TAMPEREEN TEKNILLINEN YLIOPISTO
TAMPERE UNIVERSITY OF TECHNOLOGY

Regina Gumenyuk

Generation and Interaction of Dissipative Solitons in Fiber Lasers

Julkaisu 1221 • Publication 1221

Tampere 2014

Tampereen teknillinen yliopisto. Julkaisu 1221
Tampere University of Technology. Publication 1221

Regina Gumenyuk

Generation and Interaction of Dissipative Solitons in Fiber Lasers

Thesis for the degree of Doctor of Science in Technology to be presented with due permission for public examination and criticism in Tietotalo Building, Auditorium TB109, at Tampere University of Technology, on the 11th of July 2014, at 12 noon.

Tampereen teknillinen yliopisto - Tampere University of Technology
Tampere 2014

ISBN 978-952-15-3312-9 (printed)
ISBN 978-952-15-3323-5 (PDF)
ISSN 1459-2045

Abstract

This thesis presents the study of various fiber gain materials, new laser operating regimes and pulse dynamics in mode-locked fiber lasers. Consideration was paid primarily to investigation of energy level transition in Bi-doped alumosilicate- and phosphosilicate-core fibers as promising gain media for mode-locked fiber lasers and amplifiers. The first experimental evidence of dissipative dispersion-managed soliton was obtained on basis of Tm-Ho-doped fiber laser. The role of laser cavity parameters on dissipative soliton interaction was experimentally investigated in mode-locked fiber lasers operated at different wavelengths.

The energy transition in bismuth-doped alumosilicate- and phosphosilicate-core fibers was examined using the spectroscopy of transient oscillations at room and liquid-nitrogen temperatures. Bi-doped alumosilicate fiber provides luminescence at the 1.18 μm wavelength band, while Bi-doped phosphosilicate fiber emits at 1.32 μm. The study revealed three-level transition at room temperature and a four-level system at liquid-nitrogen temperature at the 1.18 μm wavelength range. The long-wavelength range, 1.32 μm, operates via four-level transition scheme at room temperature.

The new mode-locked fiber laser regime was experimentally demonstrated in a Tm-Ho-doped fiber laser cavity operated at 2 μm. The dissipative dispersion-managed solitons, emitted by the laser in the normal net cavity dispersion regime, exhibited superior performance compared to dispersion-managed solitons in anomalous dispersion in the same cavity.

A detailed analysis of pulse dynamics in the mode-locked fiber laser was performed. Under thorough control of the laser parameters, the different soliton groups were obtained: bound solitons, bunch of solitons, soliton rains. Parameters affecting soliton

interaction include the recovery dynamics of the saturable absorber, the recovery dynamics of the gain medium, net cavity dispersion, nonlinearity, the sign of gain medium dispersion.

Preface

The work presented in this thesis was carried out at the Optoelectronics Research Centre (ORC) Tampere University of Technology. The work has been supported by Graduate school in Electronics, Telecommunications and Automation (GETA), the Elisa Foundation.

I gratefully thank my supervisor Prof. Oleg G. Okhotnikov for his belief in me, support, unquenchable energy, and plentiful source of inspiration and ideas. I would like to thank Prof. Markus Pessa for opening ORC's doors for me. I am deeply thankful to Dr. Pekka Savolainen for administrative support of my PhD study.

A thousand thanks to Eija Heliniemi and Anne Viherkoski for solving all problems and make my life in Finland much easier. Illka Hirvonen and Pauli Silanpää, thank you very much! Your help in technical issues made the scientific process smoother and faster.

I would like to thank my tutor in the lab and the fiber science world, Samuli Kivistö, for his patient and willingness anytime to support me in my enquirers.

Many thanks to Valery Filippov for helpful discussions and support.

I would like to thank my lab colleagues, former and current, Esa, Antti, Sasha, Juuso, Juho, Jussi, Chris, Tommi, Jari, Dmitrii, Andrei for the good atmosphere in the lab, taste jokes, and for help in carrying the heavy devices for me. Without you the science would not be so fun!

Special thanks to the students Teppo and Joona for being so smart and independent, what minimized my job as a lab tutor and let me come late to the work.

I am also thankful Mircea Guina for helpful discussions and perfect SESAMs.

I would like to thank Charis Reith for abiding proofreading of my written word expressed in terms of the thesis. I thank the pre-examiners, Paulo Almeida (Fianium) and

Sergey Babin (IAE SB RAS), for the review and comments.

I am gratefully thankful to my family for their patient, support in all my initiations and belief in me.

Tampere, June 2014
Regina Gumenyuk

Contents

List of Publications

This thesis is a compendium, based on the following publications that are included as appendices and referred to in the text as [P1]...[P7].

[P1] R. Gumenyuk, K. Golant and O. G. Okhotnikov, "Energy transition characterization of 1.18- and 1.3-μm bands of bismuth fiber by spectroscopy of the transient oscillations", *Applied Physics Letters*, Vol. 98, No. 19, pp. 191108 (2011)

[P2] R. Gumenyuk, I. Vartiainen, H. Tuovinen and O. G. Okhotnikov, "Dissipative dispersion-managed soliton 2 μm thulium/holmium fiber laser", *Optics Letters*, Vol. 36, No. 5, pp. 609–611 (2011)

[P3] R. Gumenyuk and O. G. Okhotnikov, "Temporal control of vector soliton bunching by slow/fast saturable absorption", *J. Opt. Soc. Am. B*, Vol. 29, No. 1, pp. 1–7 (2012)

[P4] R. Gumenyuk, M. S. Gaponenko, K. V. Yumashev, A. A. Onuschenko and O. G. Okhotnikov, "Vector Soliton Bunching in Thulium-Holmium Fiber Laser Mode-Locked with PbS Quantum-Dot-Doped Glass Absorber", *IEEE Journal of Quantum Electronics*, Vol. 48, No. 7, pp. 903–907 (2012)

[P5] R. Gumenyuk and O. G.Okhotnikov, "Impact of gain medium dispersion on stability of soliton bound states in fiber laser", *IEEE Photonics Technology Letters*, Vol. 25, No. 2, pp. 133–135 (2013)

[P6] R. Gumenyuk and O. G. Okhotnikov, "Multiple Soliton Control in Fiber Lasers by Active Intensity Modulation", *IEEE Photonics Technology Letters*, Vol. 25, No. 5, pp. 454–456 (2013)

[P7] R. Gumenyuk and O. G. Okhotnikov, ”Multiple solitons grouping in fiber lasers by dispersion management and nonlinearity control”, *J. Opt. Soc. Am. B*, Vol. 30, No. 4, pp. 776–781 (2013)

Author's contribution

The thesis includes seven original journal articles published in the international peer-reviewed press and provided as appendices to the thesis. It also contains material from supplementary publications and some new recently submitted manuscripts.

For all work reported, the author designed and built the experimental setup and made most of the experimental measurements. The author was also directly involved in designing and manufacturing passive fiber components. However, the achievements presented here are a part of team work. The author benefited from the work contribution of various co-authors, especially in the saturable absorber, high chirp phase mask and doped-fiber manufacturing. A more detailed description of the authors contribution to research work and preparation of the scientific papers is given below.

In [P1] the author built the experimental setup based on fiber laser and performed most of the investigated work. The author wrote the first draft of the paper, refined it with the help of co-authors, and was also the corresponding author.

In [P2]-[P7] the author designed and built the mode-locked fiber lasers and performed all experimental measurements. The author had a major role in writing the manuscript, refined it with help of co-authors, and was also the corresponding author.

List of Abbreviations and Symbols

ANDi	All normal dispersion
AADi	All anomalous dispersion
CW	Continuous wave
DM	Dispersion-managed
Bi	Bismuth
Yb	Ytterbium
Nd	Neodymium
Tm	Thulium
Ho	Holmium
Er	Erbium
SESAM	Semiconductor saturable absorber mirror
PbS	Lead sulfide
QD	Quantum dot
CNT	Carbon nanotubes
NPR	Nonlinear polarization rotation
DBR	Distributed Bragg reflector
QW	Quantum wells
SEM	Scanning electron microscope
SWCNT	Single-walled carbon nanotubes
SA	Saturable absorber
AOM	Acousto-optic modulator
RF	Radio-frequency

PEF	Polarization evolution frequency
PLVS	Polarization-locked vector soliton
GVLVS	Group velocity vector soliton
SPM	Self-phase modulation
XPM	Cross-phase modulation
DDM	Dissipative dispersion-managed
CFBG	Chirped fiber Bragg grating
UV	Ultraviolet
GVD	Group-velocity dispersion
AO	Acousto-optic

Symbols

ω_{relax}	Relaxation frequency
N	Total number of active ions
c	Speed of light
σ	Laser transition cross section
L	Total cavity length
l	Length of the gain medium
f^l	Fraction thermal occupation of the lower laser level
τ_c	Cavity lifetime
τ_s	Laser transition lifetime
r	Pumping rate
P_{th}	Threshold pump
ΔR	Modulation depth
α_0	Nonsaturable losses
F_{sat}	Saturation fluence
D	Dispersion parameter

Chapter 1

Introduction

Ultrashort pulse fiber lasers have attracted the attention of the scientific community for several decades. Over this time thousands of articles and several review books have been published. A growing number of new effects in soliton fiber lasers that would further enhance the practical aspect of soliton technology are still expected. The theories are expanded and augmented, definitions are corrected. Numerous nonlinear processes have been revealed and described. Progress has also been achieved in investigation of new laser materials, resulting in an ultra broad band spectral range available for promising applications. Bismuth-doped fibers are a bright example of such a gain medium. CW and mode-locked fiber lasers based on them and operated at 1.18 μm, 1.32 μm, and 1.46 μm have been developed.

Short pulse lasers can be classified according to different laser parameters. In terms of dispersion, the laser can be divided into the following groups: all normal dispersion (ANDi) fiber laser, similariton fiber laser, dispersion-managed (DM) fiber laser, all anomalous dispersion (AADi) fiber laser and stretched-pulse fiber laser (Fig. 1.1). In terms of polarization evolution of solitons, the fiber laser can be considered to be a scalar or vector soliton laser. In terms of soliton clusters/groups the lasers can be classified as lasers emitting bound solitons (or soliton molecules), bunch of solitons, and soliton rains.

The aim of this thesis is twofold. First, the design of a new type of soliton fiber laser based on new materials or new principle algorithms. Second, the investigation of

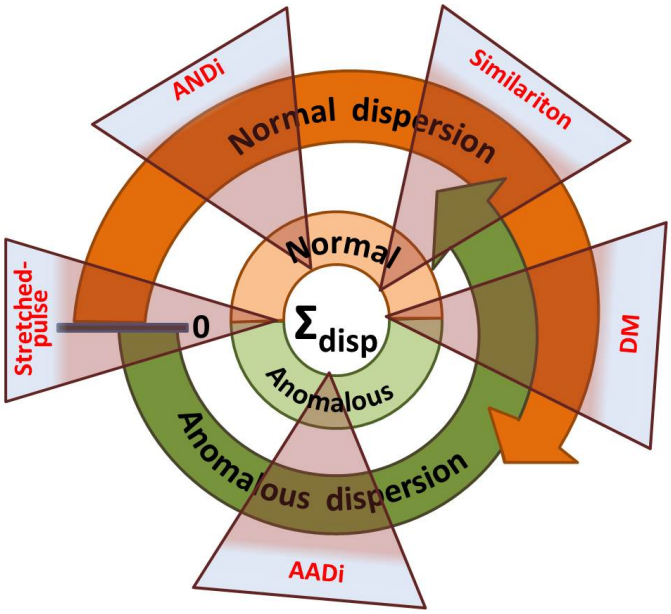

Figure 1.1: Diagram of operating soliton regimes in mode-locked fiber laser depending on the net cavity dispersion (Σ_{disp}) and dispersion map.

dissipative soliton dynamics in the fiber laser cavity.

Chapter 2 reviews the employment of relaxation oscillation as an instrument for evaluation of energy transition in rare-earth-doped fibers, widely used as active media in fiber lasers. The same method was applied for the disclosure of energy level systems in Bi-doped fibers operated at 1.18 μm and 1.32 μm.

Chapter 3 reviews the basic concept of the mode-locking regime. The definitions and physical principles of dissipative solitons, vector and scalar solitons are presented.

Chapter 4 introduces the fundamental properties and characteristics of ANDi lasers. The study includes the experimental observation of dissipative dispersion-managed soliton fiber laser operation at 2 μm.

Chapter 5 describes the main soliton interaction mechanisms and gives an overview of soliton group states. Laser parameters essentially affecting the soliton dynamics are presented.

Chapter 2

Rare-earth- and Bismuth (Bi)-doped fibers

This chapter introduces the spectrally resolved transient oscillations as a method for analysis of emission buildup, dynamics of population inversion and the nature of laser transitions. An overview of laser transitions in ytterbium, neodymium, erbium, and thulium-holmium-doped fibers, investigated by relaxation oscillations, is presented. The energy level systems in Bi-doped alumosilicate and phosphosilicated core fibers at room and liquid nitrogen temperatures are identified.

2.1 Relaxation oscillations in rare-earth-doped fiber lasers

The laser ideally exhibits three-, quasi-three or four-level systems. The energy transition mechanism affects the laser dynamics. Study of the laser transitions is typically based on optical spectroscopy and employs fluorescence and absorption processes [1,2]. However, using these tools there are some difficulties for characterization of the rare earth doped system over the entire gain spectrum. A simple method for laser transition characterization based on relaxation oscillations was proposed relatively recently [3–5].

Relaxation oscillations are small-amplitude, nearly sinusoidal, exponentially damped oscillations, which occur when a laser is on. It is a transient process, appearing

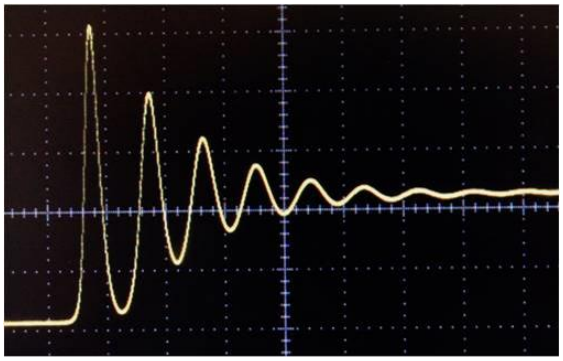

Figure 2.1: Example of typical relaxation oscillation in a fiber laser. (Bi-doped phosphosilicate-core fiber laser. Time scale: 40 μs. [P1])

as a sinusoidal variation of the photon number and, thereby, the output power. Under continuous pumping the photon number rises. Once it exceeds the steady steady-state level the laser begins to burn up excited states at a much faster rate than the pump can supply them, resulting in a decrease of photon number. This appears as an oscillation around the steady state level. These oscillations are eventually damped in a quasi-sinusoidal behavior. A typical example of relaxation oscillations is presented in Fig. 2.1.

Spectrally resolved transient oscillations offer a useful tool for analysis of emission buildup, dynamics of population inversion and the nature of laser transitions. The relaxation oscillation determines the wavelength dependence of the characteristics frequency ω^2_{relax}. The origin of this dependence for three-level systems can be understood from the small-signal analytic solution of the rate equations, taking into account the thermal population of the level as follows [6]:

$$\omega^2_{relax} = \frac{1}{\tau_c \tau_s} \left(1 + c\tau_c \sigma \eta f^1 N\right)(r-1)$$

where N is the total number of active ions, c, σ are the speed of light and the laser transition cross section, $\eta = l/[L + l(n-1)]$, where L, l are the total cavity length and the length of the gain medium, n is the refractive index, f^l is the fractional thermal oc-

cupation of the lower laser level, and τ_c , τ_s are the cavity and laser transition lifetimes. $r = \frac{P}{P_{th}}$ is a pumping rate normalized to threshold. From this relation it is clear that the wavelength dependent term in the brackets disappears for lasers operating with negligible population on the terminal level ($f^l = 0$), as is the case for four-level transitions. Thereby, the slope (ω^2_{relax} vs $(r-1)$) is wavelength-insensitive for four-level systems. In contrast, for three-level systems the slope varies notably with wavelength. Quasi-three level systems are characterized by weak wavelength-dependence of the slope. The cross sections for emission and absorption at each transition can be also determined directly using the experimentally measured wavelength dependencies of the relaxation oscillation frequency and threshold pumping rate. It should be then noted that the relaxation oscillation frequency depends directly on the absorption at the signal wavelength (σf^l) as a result of the finite thermal population of the ground level. Thus, the wavelength dependence of transient oscillation provides a method to determine the energy level scheme of optical transitions in the laser material.

Relaxation oscillations were used to determine the energy-level system in rare-earth-doped fiber lasers over the entire gain spectral range. The investigation of Yb-doped fiber laser indicated that the laser operates as a three-level system at wavelength below 1060 nm, while at longer wavelength range it is close to a four-level system [7]. Similar experiments were performed in $Nd^{(3+)}$ and Tm-Ho-doped fibers, using broad wavelength ranges of $888-1080$ nm and $1860-2020$ nm, respectively [4, 8]. The $Nd^{(3+)}$-doped fiber laser demonstrated three-level transient transitions in the wavelength range of $888-914$ nm and four-level operation at $1060-1080$ nm. The Tm-Ho-doped fiber laser operated as a three-level system at wavelengths below 1960 nm and it was wavelength insensitive to relaxation frequency at the long wavelength tail indicating four-level transition dynamics. The transient oscillation investigated in Er-doped fiber laser revealed a three-level transition below 1555 nm at room temperature, turning to four-level at 77 K. At wavelength longer than 1555 nm the four-level transition is preserved independent of temperature [3–5].

Rare-earth-doped fiber lasers were widely used and investigated in detail during the last decades. Efficient fiber lasers operating at 1, 1.3, 1.5, 1.9, 2.0, 2.1 μm bands were built. Recently, a promising new gain material, Bi-doped fiber, were successfully demon-

strated. This active medium can cover the gap in the infrared wavelength range, where laser action using rare-earth-doped fiber has not been demonstrated. Emission of Bi-doped fiber in a broad 1.1 - 1.5 μm spectral band was shown, depending on excitation wavelength and core composition. Thus, Bi-doped fibers have potential for high performance fiber lasers and amplifiers in new applications. The relaxation oscillations method was applied for investigation of the laser transition dynamics in bismuth alumosilicate and phosphosilicate-core fibers at liquid-nitrogen and room temperatures.

2.2 Energy level transitions in Bi-doped fiber lasers

The relaxation oscillations were studied in the linear laser cavity schematically shown in Fig. 2.2. Bi-doped active medium was pumped via a dichroic coupler. The resonator was terminated by a loop mirror acting as output coupler on one side, and by diffraction grating in the Littrow configuration on the other side. The diffraction grating worked as a wavelength selective element. An antireflection coated lens was used to collimate the beam from the active fiber onto the reflection grating. The chopper, placed in a collimated beam operating at rate of 650 Hz was used to observe the transient evolution of the laser emission towards its steady-state condition.

2.2.1 *Alumosilicate Bi-doped fiber*

20 m of Bi-doped fiber optimized for operation at the 1160-1180 nm band was core-pumped by a 1 W Yb-doped single-mode fiber laser, operated at 1062 nm. The fiber absorption was 1.2 dB/m at 1062 nm. The threshold pump power was in the range 55-70 mW, depending on lasing wavelength. The relaxation oscillation frequency measured at liquid-nitrogen (77 K) and room temperature (297 K) are shown in Fig.2.3. The slope $\omega^2_{relax}/(r-1)$ exhibits a valuable dependence on wavelength at room temperature, indicating a change in the population of the sublevel of the ground manifold. This behavior indicates a three-level laser transition. In contrast, at liquid-nitrogen temperature the population of the ground manifold is negligible, resulting in insignificant absorption of individual transitions from the ground sublevels and, eventually, in a four-level character of laser transition [P1].

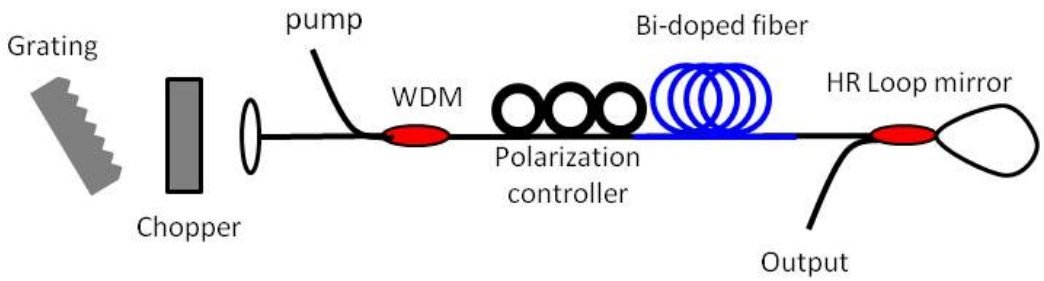

Figure 2.2: The experimental setup for measuring of relaxation oscillation in bismuth-doped fiber laser.

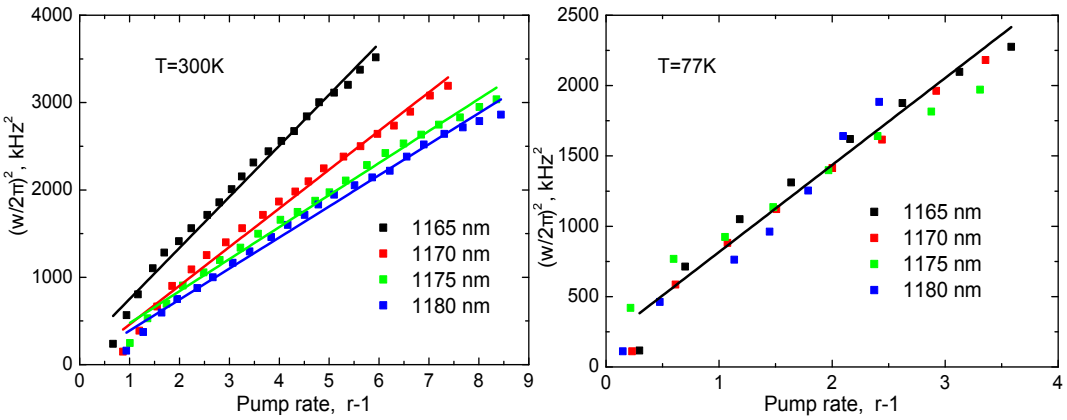

(a) (b)

Figure 2.3: $(\omega_{relax}/2\pi)^2$ vs pumping rate $(r-1)$ for 1160 - 1180 nm spectral band. a - at 300K; b - at 77K.

2.2.2 *Phosphosilicate Bi-doped fiber*

The phosphosilicate Bi-doped fiber was designed for operation at 1320-1340 nm. 30 m of Bi-doped fiber was pumped by a 200 mW 1236 nm laser diode. The threshold pump power was varied from 60 to 80 mW depending on operation wavelength. The wavelength dependent behavior of relaxation oscillation frequency versus normalized pump power is shown in Fig. 2.4. The four-level laser operation of the active medium over the whole spectral band was evident even at room temperature. The energy level system at liquid nitrogen temperature should obviously also demonstrate four-level character.

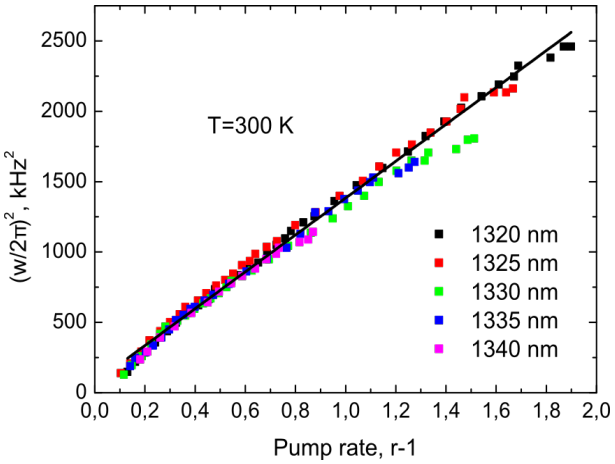

Figure 2.4: $(\omega_{relax}/2\pi)^2$ vs pumping rate $(r-1)$ dependence for 1.32 - 1.34 μm wavelength range measured at room temperature.

Chapter 3

Short pulse fiber laser

This chapter describes the basic principles of mode-locking and the general concept of the soliton pulse. The review of mode-locking methods is focused on a description of passive techniques. The concept of dissipative solitons is introduced and the differences between dissipative and conservative solitons are discussed. The properties of vector and scalar solitons in fiber lasers are considered.

3.1 Fundamentals of mode-locking

Mode-locking is a technique to produce short pulses (on the order of picoseconds (10^{-12} s) or tens of femtoseconds (10^{-15} s)). The technique is based on a fixed phase relationship between the longitudinal modes of the laser cavity. Interference between the modes causes the laser light to be produced as a train of pulses. The laser is essentially an optical oscillator requiring two basic principles, namely amplification and feedback. The stimulated emission in a gain medium provides the amplification and determines the laser's bandwidth of operation. A mirror pair surrounding the gain medium terminates the cavity and supplies the feedback. Light as a wave bounding between the mirrors constructively and destructively interferes with itself, leading to the formation of standing waves, or longitudinal modes. In a free-running laser, each of these modes oscillates independently, with no fixed phase relationship between them in the general case. By insertion of a modulation synchronous with every round trip time of the cavity, the lock-

ing between the phases of different modes can be realized, resulting in a pulse train being emitted by the laser. The mode-locking mechanism can be realized using two approaches: active or passive. In active schemes, mode-locking is achieved by using an externally driven element generating a loss modulation that is precisely synchronized with the cavity round-trip time [9]. The loss modulation can be induced by an amplitude or a phase modulator. In passive mode-locking the cavity contains an element which inserts the loss modulation based on its internal processes. Usually it is some nonlinear optical effect, such as saturation of a saturable absorber or nonlinear refractive index change of a suitable material [6]. In this chapter I will concentrate mainly on description of the passive mode-locking technique and elements that were used in the experimental work presented in this thesis .

3.1.1 *Passive mode-locking*

Passive mode-locking schemes are based on some form of saturable absorber and can be realized by a real loss component: semiconductor saturable absorber mirror (SESAM) [10–16], PbS quantum-dots-based saturable absorber (PbS QDs) [17–22], [P3], carbon nanotubes (CNT) [23–29], graphene [30–37]; or by an artificial absorber such as a nonlinear polarization rotation (NPR) [38–42]. Other mode-locking methods based on frequency shifted feedback or nonlinear amplifying loop mirrors also belong to the passive mode-locked technology.

Semiconductor saturable absorber mirror (SESAM)

A semiconductor saturable absorber mirror (SESAM) is a passive modulator used to obtain self-amplitude modulation inside the laser cavity. The working principle is based on a saturation effect exploiting relatively high losses for low intensity light and low losses for high intensity light. A SESAM structure consists of two parts: a saturable absorber and a bottom distributed Bragg reflector (DBR), grown layer by layer by state-of-art molecular beam epitaxy technology. The saturable absorber is constructed by alternation of semiconductor layers with higher and lower band gap energies, forming quantum wells (QWs). The *wavelength range* of absorption can be controlled precisely by adjusting the composition, the depth, and width of the QWs. The absorbing region is often capped with a top DBR or with an antireflection dielectric coating.

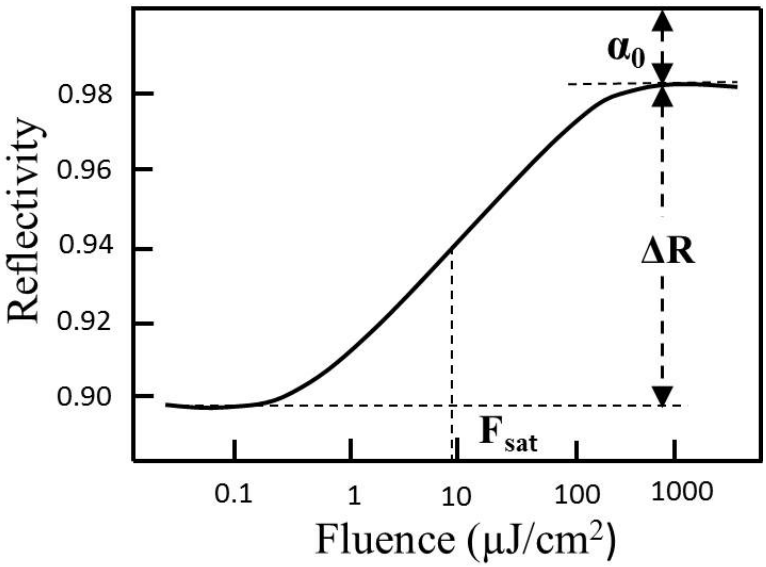

Figure 3.1: *Nonlinear reflectivity characteristics of a SESAM.*

So, as the light intensity increases, the saturable absorber becomes transparent, allowing the majority of the cavity energy to pass through the absorber to the mirror, where it is reflected back into the laser cavity. The nonlinear SESAM reflectivity is shown in Fig. 3.1. The magnitude of reflectivity variation is called the modulation depth (ΔR). This value is responsible for pulse duration optimization and for maintaining the self-starting process [43, 44]. The residual absorption, when the absorber is fully saturated, are called the nonsaturable losses (α_0). This parameter affects the efficiency of mode-locked lasers and should be minimized. The saturation fluence (F_{sat}) is defined as the fluence which produces a 1/e change in reflectivity compared to the fully saturated absorber. Low saturation fluence is desirable for low threshold and suppression of Q-switching instability [43–45].

One more key parameter is the SESAM recovery time. It is the time needed for the absorber to reach the 1/e level of its bleached transmission. The SESAM absorption has a bi-temporal response: fast and slow (Fig. 3.2). The fast response is determined by intraband thermalization processes and typically lasts from a few hundred femtoseconds to a few picoseconds. This recovery time component is responsible for stabilization

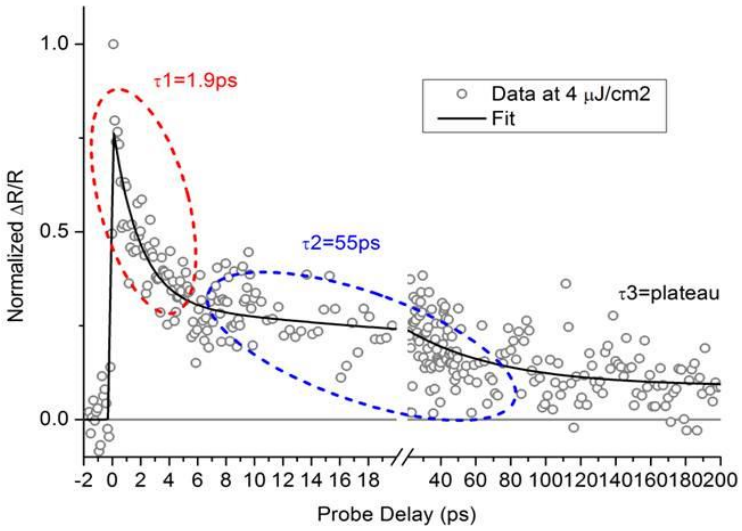

Figure 3.2: *A typical bi-temporal response of SESAM.*

of the pulse regime. The slow recovery component is due to interband recombination and varies from tens of picoseconds to nanoseconds [46]. The slow response plays an important role in starting the pulse formation process [47]. Additionally it generates the attractive force pushing the pulses close to each other and resulting in a stable group formation with closely spaced pulses [48], [P3, P7]. When the temporal length of the group is below the decay time of the absorber, the joint action of the pulses forming the group provides more complete saturation of absorption, and thus the pulses exhibit lower losses compared to the regime with the absorber saturated by individual pulses. The recovery time of SESAM can be reduced by creating fast non-radiative recombination centers in the absorber structure. Methods to achieve this include low temperature [49] or metamorphic growth [50, 51], and post-growth or in-situ heavy-ion implantation [52–55].

Carbon nanotube-based saturable abrorbers

Carbon nanotubes (CNTs) represent low-dimensional carbon nanostructures - tiny, hollow cylinders constructed by rolling up a single layer of graphite. The diameters of nanotubes are in the range of several nanometers, while their length can reach several micrometers. As a result, they are prototypical one-dimensional systems, in which car-

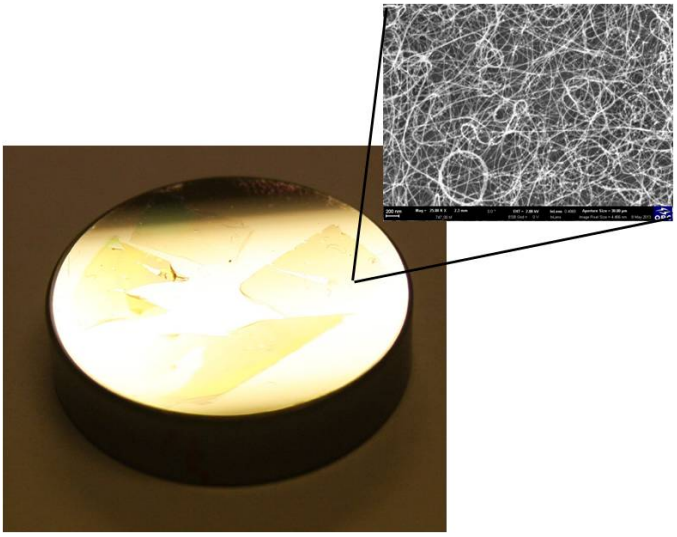

Figure 3.3: *SEM image of CNT (inset) embedded on silver reflective mirror.*

riers can move freely only along the axis of the cylinder. Depending on the specific geometry the quantum confinement, they can be either metallic or semiconducting, with a tunable bandgap depending on nanotube diameter [56, 57]. Since it is quite challenging to make uniform structures of carbon nanotubes film, and, thereby, the film usually contains nanotubes with a broad range of parameters. This feature results in broadband absorption of the structure, which can range from 1 to 2 μm [58].

CNTs are usually fabricated in quite simple and cost-efficient ways with spin coating or spray methods [56, 59–61]. They can be performed to operate either in transmission or reflection, which gives the freedom to use them in either ring or linear cavity configurations [27, 58]. So far CNT-based absorbers have been widely used in fiber lasers. Most of them contain single-walled carbon nanotubes (SWCNT) typically embedded into polymer and transferred afterward onto different surfaces: on top of a reflective mirror (Fig. 3.3), silica glass substrate [55], or fiber connectors [62, 63]. A combination of SWCNT and evanescent field interaction in tapered and D-shape fibers has been also reported [64]. Recently, a multi-walled CNT was synthesized and investigated [65], and used as a saturable absorber in a fiber laser [66].

Ordinary, carbon nanotubes have a chaotic surface structure. Inoue et al. reported

a new generation of CNT-based absorber with vertically aligned CNT, what has been implemented in an Er-doped fiber laser as a mode-locking element [67]. It exhibited no absorption, when the light was incident perpendicular to the substrate.

As a saturable absorber, CNT offers a small modulation depth, usually not exceeding a few percent. By increasing the thickness or concentration of the film it is possible to increase the modulation depth [68, 69] and achieve better pulse shaping. However, the increase in the nonlinear absorption also typically results in an increase in the nonsaturable losses. In terms of carrier dynamics, the advantage of CNT-SA is fast relaxation decay, which can be described primarily by one exponential component. The recovery time is within the range of 300 fs to 1 ps [70–74].

PbS quantum dot saturable absorbers

This type of saturable absorber is based on II-VI semiconductor nanoparticles incorporated in glass matrices. They are fabricated by using deposition in porous glasses by simple and low-cost batch-melting techniques [21,75]. By variation of the heat treatment regime, the size of the quantum dots can be controlled. Usually, the radius of the PbS nanoparticles is within the range of 1.7 - 9 nm [18,21,22,76–79]. The nanometer size of PbS quantum dots provides a strong quantum confinement effect, resulting in a blue shift of the energy band gap and a strong nonlinearity close to the first excitation resonance. The large exciton Bohr radius of 18 nm and the narrow bandgap (0.3 - 0.4 eV) produce a strong confinement affect even with relatively large crystals, and allow the absorption resonance to be tuned in the spectral range of about 0.5 - 3 μm [45]. The typical linear and nonlinear absorption spectra of the PbS QD sample used as saturable absorber in a mode-locked Tm-Ho fiber laser can be seen in Fig. 3 and 4 in [P4]. The nonlinear response shows bi-temporal recovery dynamics [P4], [18, 45, 79]. The typical bleaching relaxation process is presented in Fig. 5 [P4]. The fast and slow time components were equal to 6.5 and 220 ps, respectively.

Frequency shifted feedback mode-locking

Another type of passive mode-locking mechanism is based on the frequency-shifted feedback technique. In this case the pulse is formed in the laser cavity by a combination of a Kerr nonlinearity and spectral filtering. An acousto-optic modulator (AOM) placed inside the resonator introduces the continuous frequency shift of the spectrum at each

roundtrip. The spectrum moves away from the peak wavelength of the filter usually presented by the gain medium. The frequency dependent amplification and self-modulation restore the spectrum in a way opposite to the shift. Thereby the optical pulse is trapped in the frequency domain. The frequency-shifted feedback is used as an alternative to mode-locking with a saturable absorber or nonlinear polarization rotation for generation of ultrashort pulses [80–83]. In addition, the wide wavelength tuning of mode-locked fiber laser has been demonstrated [84, 85].

3.2 *Dissipative nature of soliton*

The pulses forming in the mode-locked fiber lasers frequently take the shape of a soliton. The shape and energy of a soliton are preserved during the propagation. In general, a pulse propagating in a fiber laser is formed by a combination of nonlinear self-phase modulation and dispersion. Dispersion spreads the pulse in the time domain, while nonlinearity broadens it in frequency domain. Furthermore, a laser is characterized by continuous energy flow, which leads to a strong requirement of an additional balance between gain and loss in order for soliton formation to occur. In order to produce stationary state in fiber laser, the balance of four parameters (gain and loss, dispersion and nonlinearity) is needed (Fig. 3.4). This fact reveals the dissipative nature of solitons formed in a fiber laser, meaning that energy leakage is always present in the system [86–88]. The energy dissipation in the cavity leads to the pulse dynamics resulting in interaction of solitons and formation of multi-soliton complexes such as bound solitons, bunch of solitons and soliton rains [89–97].

Though solitons in fiber lasers are dissipative, there is a difference between pulse properties depending on the net cavity dispersion. In the anomalous net cavity dispersion regime with increasing pump energy the accumulative phase shift can not be eventually compensated for by the dispersion, giving rise to a phenomenon known as pulse breaking. Multiple pulsing is a result of energy quantization and a general attribute of soliton regime in a laser operated at net anomalous dispersion. The typical pulse spectrum can be seen in Fig. 2 in [P4]. The spectrum indicative for this regime has a gaussian or hyperbolic shape and contains narrow Kelly sidebands [98]. When the gain and loss balance

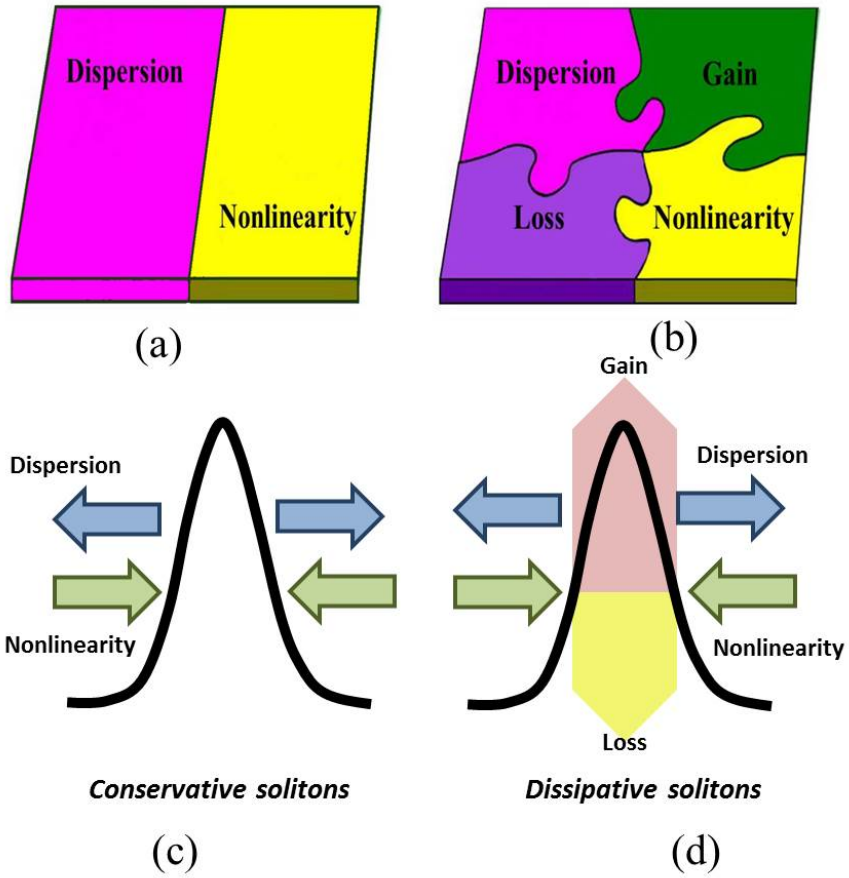

Figure 3.4: *Qualitative representation of a family of conservative solitons solutions (a, c) and fixed soliton solution for dissipative solitons (b, d).*

does not play a primary role, the pulses, formed in this regime, do not display complex dynamics and are considered as Schrödinger solitons, meaning that the main factors in their formation are nonlinearity and dispersion [89]. They are also called *conservative (conventional)* solitons (Fig. 3.4). In normal net cavity dispersion, the pulse is continuously stretched and is characterized by high chirp at every single point in the cavity [99]. As a result, the peak power is reduced while a large spectral content is maintained and conditions preventing the pulse-breaking are created [100]. This concept leads to the formation of high-energy single pulse operation in the cavity. The typical pulse spectrum with steep spectral edges can be seen in Fig. 2 in [P2].

3.3 *Scalar and vector solitons*

An ordinary soliton maintains its shape during propagation in the cavity and has effectively only one polarization component, and is, thereby, characterized by linear polarization state. In terms of polarization this soliton is termed a *scalar soliton*. Scalar solitons are formed primarily in all-polarization maintaining fiber lasers, where only light of the specific linearly-polarized state is guided [101]. In conventional (non-polarization-maintaining) fiber two polarization components propagate with the same nominal phase velocity, due to the fiber's circular symmetry. However, even small amounts of random birefringence in such fiber, due to arbitrary stress, fiber bending or imperfection of the circular core cross-section along a fiber length, will cause phase shift and polarization crosstalk between two polarization modes (*linear birefringence*) [102]. Even small amounts of crosstalk can lead to a large power transfer from one mode to another, completely changing the state of polarization. If the energy distribution between components is unequal it creates *nonlinear birefringence*. The presence of coupling between two orthogonal polarization components may cause vector soliton formation. During the propagation of vector solitons, two orthogonal polarization components can copropagate as one unit without splitting, due to the strong cross-phase modulation and coherent energy exchange between them, which may induce intensity differences between polarization modes. Because of the nonlinear interaction among these two polarization components, despite the existence of birefringence, they can still adjust their group velocities and be trapped together [103–106].

The polarization state evolves from pulse to pulse, or even within the duration of a single pulse [107]. The evolution of the polarization state can be examined by monitoring the radio-frequency (RF) spectrum of the pulse passed through polarizing beam splitter (Fig. 3.5) [108–110]. The sidebands around the harmonics of the repetition rate frequency are the signature of the evolution of the pulse polarization transforming into amplitude modulation at the output of the polarizer. The rate of polarization evolution is expressed in polarization evolution frequency (PEF). When polarization is locked, PEF=0 [P3]. When polarization pertubation of soliton occurs, the PEF takes values other than zero [107].

Depending on the strength of birefringence different types of vector soliton can be

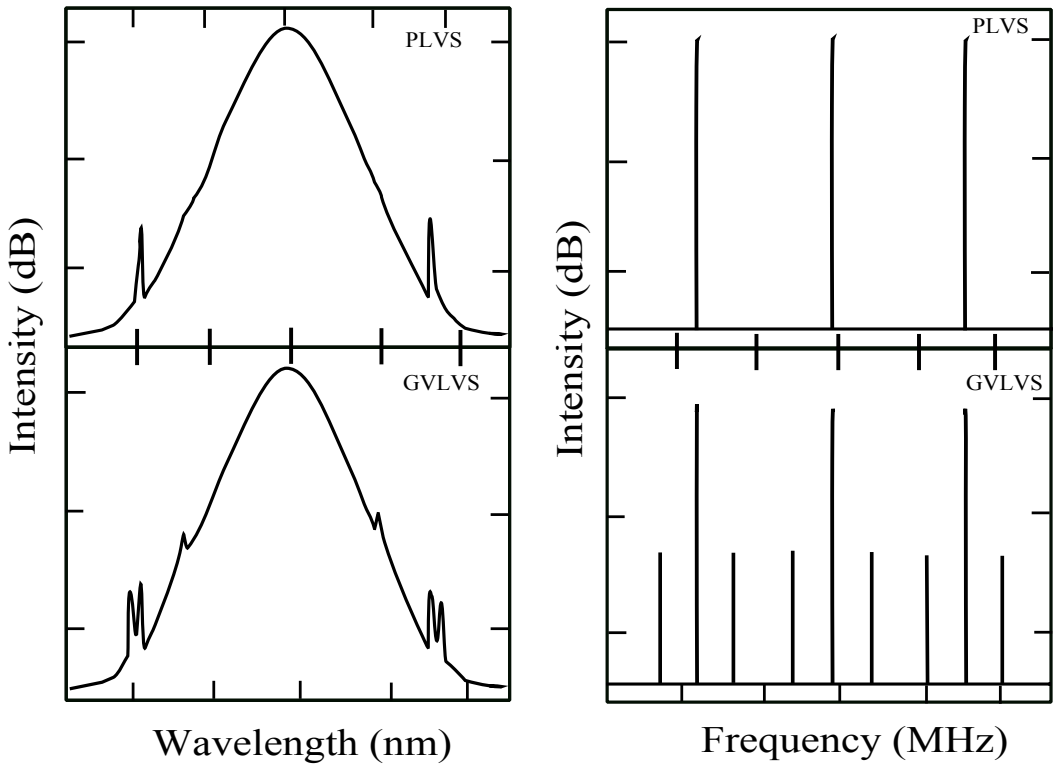

Figure 3.5: *Qualitative representation of PLVS's and GVLVS's optical and RF spectra.*

formed in the cavity. For the *low-birefringence* condition, in which the linear birefringence is comparable with the nonlinear birefringence, the group velocity difference is assumed to be negligible. Within this regime elliptically polarized vector solitons are formed in the cavity. These stationary solitons are composed of two orthogonally polarized and optically phase-locked components and are defined as *phase-locked* or *polarization-locked vector solitons* (PLVS). PLVSs maintain both their temporal and polarization state profiles during propagation within birefringent environments and have a $\pm\pi/2$ fixed relative phase difference. Therefore, when PLVSs are formed in the laser, PEF=0. The polarization state of PLVSs can be either elliptical, or linear. In case of linearly polarized vector solitons, the total energy of the soliton is carried by the component polarized along the slow axis. The existence of such solitons is related to the polarization instability of light polarized along the fast axis [109, 111].

In the presence of *moderate* or *large birefringence*, group velocity vector solitons

(GVLVSs) are formed in the cavity [112]. This type of vector soliton is composed of two orthogonal components with equal group velocities. It has been shown that GVLVS can be formed by nonlinearly induced central frequency shifting of two polarization modes in order to compensate for the self-phase modulation (SPM) and cross-phase modulation (XPM) (Fig. 3.5) [113–115]. Contrary to PLVSs, for which the polarization state is locked, GVLVSs are characterized by polarization rotation during the propagation. Therefore, a GVLVSs exhibit PEF in the RF spectrum and polarization sidebands in the optical spectrum (Fig. 3.5) [115].

Chapter 4

Mode-locked fiber laser operated in normal net cavity dispersion regime

In order to get the desired fiber laser output performance it is necessary to select the laser components carefully, since the fiber laser regime is affected not only by cumulative laser parameters, but also by its individual components. In particular, the pulse formation mechanism depends not only on total net cavity dispersion but rather on a dispersion map. In a fiber laser constructed using only anomalous dispersion segments, the pulses are formed by the balance of nonlinear and dispersive shifts. In the case when the nonlinear phase cannot be compensated for by dispersion, the pulse will break up into two or more pulses. The multiple pulse regime restricts the maximum pulse energy that can be acquired.

A dispersion-managed fiber laser contains elements with anomalous and normal dispersion, which make up a dispersion map with a certain strength. In the case when the net cavity dispersion is anomalous, the pulse-shaping is soliton-like, as nonlinearity balances the dispersion in an average sense. The variation of the dispersion sign results in a reduction of the accumulative linear phase, and allows the pulse energy to be increased by an order of magnitude. The maximum pulse energy, that can be achieved in the cavity, can be further increased by removing anomalous dispersion segments from the cavity. This laser is called an *all normal dispersion (ANDi) laser*. The pulses are formed when four components (gain and losses, dispersion and nonlinearity) are in bal-

ance, and are denoted dissipative solitons. In this chapter the formation of high power dissipative solitons in ANDi and dispersion-managed soliton fiber laser operated at 2 μm are considered.

4.1 All normal dispersion fiber laser (ANDi)

All normal dispersion fiber laser is constructed of segments with normal dispersion [116, 117], or at least they provide the dominant contribution to the cavity [118]. The presence of normal dispersion, in combination with self-phase modulation and gain, leads to the formation of pulses with high positive frequency chirp propagating through the cavity. The chirped pulses are more resistant to the restrictions imposed by fiber nonlinearity, which is reflected in to prevention of pulse breaking, and therefore superior performance in terms of pulse energy [119]. ANDi lasers operate primarily in the single mode regime, but under excessive pumping a second pulse can appear in the cavity [116]. The typical spectrum exhibits the steep edges with a Gaussian-shaped or M-shaped top, depending on cavity design and the position of the cavity output [117, 119–121].

The pulse chirp increases monotonically during propagation along the normal dispersion fiber segments and decreases after the saturable absorber, which converts the frequency chirp to self-phase modulation. From the other side the spectral filter restores the pulse to its original duration, and this effect dominates the self-amplitude modulation occurring in the saturable absorber. Therefore, the main pulse shaping mechanism of ANDi laser is referred to as chirped-pulse spectral filtering [99, 122]. Three main laser parameters that play a primary role in pulse evolution and characteristics can be distinguished. These are nonlinear phase, spectral filter bandwidth and dispersion. All of them affects in similar way on the qualitative behavior and laser performance [99, 120]. A summary of laser parameter contributions is presented in Fig. 4.1(a) and (b). In case of variation of nonlinear phase shift, the breathing ratio, defined as the ratio of maximum and minimum pulse duration in the cavity, increases, while the pulse chirp decreases. Variation of dispersion has the opposite effect. When dispersion increases the breathing ratio decreases and pulse chirp increases. A similar characteristic is demonstrated by the variation of the spectral filtering.

The location of the spectral filter, output coupler and the output coupler ratio have a crucial influence on the pulse dynamics and derivation of high pulse energy [123, 124]. It was first theoretically predicted [120, 125, 126] and then experimentally proved [127] that at certain sets of laser parameters the energy of solitons in a dissipative system may become infinitely high. This phenomenon is defined as *dissipative soliton resonance*.

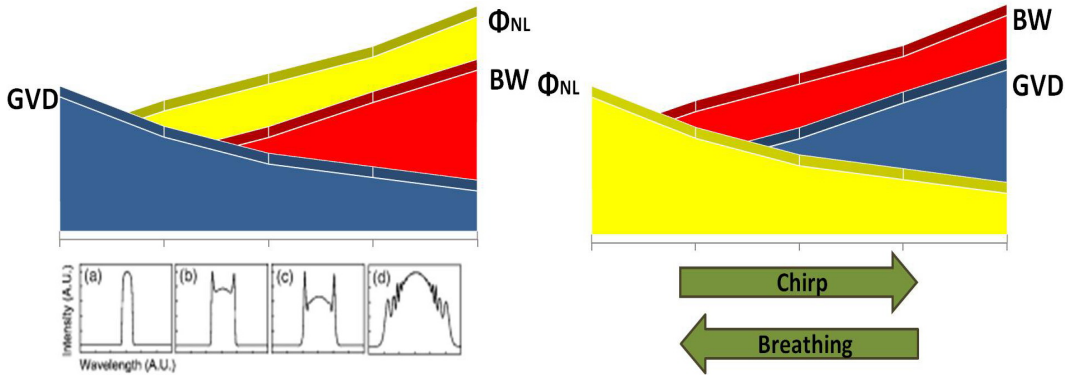

(a) (b)

Figure 4.1: Schematic representation of ANDi laser performance depending on the laser parameters: the optical spectrum (a) and pulse duration (b) evolutions. BW - bandwidth, GVD - group-velocity dispersion, Φ_{NL} - nonlinear phase. The data were taken from [99, 120]

At the time of writing, ANDi lasers were broadly represented in a variety of different laser cavity configurations. This type of laser has been realized in a ring cavity with nonlinear polarization rotation as mode-locker implemented by bulk elements [117, 121], or by fiber components [128–130]. ANDi lasers mode-locked by SESAMs in ring cavities [14, 118, 131] and linear cavities have also been demonstrated [132, 133]. Active mode-locking has been implemented in ANDi lasers in the work of Wang et al. [134] and Koliada et al. [135]. In order to increase the pulse energy in ANDi laser, core-size scaling has been applied by introducing double-clad [121] or photonic crystal fiber [136, 137] into the laser cavity.

In spite of the wide range of publications, all demonstrated ANDi lasers operate at the wavelength range from 1 to 1.55 μm, where a fiber is capable of providing normal dispersion. At present, it is not possible to construct ANDi laser operating at longer

wavelength bands. Bale et al. [138] proposed a solution, when they extended the theory of dispersion-managed (DM) solitons to dissipative systems opening the route to long-wavelength high-energy solitons.

4.2 Dispersion-managed dissipative soliton laser

The theory of dissipative dispersion-managed (DDM) solitons was demonstrated experimentally in Tm-Ho-doped fiber laser with moderate dispersion map strength composed of anomalous dispersion fiber and normal dispersion highly chirped fiber Bragg grating. The change in sign of the dispersion causes the dispersion-managed (DM) solitons to temporally broaden and recompress as they propagate. These periodic pulse duration breathers are a distinctive feature of conservative DM solitons, but in contrast to conservative DM solitons, for dissipative DM case these variations act as stable attractors to the system. The sign of the net cavity dispersion determines whether conservative or dissipative DM solitons are formed in the resonator. By variation of the fiber segment length, and thereby by changing the sign of the net cavity dispersion, it was possible to achieve both conservative and dissipative DM soliton regimes in the same laser cavity [P2].

The Tm-Ho fiber laser setup is shown in Fig. 4.2. It consists of linear cavity with a total length varied from 3 to 8.5 m changing the repetition rate in the range of 12.2 to 33.3 MHz. The gain was provided by a 1.2 m-long Tm-Ho fiber with anomalous dispersion of 0.13 ps^2/m at 1985 nm and pumped by a 1565 nm Er-doped fiber laser via a fiber pump combiner. The cavity was terminated by a chirped fiber Bragg grating (CFBG) from one side and an antimonide-based SESAM from the other side. The SESAM is described in detail elsewhere [139]. The CFBG had a chirp of 130 nm/cm and was spliced at the long wavelength range side to the cavity. It acted as an output coupler and dispersion compensator, which provided the normal dispersion.

The CFBG was inscribed by exposing the fiber to 248 nm UV light from a KrF excimer laser through a phase mask using the beam scanning technique. The single-mode fiber was loaded with hydrogen prior to grating imprinting. The linearly chirped phase mask, with a central period of 1373 nm and a chirp rate of 130 nm/cm over a length of

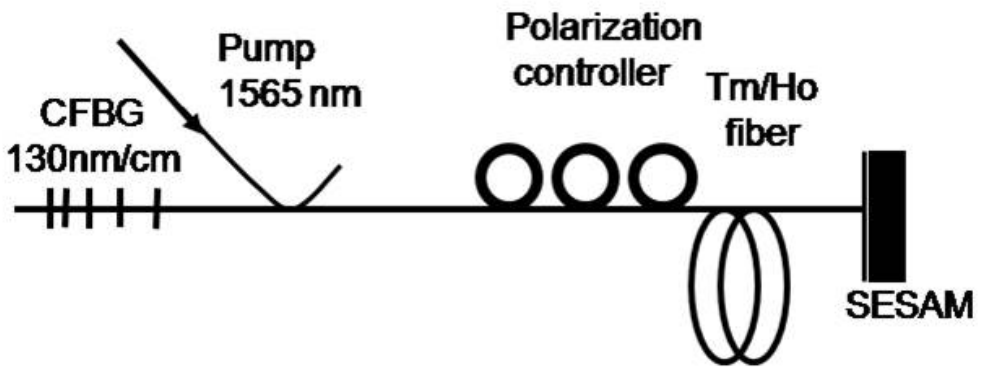

Figure 4.2: Schematic of mode-locked Tm-Ho fiber laser.

10 mm, was designed using diffraction theory based on rigorous coupled wave analysis, and then fabricated by an advanced e-beam lithography process. The 4 mm-long grating had a bandwidth of 82 nm with a central wavelength of 1986 nm, a reflectivity of 30% generated a normal dispersion of 1.07 ps^2. Thus, the dispersion map of the cavity consisted of fiber segments with anomalous dispersion and normal-dispersion CFBG, and thereby the laser supported DM solitons. By changing the length of passive fiber, the net cavity dispersion was varied from normal $0.47ps^2$ to anomalous -$0.32ps^2$.

The evolution of the pulse spectrum with the cavity dispersion is presented in Fig. 4.3. As normal group-velocity dispersion (GVD) decreases from 0.47 to 0.014 ps^2, the spectrum bandwidth increases from 3 to 10 nm (Fig. 4.3a-c). The spectrum exhibits steep spectral edges and a M-top shape, which are the signature of dissipative solitons in net normal cavity dispersion, and is similar to the spectrum shape obtained in the ANDi laser. Single pulse operation was maintained over the whole range of pump power since the normal-dispersion regime of the cavity prevents wave breaking. The measured autocorrelation for a dispersion value of 0.25 ps^2 is shown in Fig. 4.4. The cavity length was 4.5 m, corresponding to a repetition rate of 22.7 MHz and a bandwidth of 5 nm with a central wavelength of 1987 nm. The laser delivered 11.7 ps strongly up-chirped pulses corresponding to a time-bandwidth product of 15.69, which is also distinctive for a laser operated in normal dispersion. The average output power was limited to 50 mW at a pump power of 470 mW, due to the excessively large outcoupling provided by the

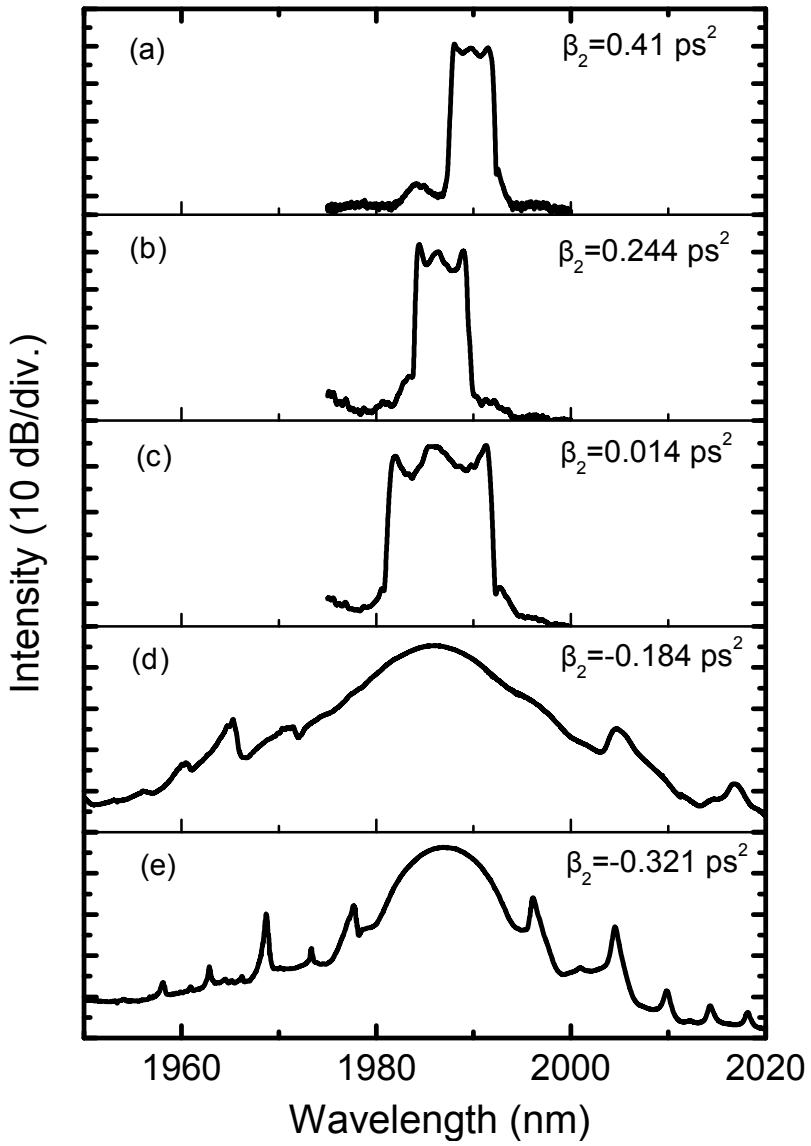

Figure 4.3: The evolution of the pulse spectrum with cavity dispersion.

CFBG.

For a net anomalous GVD increasing from -0.18 to -0.321 ps^2, the spectrum spectral width decreases from 7.6 nm to 7.3 nm (Fig. 4.3d, e). The spectrum exhibits a Gaussian shape and contains Kelly sidebands, which is indicative of solitons in the anomalous net cavity dispersion regime. The laser delivered slightly chirped 1.54 ps pulses, cor-

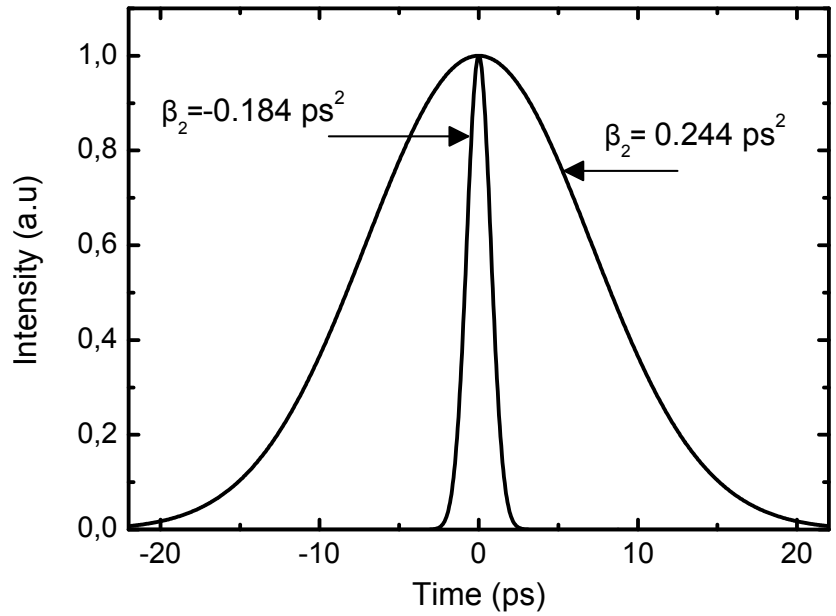

Figure 4.4: The pulse autocorrelation traces for large net normal dispersion of 0.25 ps^2 and anomalous of -0.18 ps^2.

responding to 0.85 of time-bandwidth product. The average power was within 20 mW. Multiple pulse operation set in with a minor increase in pump power.

A comparison of conservative and dissipative DM solitons in the net anomalous and normal dispersion regimes provides the following conclusions. First of all, there are fundamental differences in the laser output performance between conservative solitons in the anomalous disperion regime, and dissipative solitons in normal dispersion regime. The DDM laser operated in normal dispersion demonstrates behavior similar to that of an ANDi laser. Highly chirped pulses with a typical rectangular shaped spectrum are formed in the cavity. The output power is more than twice that of the conservative DM solitons. Additionally, the dissipative DM laser is characterized by single pulse operation over the whole range of pump power.

Chapter 5

Pulse dynamics in mode-locked fiber laser

The optical pulses formed in a mode-locked fiber laser cavity have a dissipative nature due to the inevitable presence of losses, which are compensated for by the gain. Additionally, the pulses experience nonlinearity and dispersion, the proper balance of which is essential for pulse formation and stability. When the accumulative nonlinear phase shift can not be compensated for by dispersion the pulse breaks up into two. This multiple pulsing is a distinctive feature of mode-locked lasers operated in the anomalous dispersion regime. The energy dissipation leads to the pulses interaction through various mechanisms. Depending on the particular laser parameters as well as their combination, different soliton groups/clusters can be formed such as bound solitons, bunch of solitons and soliton rains. All of them are considered in this chapter. Among the laser parameters, governing attraction and repulsion, the bi-exponential dynamics of the saturable absorber, the amount of net cavity dispersion, nonlinearity, gain dispersion and saturation dynamics can be highlighted.

5.1 Soliton interaction mechanisms

The formation of soliton groups can be affected by various intracavity pulse interaction mechanisms. The dominance of one or other interaction mechanism, being dependent

on laser configuration, determines the formation and the dynamics of the bounded states. The following mechanisms were investigated in the fiber laser cavity:

1. Gain depletion and recovery. This mechanism is based on the interaction of the pulses with the transient depletion and recovery dynamics of the gain medium. Thus, the solitons effectively repulse each other, due to a group-velocity drift caused by time-dependent amplifying medium depletion acting in conjunction with the gain recovery [140].

2. Acoustic effect and electrostriction. The pulse circulating in the cavity might interact with the fiber material and create an acoustic wave, due to the large transverse electric field gradient (electrostriction). It induces a small frequency shift resulting in a temporal shift of pulses relative to one another. Since the lifetime of acoustic waves in an optical fiber is of the order of 100 ns, it gives rise to long-range interaction, that can either trap pulses in bunch or lead to regularly spaced pulse sequences [141, 142].

3. Direct soliton-soliton interaction. This type of interaction occurs when soliton profiles are overlapped. The optical pulse tails are phase-sensitive, and depending on the phase difference they can attract or repel each other. A repulsive force appears when the pulse phase difference is a multiple of $\pi/2$, while attraction occurs when they are in phase. The solitons formed under direct soliton interaction have a very strong binding energy [38, 100].

4. Soliton and dispersive wave interaction. This is related to long-range soliton interaction. Propagating along the cavity, solitons suffer periodical perturbations, resulting in radiation of resonant dispersive waves. This interaction is phase-independent and causes random, irregular relative soliton movement [38, 143–145].

5. Soliton interaction caused by existence of unstable CW components (or global interaction). It is the interaction with the largest interaction range but the weakest interaction strength among the types listed above. The stable CW component contributes to the cw noise background and causes a central frequency shift in

each soliton. The overall relative soliton velocity will not change unless the cw component becomes unstable. In this case each soliton will experience different perturbations and acquire a different central frequency shift [38, 146].

5.2 Soliton group states

Bound solitons

Bound solitons are stable and tight packets of solitons, characterized by a fixed, discrete pulse separation independent of propagation. In relation to interaction mechanisms and binding energy, bound solitons can be classified into two categories. *Tightly bound solitons* are formed due to direct soliton interaction. They are characterized by strong binding energy and a pulse separation less than 5 times of the pulse width. *Loosely bound solitons* are separated by more than 10 times of pulse width. This type of soliton group is affected by a combination of direct and dispersive wave soliton interactions. Since the pulse separation in loosely bound solitons is relatively high, the binding energy become weaker, and long-range interactions start to play a dominant role in their formation [147–152]. The pulse separation within the group is the result of a combination of laser parameters, for example, the net cavity dispersion and the relaxation dynamics of the SESAM.

Optical spectra of bound solitons exhibits interference pattern, indicating that the different solitons have a fixed phase relationship. The period of spectral modulation corresponds to the pulse separation. So far, bound solitons with phase differences of π, 0, $\pm\pi/2$ have been demonstrated [153–156]. In most cases the formation of bound solitons was considered in fiber laser operated in the net anomalous cavity dispersion regime. Even though the bound pulses tend to become out-of-phase in the normal dispersion regime, the presence of a proper attractor allowed them to be achieved in this regime too [157–160].

Bunch of solitons

A bunch of solitons is called a tightly bounded solitons packet, where the solitons continuously oscillate within the bunch width. The bunch of solitons has been observed in fiber laser mode-locked by saturable absorber mirrors [P3, P4, P6, P7], [48]. Since

the SESAM is characterized in the general case by bi-exponential relaxation dynamics, the fast component is responsible for pulse formation, while the slow one works as an attractive force pushing the pulses close together, and causing the group formation with closely spaced pulses. When the temporal length of the group is below the decay time of the absorber, the joint action of the pulses forming the group provides more complete saturation of the absorption, and thus the pulses suffer lower losses compared to the regime with the absorber saturated by individual pulses. Thus, the absorber strongly enhances the pulse interaction by keeping them in a compact group with a short interpulse interval. From the other side the repulsive force induced by direct soliton-soliton interaction moves the pulses away from each other. The joint action of the contraction force induced by the saturable absorber, and the repulsive force due to soliton-soliton interaction results in the soliton oscillation within the bunch. The bunch of solitons propagates as unit along the cavity with the fundamental repetition rate.

The dynamic properties of bunch of solitons lead to a reduced spectral bandwidth, suppressed large-width soliton sidebands and a noticeable pedestal in the autocorrelation. The large timing jitter of the pulses results in large deviations of the carrier frequency, which deteriorates the coherence of the soliton perturbation inside the cavity, providing a larger width of soliton sidebands. This was confirmed by observation of the correlation between the temporal width of the sidebands and the spacing between the pulses for the multiple-pulse regime [P6]. The soliton interaction is too rapid to be resolved by the autocorrelator and is therefore manifested as an autocorrelation trace with a large pedestal.

The irregular motion of the solitons leads to random phase variations. By applying the loss modulation at a high harmonic of the cavity, which provided efficient control of the relative phases of the solitons, it was possible to switch the operation mode from bunch of solitons to bound solitons. This fact discloses the similar nature of bound solitons and bunch of solitons states [P6].

Soliton rains

Soliton rains are another example of dissipative soliton dynamics. They are named in analogy with the water cycle in nature. The appearance of this type of soliton cluster in the cavity is determined by the interaction of three components: bunch of several tens

of bounded jittering solitons (condensed soliton phase), a group of drifting pulses, and noisy cw background [96, 100, 161, 162]. The condensed phase emits a large amount of radiation, which in combination with preexisting cw modes produces a noisy, inhomogeneous background. The further amplification of the background fluctuations leads to creation of new solitons, which drift back to the condensed phase. The size of the condensed phase remains constant on average, therefore the arrival of new solitons causes dissipation of a similar number of solitons through collective rearrangements inside the condensed phase. The dissipation in turn can produce additional radiation and dispersive waves that contribute to the background [96, 161]. The soliton rains cluster is characterized by chirped allocation of the pulses inside it. This fact might be related to three possible mechanisms. These mechanisms have different origins, but all of them can work as repulsive force pushing the solitons away from each other. Among them are: gain relaxation dynamics (gain depletion), interaction of solitons with a dispersive wave, and the electrostriction effect. Soliton rains were discovered in anomalous dispersion fiber laser, but quite recently this type of dissipative soliton dynamics was demonstrated in the net normal dispersion regime [163].

5.3 Impact of laser parameters on dissipative soliton dynamics

As has been shown, various parameters or their combination are responsible for the formation of multisoliton complexes. In particular, the impact of the relaxation dynamics of the saturable absorber, the value of the net cavity dispersion, nonlinearity, the sign of gain dispersion and the gain dynamics has been demonstrated. It should be noted that in all cases described below the mode-locked fiber laser emitted vector solitons.

5.3.1 *Relaxation dynamics of the saturable absorber*

As was mentioned earlier, the bi-exponential recovery dynamics of the saturable absorber enhance the soliton interaction. The slow recovery time induces the formation of an attractive force, which in association with the repulsive force formed due to the

direct soliton interaction, leads to a continuous relative motion of the pulses within the bunch. The joint action of two counteractive forces causes the phase jittering of the pulses, which results in greatly reduced and broadened Kelly sidebands of the spectrum and a pedestal in the autocorrelation trace. These features describe the non-stationary regime so-called bunching.

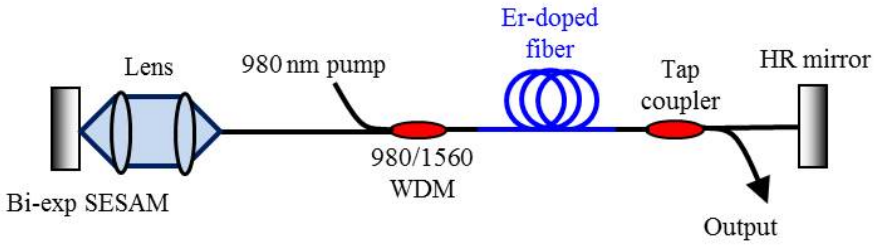

Figure 5.1: *Soliton erbium-doped fiber laser setup.*

The investigation of the effect of the saturable absorber on the pulse dynamics was performed in Er-doped fiber laser, whose experimental setup is shown in Fig. 5.1. The laser details can be found in [P3]. The examination was based on comparison of the laser performance when it was mode-locked by either one bi-exponential SESAM, or two separate SESAMs with fast and slow recovery dynamics representing a combined bitemporal fast-and-slow response. Otherwise the laser cavity remained unchanged.

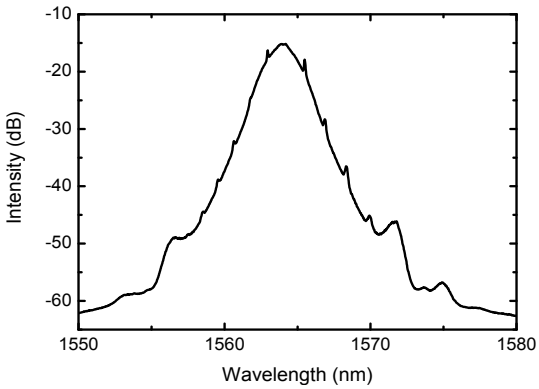

(a)

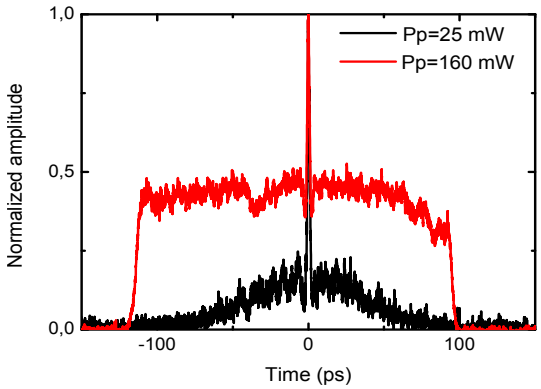

(b)

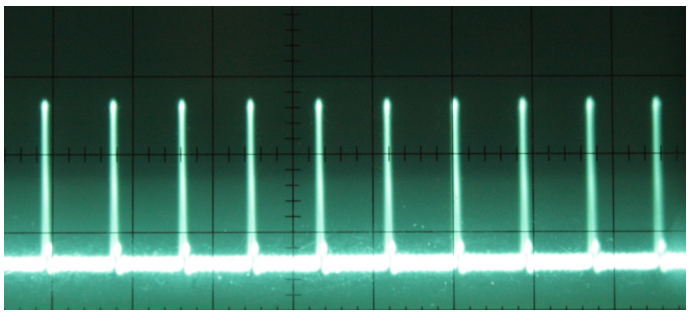

(c)

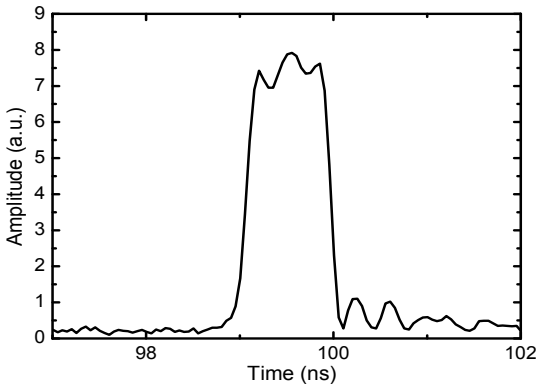

(d)

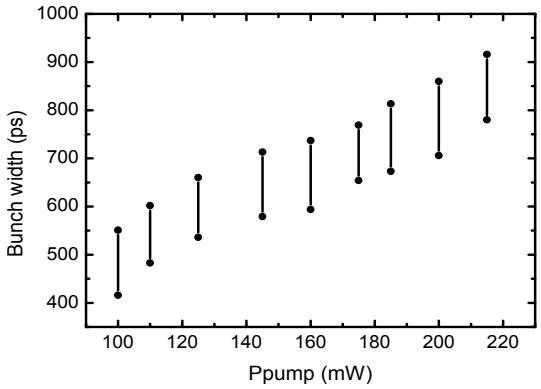

(e)

Figure 5.2: Output parameters of Er-doped fiber laser mode-locked by SESAM with bi-exponential response. (a) optical spectrum; (b) autocorrelation traces at different pump powers; (c) oscilloscope picture of the pulse train; (d) the oscilloscope picture of a generated pulse bunch observed with 9 GHz detection system; (e) the bunch duration versus pump power. Dots limit the upper and lower values of bunch width variation with time.

The laser output spectrum and autocorrelation with the SESAM characterized by a bi-temporal response are shown in Fig. 5.2a,b. The oscilloscope picture of the pulse train disclosed a "single" pulse observed in Fig. 5.2c, which is in fact a bunch of closely spaced pulses (Fig. 5.2d). The bunch amplitude does not depend on output power, confirming the soliton nature of the pulses comprised in the bunch. The temporal length of the bunch increased with output power, as shown in Fig. 5.2e. In addition, the bunch width was "breathing" continuously, which confirmed the fact that the pulses oscillate within the bunch. Similar laser behavior was observed with a combination of two SESAMs with dominant fast and slow recovery components (or a combination of CNT as fast absorber and a slow SESAM). The output laser characteristics in this case are presented in Fig. 5.3. The spectrum and autocorrelation possess the same attributes as with the bi-temporal SESAM, confirming the dominant role of saturable absorber relaxation dynamics in bunch formation.

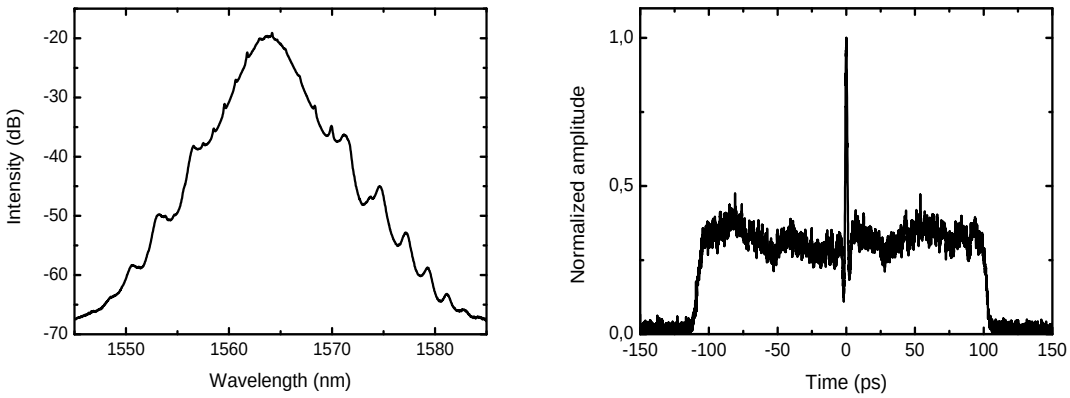

(a) (b)

Figure 5.3: *(a) Laser spectrum and (b) autocorrelation trace with separate slow and fast SESAMs in the cavity.*

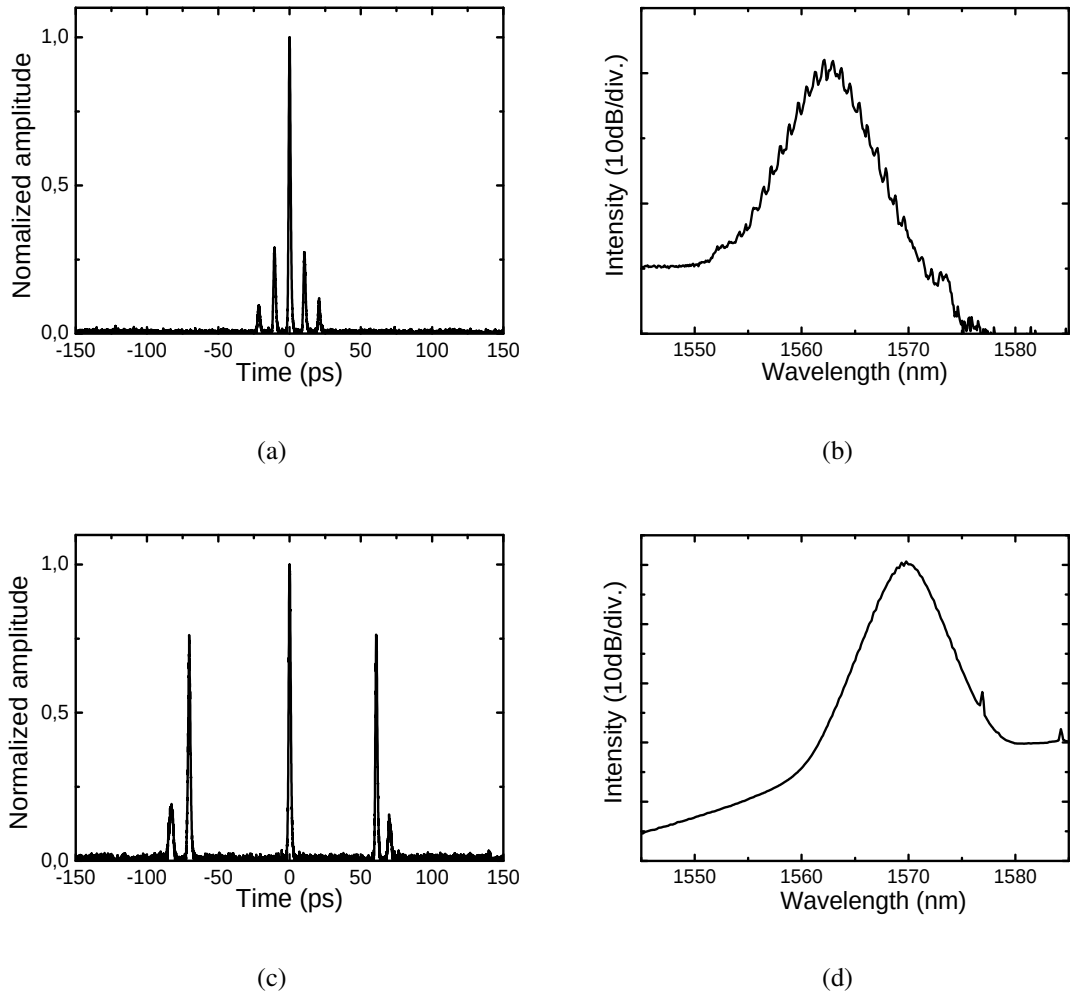

Figure 5.4: *Bound soliton group autocorrelations and corresponding spectra for SESAMs with a recovery time of saturable absorption of (a) and (b) 1 ps, (c) and (d) 100 ps.*

A notable feature was demonstrated by bi-temporal SESAM in the case of bound solitons mode-locked fiber laser. The laser setup was similar to the one shown in Fig. 5.1. It was found that the separation of bound solitons increases with an increase in the recovery time of the saturable absorber, as seen in Fig. 5.4, since a slower recovery time provides a larger time window for the group [P5].

The PbS QDs saturable absorber is also characterized by bi-temporal recovery dynamics and therefore has the same effect on pulse dynamics in Tm-Ho-doped fiber laser as the bi-exponential SESAM in the Er-doped fiber laser. The details of the experiments and laser output parameters can be found in [P4].

The bunch of solitons state can be transformed into the bound soliton state by inserting amplitude modulator in the cavity [P6]. Amplitude modulator causes the loss modulation at high harmonic of cavity frequency, thereby synchronizes the pulses and provides the selectivity to separate and stabilize the temporal position of solitons within the group.

The balance of the fast and slow time constants and their relative contribution to the nonlinear response were shown to be a valuable instrument in laser dynamics control. It was clearly observed that a adding a slow recovery component to the absorption allows the soliton interaction to be changed radically.

5.3.2 *Net cavity dispersion*

In order to investigate the impact of net cavity dispersion on pulse dynamics, a mode-locked Er-doped fiber laser with a grating pair as dispersion compensator was used (Fig.5.5). The essential feature of this setup is the possibility for nonlinearity-free dispersion measurement. The laser was mode-locked by a bi-exponential SESAM and operated in the stable bound soliton regime.

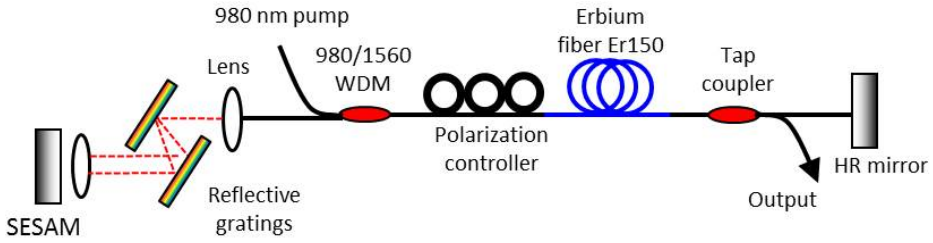

Figure 5.5: *Soliton erbium fiber laser setup with 600 grooves/mm grating pair dispersion compensator.*

Fig. 5.6 shows the evolution of the laser output parameters with the net cavity dispersion, which demonstrates that the character of the laser operation did not change with an increase of the cavity dispersion from 0.37 to 0.75 ps/nm. Stationary bound soliton pairs have been observed for the entire ranges of available pump power and dispersion, while the soliton separation in a group increased with increasing dispersion. The bound soliton regime in this case was determined by the bi-exponential recovery dynamics of SESAM which refrain the pulses in the group. In the presence of only a fast mode-locker in the cavity (for example an AO frequency-shifter) even a slight increase of dispersion leads to pulse repulsion and the destruction of bound states, resulting in the establishment of a weakly-interacting soliton regime (or conservative solitons) in the cavity [164]. Therefore, the cavity dispersion plays the role of a repulsive force in soliton interactions.

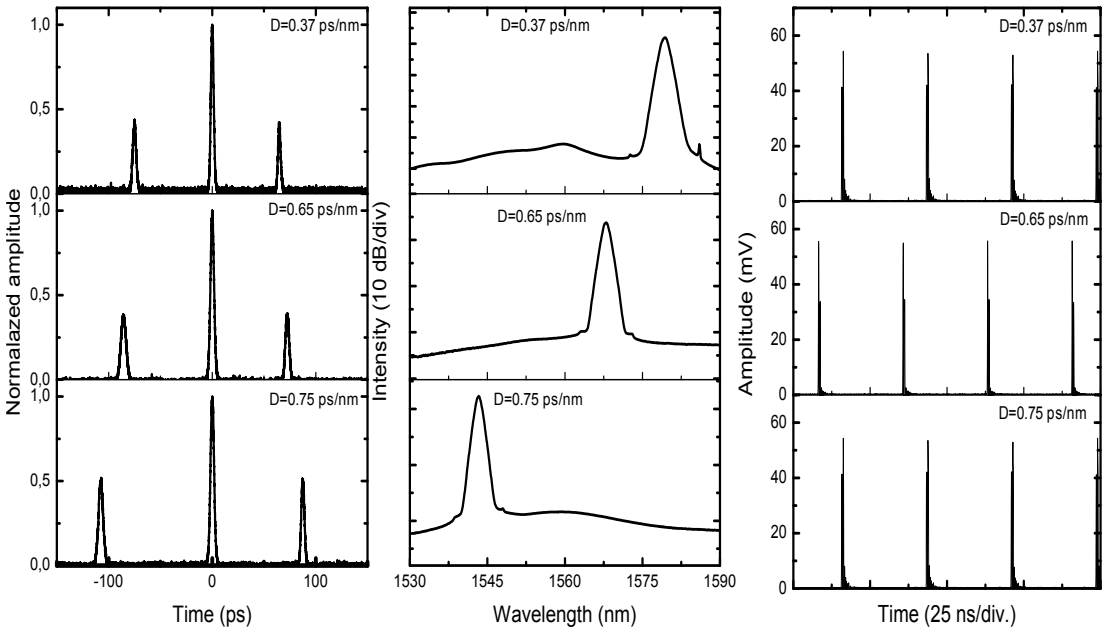

Figure 5.6: *(a) Pulse autocorrelations, (b) pulse spectra, and (c) oscilloscope waveforms of the pulse train for net anomalous cavity dispersion of D=0.37, 0.65, and 0.75 ps/nm corresponding to 600/mm grating pair separation of 7, 12.3, and 13.5 cm.*

5.3.3 *Nonlinearity*

Nonlinearity in a cavity leads to a nonlinear phase shift accumulation, which increases with pulse energy and eventually cannot be controlled by adjusting the dispersion. This effect causes pulse distortion and break-up, resulting in a multiple pulse regime. The presence of a long-range soliton interaction mediated by a dispersive wave, may cause irregular soliton movements, while the stability of the relative separation between solitons increases with the spacing [38]. Therefore with an increase in the number of pulses and a corresponding decrease in the average soliton spacing, the bound state of solitons collapses, and bunch of pulses with random soliton oscillations sets in.

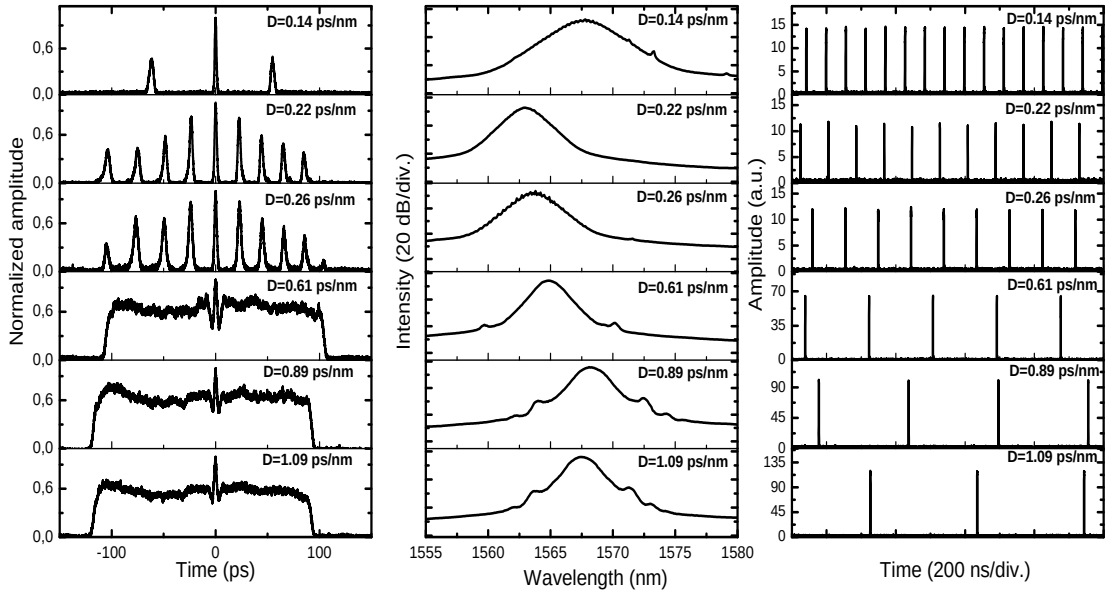

(a) (b) (c)

Figure 5.7: *Multiple pulse regime evolution with net cavity dispersion varied by length of compensating fiber. (a) Pulse autocorrelations, (b) pulse spectra and (c) oscilloscope pulse trains.*

The experimental demonstration of this statement was performed in Er-doped fiber laser with a bi-temporal SESAM. Initially, the laser operated in bound soliton regimes. By adding from 5.5 to 30 m of the passive compensating fiber the cavity dispersion was tuned in the range of 0.15 - 1.1 ps/nm. Fig. 5.7 shows that by increasing the cavity

dispersion, the type of the soliton group can be changed from stationary bound state to bunch. At low values of cavity dispersion, $D \leq 0.29$ ps/nm, the laser operated with bound solitons for the whole range of available pump power, as seen from the autocorrelation plotted in Fig. 5.7a. With increasing dispersion value, the solitons grouped together and circulated in the cavity as a unified bunch with continuous irregular pulse motion, which was reflected in the laser output characteristics, which revealed all the attributes of the bunch of solitons regime. Though the increase of anomalous dispersion apparently promotes soliton bunch formation through enforced soliton-soliton interaction, it should be noted that the dispersion offset performed by changing the length of the fiber unavoidably changes the nonlinearity of the cavity, which also affects the soliton interaction. However, as it was shown earlier, the dispersion works as a repulsive force in soliton interaction, thereby transferring the responsibility for bunch formation to nonlinearity.

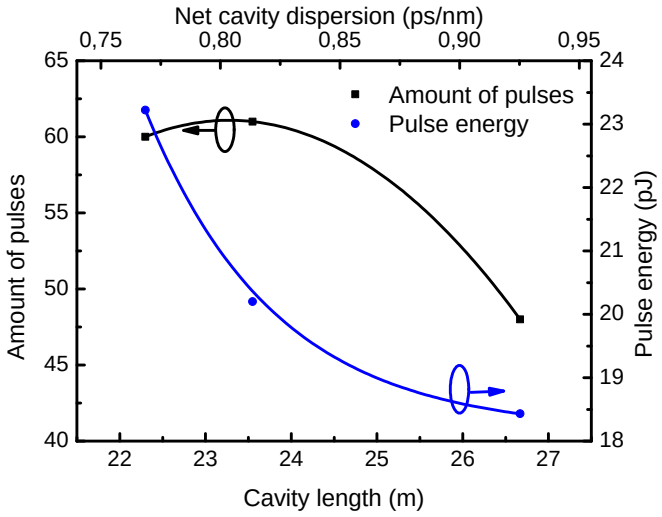

Figure 5.8: *Soliton energy threshold of transition to bunch formation depending on length/dispersion of the compensating fiber.*

To further validate the impact of nonlinearity, the critical number of pulses corresponding to the transition from bound state to soliton bunching was measured (Fig. 5.8). The typical scenario of soliton dynamics consists of steady bound soliton formation at low pump power, while above the critical pumping level, dependent on the cavity dispersion, the bunches of solitons develop. The soliton energy corresponding to the onset

of the transition from bound state to bunched solitons was varied by changing the length of fiber segment in the cavity. The pumping threshold for bunch formation gradually decreased with the cavity dispersion, starting from a dispersion value of 0.27 ps/nm. At a cavity dispersion of 0.89 ps/nm the soliton bunch regime was observed for the entire range of pump power. Thus, if the pulse energy or/and number of pulses circulating within the cavity become too large, the bound states of solitons become unstable, eventually resulting in the transition to bunch formation with chaotic motion of solitons within the group. The evolution of the bound solitons toward the bunch regime was thus ascribed to enforced soliton-soliton interaction [P3].

5.3.4 *Gain medium dispersion*

The effect of gain medium dispersion has been experimentally examined in two similar versions of Er-doped fiber laser, one with anomalous and the other with normal dispersion active fiber. The laser was mode-locked by a bi-exponential SESAM in a setup similar to that shown in Fig. 5.1. The net cavity dispersion was kept unchanged after switching the sign of the gain medium dispersion. The laser behavior with Er-doped active fiber providing anomalous and normal dispersion is presented in Fig. 5.9 and Fig. 5.10, respectively. The results reveal that the cavity with normal dispersion gain medium supports stable bound solitons, while the anomalous gain dispersion leads to soliton bunch formation with irregular pulse motion. Thus, the switching of the gain dispersion from normal to anomalous changes the soliton dynamics radically [P5].

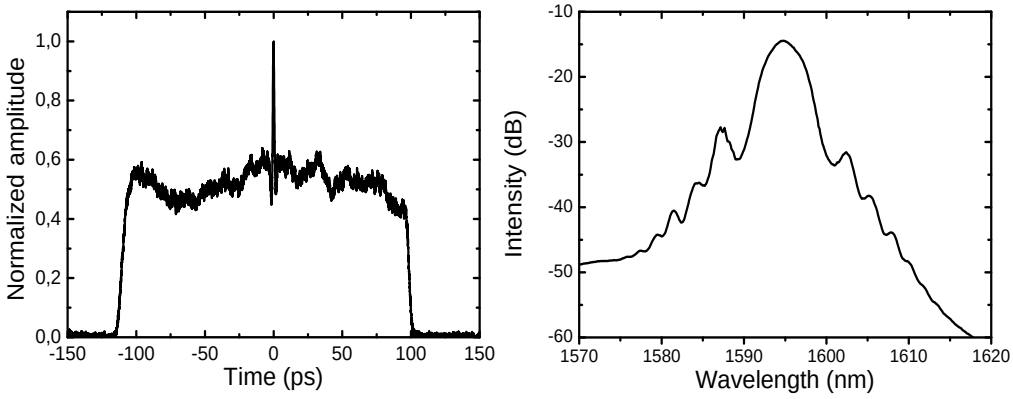

(a) (b)

Figure 5.9: *Output laser characteristics with anomalous dispersion of Er-doped fiber: (a) auto-correlation trace and (b) corresponding spectrum.*

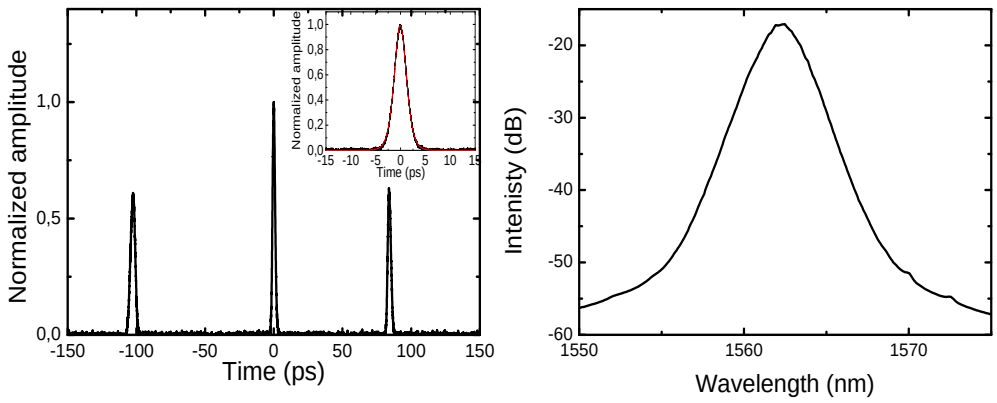

(a) (b)

Figure 5.10: *Output laser characteristics with normal dispersion of Er-doped fiber: (a) auto-correlation trace (Inset: central pulse and its fitting) and (b) corresponding spectrum.*

5.3.5 *Gain saturation*

The impact of gain saturable absorption on soliton dynamics was disclosed in Bi-doped fiber laser operated at 1460 nm. The particular peculiarity of Bi-doped fiber compared to rare-earth doped fibers is that it is characterized by bi-exponential, but relatively fast, decay [165, 166]. The fast component typically varies from hundreds of nanoseconds to a few microseconds depending on the fiber core composition, while the slow recovery factor is around 700 μs. Additionally, Bi-doped fiber lasers can exhibit reduced efficiency owing to a significant amount of unbleachable absorption at the lasing wavelength. The nature of this absorption has not been determined yet. However, it was observed that absorption can be partially saturated, but a certain level of unbleachable losses is always present in the fiber.

The fiber laser setup has similar to that shown in Fig. 5.1. The laser cavity comprised SESAM to ensure mode-locked operation. The SESAM was characterized by bi-temporal dynamics with a fast component of 2 ps and a slow component of 17 ps. The Bi-doped fiber laser generated multiple pulses with a typical spectrum and autocorrelation presented in Fig. 5.11 (a). No cw component was exhibited in the cavity. Due to the high absorption of Bi-doped fiber at the signal wavelength and a relatively fast gain recovery, comparable to the cavity round trip time, the time window for soliton group was set by the number of pulses within the cavity, the gain recovery and the saturation energy. The Fig. 5.11 (c) demonstrates the multiple soliton group evolution with pump power. This observation indicates that the soliton group with a temporal length comparable or less than the bismuth gain recovery effectively sees the reduced cavity loss. The group consists of stationary solitons with a fixed position, without any tendency to timing disordering or large jitter. With increasing pump power the number of pulses and the group width gradually increase. The size of the group approaches the cavity round trip period and eventually occupies the whole cavity. Since the slowest component in the SESAM recombination decay (17 ps) was much shorter than the pulse separation of a few nanoseconds, the SESAM did not assist in pulse group formation. The soliton group was composed of chirped trains of pulses, characteristic of soliton rains (Fig. 5.11 (b)) [167].

Thus, the gain saturation and bleachable absorption of bismuth fiber induced the

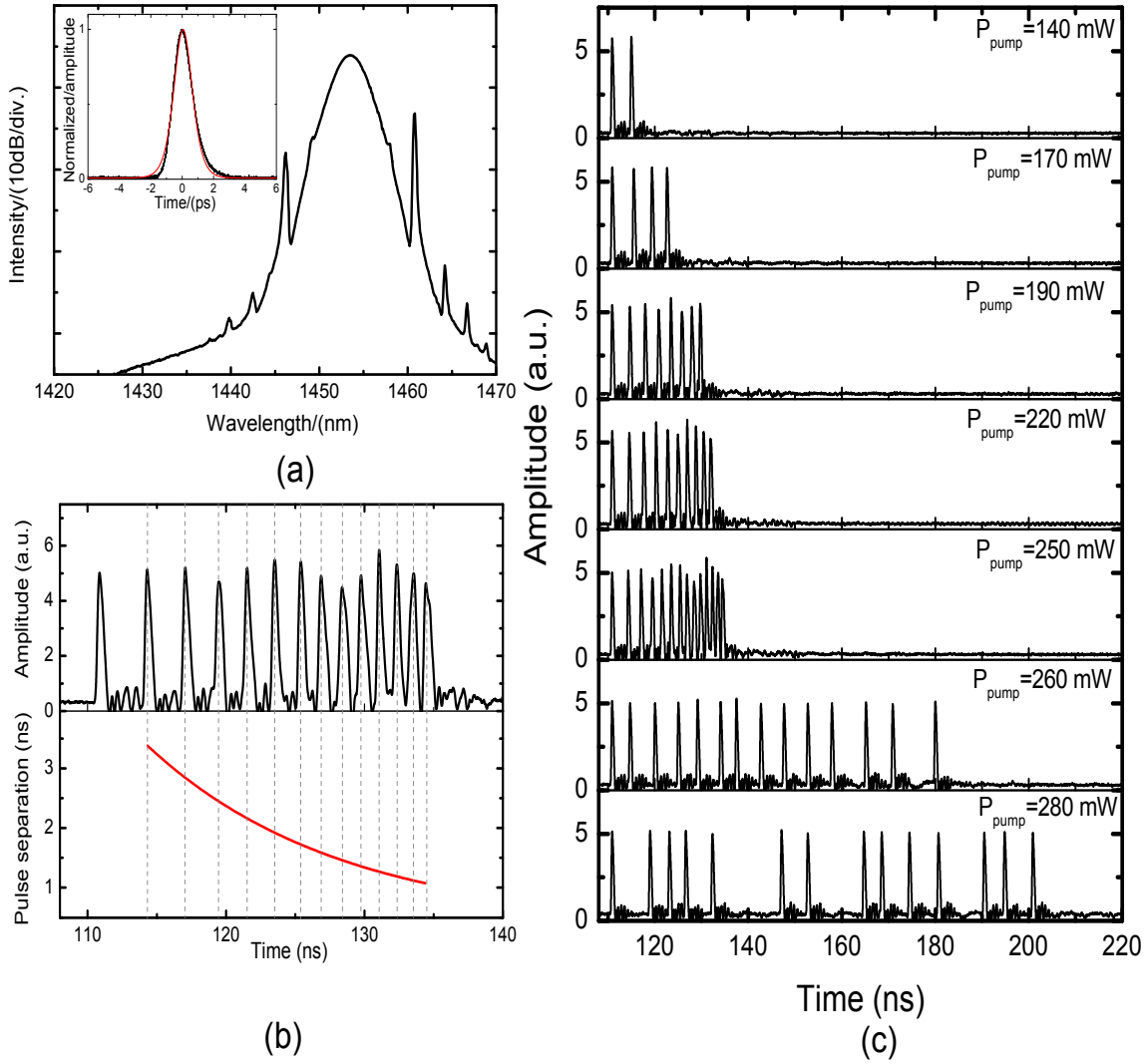

Figure 5.11: *(a) Typical output spectrum and autocorrelation with sech^2−fitting (inset); (b) Chirpy pulse train and pulse separation inside the bunch ($Pp = 250mW$); (c) Oscilloscope picture of soliton group evolution with pump power.*

distinctive features of soliton interaction and grouping, and contributed to soliton organization in stationary groups/clusters.

Chapter 6

Conclusions

The thesis presents detailed experimental study of the generation, interaction and group formation of solitons in fiber lasers. Special attention was paid to dynamics of dissipative solitons in lasers with various dispersion maps. The research objectives include the examination of energy transitions in Bi-doped fibers, the generation of dissipative dispersion-managed solitons in the normal dispersion regime and the role of laser parameters in the formation of solitons clusters, such as bound solitons, bunch of solitons and soliton rains. The major achievements of the thesis are as follows:

- The energy transition type in Bi-doped fibers operating at the 1.18 and 1.3 μm spectral bands was identified using spectrally resolved transient relaxation oscillations. The study included the investigation at room and liquid-nitrogen temperatures. The 1.18 μm wavelength band was found to be a three-level system at room temperature while it switched to a four-level system at liquid-nitrogen temperature. The four-level energy transition was observed at 1.32 μm at room temperature.

- Dissipative dispersion-managed solitons were generated in a Tm-Ho-doped fiber laser operated in the normal dispersion regime. The laser demonstrated an increase of output power compared with a laser operated in the anomalous dispersion regime.

- A detailed investigation of pulse dynamics in mode-locked fiber laser revealed the impact of various laser parameters on pulse interaction and soliton group forma-

tion:

1. The slow recovery component of the saturable absorber works as a soliton attractor in the cavity. It pushes the pulses close to each other, which in combination with a strong repulsive force due to the direct soliton-soliton interaction leads to a continuous oscillation of the solitons within the bunch.
2. Excessive nonlinearity and dispersion tend to destroy stable bound solitons. Dispersion pushes the pulse apart, while nonlinearity leads to bunch formation with chaotic motion of the pulses within the group.
3. Switching of the gain dispersion from normal to anomalous changes the soliton dynamic radically. A cavity with a normal dispersion gain medium supports stable bound solitons, while anomalous gain dispersion leads to soliton bunch formation with irregular pulse motion.
4. The role of gain recovery dynamics on pulse grouping was experimentally studied in Bi-doped fiber laser operating at 1460 nm. It was discovered that, when the gain saturation relaxation time is comparable with the cavity round trip time, the formation of stationary soliton groups, with widths occuping the whole cavity length, occurs .

Bibliography

[1] D. E. McCumber, "Einstein relations connecting broadband emission and absorption spectra," *Physical review A*, vol. 136, pp. A954–A957, 1964.

[2] S. A. Payne, L. L. Chase, L. K. Smith, W. L. Kway, and W. Krupke, "Infrared cross-section of $Er^{(3+)}$ doped silica fibers," *IEEE Journal of Quantum Electronics*, vol. 28, pp. 2619–2630, 1992.

[3] O. G. Okhotnikov, V. V. Kuzmin, and J. R. Salcedo, "General intracavity method for laser transition characterization by relaxation oscillations spectral analysis," *IEEE Photonics Technology Letters*, vol. 6, pp. 362–364, 1994.

[4] O. G. Okhotnikov and J. R. Salcedo, "Laser transition characterization by spectral and thermal dependences of the transient oscillations," *Optics Letters*, vol. 19, pp. 1445–1447, 1994.

[5] ——, "Stable relaxation-oscillation $Er^{(3+)}$-doped fiber laser," *IEEE Photonics Technology Letters*, vol. 6, pp. 369–371, 1994.

[6] O. Svelto, *Principles of Lasers*, 5th ed. London: Springer, 2010.

[7] L. Orsila and O. G. Okhotnikov, "Three- and four-level transition dynamics in Yb-fiber laser," *Optics Express*, vol. 13, pp. 3218–3223, 2005.

[8] L. Orsila, S. Kivistö, R. Herda, and O. G. Okhotnikov, "Spectroscopy of relaxation dynamics in Tm-Ho-fiber lasers," in *Conference digest of European Conference on Lasers and Electro-Optics*, 2007, pp. CE–24–TUE.

[9] M. E. Fermann, A. Galvanauskas, and G. Sucha, *Ultrafast lasers: Technology and Applications*, 1st ed. Switzerland: Marcel Dekker, Inc., 2003.

[10] O. G. Okhotnikov, L. Gomes, N. Xiang, T. Jouhti, and A. B. Grudinin, "Mode-locked ytterbium fiber laser tunable in the 980 - 1070 nm spectral range," *Optics Letters*, vol. 28, pp. 1522–1524, 2003.

[11] O. Shtyrina, M. Fedoruk, S. Turitsyn, R. Herda, and O. G. Okhotnikov, "Evolution and stability of pulse regimes in SESAM-mode-locked femtosecond fiber lasers," *Journal of Optical Society America B*, vol. 26, pp. 346–352, 2009.

[12] O. G. Okhotnikov, T. Jouhti, J. Konttinen, S. Karirinne, and M. Pessa, "1.5-μm monolithic GaInNAs semiconductor saturable-absorber modelocking of an erbium fiber laser," *Optics Letters*, vol. 28, pp. 364–366, 2003.

[13] X. Tian, M. Tang, P. P. Shum, Y. Gong, C. Lin, S. Fu, and T. Zhang, "High-energy laser pulse with a submwgahertz repetition rate from a passively mode-locked fiber laser," *34*, vol. 34, pp. 1432–1434, 2009.

[14] H. Zhang, D. Y. Tang, X. Wu, and L. M. Zhao, "Multi-wavelength dissipative soliton operation of an erbium-doped fiber laser," *Optics Express*, vol. 17, pp. 12 692–12 697, 2009.

[15] R. Herda and O. G. Okhotnikov, "Dispersion compensation-free fiber laser mode-locked and stabilized by high-contrast saturable absorber mirror," *IEEE Journal of Quantum Electronics*, vol. 40, pp. 893–899, 2004.

[16] C. Lecaplain, C. Chédot, A. Hideur, B. Ortaç, and J. Limpert, "High-power all-normal dispersion femtosecond pulse generation from a Yb-doped large-mode-area microsrtructure fiber laser," *Optics Letters*, vol. 32, pp. 2738–2740, 2007.

[17] J. M. Auxier, A. Schülzgen, M. M. Morrell, B. R. West, S. Honkanen, S. Sen, N. F. Borrelli, and N. Peyghambarian, "Quantum dots for fiber sources," in *Fiber Laser II: Technology, Systems, and Appllications*, 2005.

[18] V. G. Savitski, N. N. Posnov, P. V. Prokoshin, A. M. Malyarevich, K. V. Y. M. I. Demchuk, and A. A. Lipovskii, "PbS-doped phosphate glasses saturable absorbers for 1.3-μm neodymium lasers," *Applied Physics B*, vol. 75, pp. 841–846, 2002.

[19] E. U. Rafailov, M. A. Cataluna, and W. Sibbett, "Mode-locked quantum-dot lasers," *Nature Photonics*, vol. 1, pp. 395–401, 2007.

[20] P. T. Guerreiro, S. Ten, N. F. Borrelli, J. B. G. E. Jabbour, and N. Peyghambarian, "PbS quantum-dot doped glasses as saturable absorbers for mode-locking of a Cr:forsterite laser," *Applied Physics Letters*, vol. 71, pp. 1595–1597, 1997.

[21] A. M. Malyarevich, V. G. Savitski, P. V. Prokoshin, N. N. Posnov, K. V. Yumashev, E. Raaben, and A. A. Zhilin, "Glass doped with PbS quantum dots as a saturable absorber for 1 μ m neodymium lasers," *Journal of Optical Society America B*, vol. 19, pp. 28–32, 2002.

[22] A. M. Malyarevich, V. G. Savitski, M. G. Gaponenko, K. V. Yumashev, A. A. Lagatsky, W. Sibbett, A. A. Lipovskii, H. Raaben, and A. A. Zhilin, "PbS-doped glass satrable absorbers for mode-locked and Q-switched near IR lasers," in *Advanced Solid-State Photonics*, 2005.

[23] Z. Sun, T. Hasan, F. Wang, A. G. Rozhin, I. H. White, and A. C. Ferrari, "Ultrafast stretched-pulse fiber laser mode-locked by carbon nanotubes," *Nano Research*, vol. 3, pp. 404–411, 2010.

[24] F. Wang, A. G. Rozhin, V. Scardaci, Z. Sun, F. Hennrich, I. H. White, W. I. Milne, and A. C. Ferrari, "Wideband-tunable nanotube mode-locked fibre laser," *Nature Nanotechnology*, vol. 3, pp. 738–742, 2008.

[25] S. Y. Set, H. Yaguchi, Y. Tanaka, and M. Jablonski, "Laser mode locking using a saturable absorber incorporating carbon nanotubes," *IEEE Journal of Lightwave Technology*, vol. 22, pp. 51–56, 2004.

[26] S. Yamashita, Y. Inoue, S. Maruyama, Y. Murakami, H. Yaguchi, M. Jablonski, and S. Y. Set, "Saturable absorbers incorporating carbon nanotubes directly

synthesized onto substrates and fibers and their application to mode-locked fiber lasers," *Optics Letters*, vol. 29, pp. 1581–1583, 2004.

[27] M. A. Solodyankin, E. D. Obraztsova, A. S. Lobach, A. I. Chernov, A. V. Tausenev, V. I. Konov, and E. M. Dianov, "Mode-locked 1.93 μm thulium fiber laser with a carbon nanotube absorber," *Optics Letters*, vol. 33, pp. 1336–1338, 2008.

[28] A. V. Tausenev, E. D. Obraztsova, A. Lobach, A. I. Chernov, V. I. Konov, P. G. Kryukov, A. Konyashchenko, and E. M. Dianov, "177 fs erbium-doped fiber laser mode locked with a cellulose polymer film containing single-wall carbon nanotubes," *Applied Physics Letters*, vol. 92, p. 171113, 2008.

[29] Z. Sun, A. G. Rozhin, F. Wang, T. Hasan, D. Popa, W. O'Neil, and A. C. Ferraril, "A compact, high power, ultrafast laser mode-locked by carbon nanotubes," *Applied Physics Letters*, vol. 95, p. 253102, 2009.

[30] H. Zhang, D. Y. Tang, L. M. Zhao, Q. L. Bao, and K. P. Loh, "Large energy mode-locking of an erbium-doped fiber laser with atomic layer graphene," *Optics Express*, vol. 17, pp. 17 630–17 635, 2009.

[31] H. Zhang, Q. Bao, D. Tang, L. Zhao, and K. Loh, "Large energy soliton erbium-doped fiber laser with a graphene-polymer composite mode-locker," *Applied Physics Letters*, vol. 95, p. 141103, 2009.

[32] H. Zhang, D. Y. Tang, L. M. Zhao, Q. L. Bao, K. P. Loh, B. Lin, and S. C. Tjin, "Compact graphene mode-locked wavelength-tunable erbium-doped fiber lasers: from all anomalous dispersion to all normal dispersion," *Laser Physics Letters*, vol. 7, pp. 591–596, 2010.

[33] D. Popa, Z. Sun, F. Torrisi, T. Hasan, F. Wang, and A. Ferrari, "Sub 200 fs pulse generation from a graphene mode-locked fiber laser," *Applied Physics Letters*, vol. 97, p. 203106, 2010.

[34] Z. Sun, T. Hasan, F. Torrisi, D. Popa, G. Privitera, F. Wang, F. Bonaccorso, D. M. Basko, and A. C. Ferrari, "Graphene mode-locked ultrafast laser," *ACS Nano*, vol. 4, pp. 803–810, 2010.

[35] M. . Zhang, E. J. R. Kelleher, F. Torrisi, Z. Sun, T. Hasan, D. Popa, F. Wang, A. C. Ferrari, S. P. Popov, and J. R. Taylor, "Tm-doped fiber laser mode-locked by graphene-polymer composite," *Optics Express*, vol. 20, pp. 25 077–25 084, 2012.

[36] Z.-B. Liu, X. He, and D. N. Wang, "Passively mode-locked fiber laser based on a hollow-core photonic crystal fiber filled with few-layered graphene oxide solution," *Optics Letters*, vol. 36, pp. 3024–3026, 2011.

[37] Y.-W. Song, S.-Y. Jang, W.-S. Han, and M.-K. Bae, "Graphene mode-lockers for fiber lasers functioned with evanescent field interaction," *Applied Physics Letters*, vol. 96, p. 051122, 2010.

[38] D. Y. Tang, B. Zhao, and L. M. Zhao, "Soliton interaction in a fiber ring laser," *Physical review E*, vol. 72, p. 016616, 2005.

[39] A. Chong, J. Buckley, W. Renninger, and F. Wise, "All-normal-dispersion femtosecond fiber laser," *Optics Express*, vol. 14, pp. 10 095–10 100, 2006.

[40] F. Ö. Ilday, J. R. Buckley, H. Lim, F. W. Wise, and W. G. Clark, "Generation of 50-fs, 5-nJ pulses at 1.03 μm from a wave-breaking-free fiber laser," *Optics Letters*, vol. 28, pp. 1365–1367, 2003.

[41] J. R. Buckley, S. W. Clark, and F. W. Wise, "Generation of ten-cycle pulses from and ytterbium fiber laser with cubic phase compensation," *Optics Letters*, vol. 31, pp. 1340–1342, 2006.

[42] M. Schultz, O. Prochnow, A. Ruehl, D. Wandt, D. Kracht, S. Ramachandran, and S. Ghalmi, "Sub-60-fs ytterbium-doped fiber laser with a fiber-based dispersion compensation," *Optics Letters*, vol. 32, pp. 2372–2374, 2007.

[43] O. Okhotnikov, A. Grudinin, and M. Pessa, "Ultra-fast fibre laser systems based on SESAM technology: new horizons and applications," *New Journal of Physics*, vol. 6, p. 177, 2004.

[44] R. Herda, "Semiconductor mirrors for ultrashort fiber technology," Ph.D. dissertation, Tampere University of Technology, 2006.

[45] A. A. Lagatsky, C. G. Lerburn, C. T. A. Brown, W. Sibbett, S. A. Zolotovskaya, and E. Rafailov, "Ultrashort-pulse lasers passively mode locked by quantum-dot-based saturable absorber," *Progress in Quantum Electronics*, vol. 34, pp. 1–45, 2010.

[46] U. Keller, k. J. Weingarten, F. X. Kartner, D. Kopf, B. Braun, I. D. Jung, R. Fluck, C. Honninger, N. Matuschek, and J. der Au, "Ultrashort-pulse lasers passively mode locked by quantum-dot-based saturable absorber," *IEEE Journal of Selected Topics in Quantum Electronics*, vol. 2, pp. 435–453, 1994.

[47] R. Paschotta and U. Keller, "Passive mode locking with slow saturable absorbers," *Applied Physics B*, vol. 73, pp. 653–662, 2001.

[48] L. M. Zhao, D. Y. Tang, H. Zhang, and X. Wu, "Bunch of restless vector solitons in a fiber laser with SESAM," *Optics Express*, vol. 17, pp. 8103–8108, 2009.

[49] S. Gupta, J. F. Whitaker, and G. A. Mourou, "Ultrafast carrier dynamics in III-V semiconductors grown by molecular-beam epitaxy at very low substrate temperatures," *IEEE Journal of Quantum Electronics*, vol. 28, pp. 2464–2472, 1992.

[50] S. Suomalainen, A. Vainionpaa, O. Tengvall, T. Hakulinen, S. Karirinne, M. Guina, O. G. Okhotnikov, T. G. Euser, and W. L. Vos, "Long-wavelength fast semiconductor saturable absorber mirrors using metamorphic growth on GaAs substrates," *Applied Physics Letters*, vol. 87, p. 121106, 2005.

[51] S. Suomalainen, M. Guina, T. Hakulinen, O. G. Okhotnikov, T. G. Euser, and S. Marcinkevicius, "1 μ m saturable absorber with recovery time reduced by lattice mismatch," *Applied Physics Letters*, vol. 89, p. 071112, 2006.

[52] M. Guina, P. Tuomisto, O. G. Okhotnikov, S. Marcinkeviciusc, K. Mizohatad, and J. Keinonen, "Semiconductor saturable absorbers with recovery time controlled through growth conditions," *Photonics West SPIE Proc.*, vol. 6451, p. 642113, 2007.

[53] M. J. Lederera, B. Luther-Davies, H. H.Tan, and C. Jagadish, "GaAs based anti-resonant Fabry-Perot saturable absorber fabricated by metal organic vapor phase epitaxy and ion implatation," *Applied Physics Letters*, vol. 70, pp. 3428–3430, 1997.

[54] E. L. Deplon, J. L. Oudar, N. Bounch, R. Raj, A. Shen, N. Stelmakh, and J. M. Lourtioz, "Utrafast excitonic saturable absorption in ion-implantted InGaAs/InAlAs multiple quantum wells," *Applied Physics Letters*, vol. 72, pp. 759–761, 1998.

[55] S. Kivistö, R. Gumenyuk, J. Puustinen, M. Guina, E. M. Dianov, and O. Okhotnikov, "Mode-locked Bi-doped all-fiber laser with chirped fiber Bragg grating," *IEEE Photonics Technology Letters*, vol. 21, pp. 599–601, 2009.

[56] E. by Q. Zhang, *Carbon nanotubes and their applications*. USA: Pan Stanford Publishing Pte, Ltd., 2012.

[57] E. Malic and A. Knorr, *Graphene and carbon nanotubes: ultrafast optics and relaxation dynamics*. Germany: WILEY-VCH, 2013.

[58] S. Kivistö, T. Hakulinen, A. Kaskela, B. Aichison, D. P. Brown, A. G. Nasibulin, E. I. Kauppinen, A. Härkönen, and O. Okhotnikov, "Carbon nanotubes films ultrafast broadband technology," *Optics Express*, vol. 17, pp. 2358–2363, 2009.

[59] J. H. Yim, W. B. Cho, S. Lee, Y. H. Ahn, K. Kim, H. Lim, G. Steinmeyer, V. Petrov, U. Griebner, and F. Rotermund, "Fabrication and characterization of ultrafast carbon nanotube saturable absorbers for solid-state laser mode-locking near 1 μm," *Applied Physics Letters*, vol. 93, p. 161106, 2008.

[60] K. K. Chow, S. Yamashita, and Y. W. Song, "A widely tunable wavelength converter based on nonlinear polarization rotation in a carbon-nanotube-deposited D-shaped fiber," *Optics Express*, vol. 17, pp. 7664–7669, 2009.

[61] I. H. Baek, S. Y. Choi, H. W. Lee, W. B. Cho, V. Petrov, A. Agnesti, V. Pasiskevicius, D. Yeom, K. Kim, and F. Rotermund, "Single-walled carbon nanotubes saturable absorber assisted high-power mode-locking of a Ti:sapphire laser," *Optics Express*, vol. 19, pp. 7833–7838, 2011.

[62] C. E. S. Castellani, E. J. R. Kelleher, D. Popa, T. Hasan, Z. Sun, A. Ferrari, S. V. Popov, and J. Taylor, "CW-pumped short pulsed 1.12 μm Raman laser using carbon nanotubes," *Laser Physics Letters*, vol. 10, p. 015101, 2013.

[63] S. Yamashita, Y. Inoue, S. Maruyama, Y. Murakami, H. Yaguchi, M. Jablonski, and S. Y. Set, "Saturable absorbers incorporating carbon nanotubes directly synthesized onto substrates and fibers and their application to mode-locked fiber lasers," *Optics Letters*, vol. 29, pp. 1581–1583, 2003.

[64] Y.-W. Song, S. Yamashita, C. S. Goh, and S. Y. Set, "Carbon nanotube mode lockers with enhanced nonlinearity via evanescent field interaction in D-shaped fibers," *Optics Letters*, vol. 32, pp. 148–150, 2007.

[65] S. Bakshi, J. Tercero, and A. Agarwal, "Synthesis and characterization of multiwalled carbon nanotube reinforced ultra high molecular weight polyethylene composite by electrostatic spraying technique," *Composites: Part A*, vol. 38, pp. 2493–2499, 2007.

[66] X. C. Lin, L. Zhang, Y. H. Tsang, Y. G. Wang, H. J. Yu, S. L. Yan, W. Sun, Y. Y. Yang, Z. Han, and W. Hou, "Multi-walled carbon nanotube as a saturable absorber for a passively mode-locked ND:YVO4 laser," *Laser Physics Letters*, vol. 10, p. 055805, 2013.

[67] Y. Inoue, S. Yamashita, S. Maruyama, Y. Murakami, H. Yaguchi, T. Kotake, and S. Y. Set, "Mode-locked fiber lasers using vertically aligned carbon nanotubes di-

rectly synthesized onto substrates," in *Optical Fiber Communication Conference*, 2005.

[68] J. C. Chiu, Y. F. Lan, C. M. Chang, X. Z. Chen, C. Y. Yeh, C. K. Lee, G. R. Lin, J. J. Lin, and W. H. Cheng, "Concentration effect of carbon nanotube based saturable absorber on stabilizing and shortening mode-locked pulse," *Optics Express*, vol. 18, pp. 3592–3600, 2010.

[69] J. C. Chiu, C. M. Chang, B. Z. Hsieh, S. C. Lin, C. Y. Yeh, G. R. Lin, C. K. Lee, J. J. Lin, and W. H. Cheng, "Pulse shortening mode-locked fiber laser by thickness and concentration product of carbon nanotube based saturable absorber," *Optics Express*, vol. 19, pp. 4036–4041, 2011.

[70] J. S. Lauret, C. Voisin, G. Cassabois, C. Delalande, P. Roussignol, O. Jost, and L. Capes, "Ultrafast carrier dynamics in single-wall carbon nanotubes," *Physical Review Letters*, vol. 90, p. 057404, 2003.

[71] A. Gambetta, G. Galzerano, A. G. Rozhin, A. C. Ferrari, R. Ramponi, P. Laporta, and M. Marangoni, "Sub-100 fs two-color pump probe spectroscopy of single wall carbon nanotubes with a 100 MHz Er-fiber laser system," *Optics Express*, vol. 16, pp. 11 727–11 734, 2008.

[72] E. N. Lalanne, A. M. Johnson, A. Lan, Z. Iqbal, and H. Grebel, "Femtosecond non-degenerate pump-probe measurements of single-wall carbon nanotubes (SWCNTs) within an ordered array of nanosize silica," in *Quantum Electronics and Laser Science*, 2003.

[73] J. S. Lauret, C. Voisin, G. Cassabois, C. Delalande, P. Roussignol, L. Capes, and O. Jost, "Ultrafast pump-probe measurements in single wall carbon nanotubes," *Physica E*, vol. 17, pp. 380–383, 2003.

[74] Z. Zhu, "Ultrafast pump probe spectroscopy of single-wall carbon nanotubes," Ph.D. dissertation, Vanderbilt University, 2008.

[75] A. A. Lipovskii, E. V. Kolobkova, A. Plkhovets, V. D. Petrikov, and F. Wise, "Synthesis of monodisperse PbS quantum dots in phosphate glass," *Physica E*, vol. 5, pp. 157–160, 2000.

[76] K. Wundke, S. Plötting, J. Auvier, A. Schülzgen, N. Peyghambarian, and N. F. Borrelli, "PbS quantum-dot-doped glasses for ultrashort-pulse generation," *Applied Physics Letters*, vol. 76, p. 10, 2000.

[77] I. Kang and F. W. Wise, "Electronic structure and optical properties of PbS and PbSe quantum dots," *Journal of Optical Society America B*, vol. 14, pp. 1632–1646, 1997.

[78] G. Tamulaitis, V. Guibinas, G. Kodis, A. Dementjev, and L. Valkunas.

[79] A. M. Malyarevich, I. A. Denisov, V. G. Savitsky, K. V. Yumashev, and A. A. Lipovskii, "Glass doped with PbS quantum dots for passive Q swiching of a 1.54-μ m laser," *Applied Optics*, vol. 39, pp. 4345–4347, 2000.

[80] A. M. Heidt, J. P. Burger, J.-N. Maran, and N. Traynor, "High power and high energy ultrashort pulse generation with a frequency shifted feedback fiber laser," *Optics Express*, vol. 15, pp. 15 892–15 897, 2007.

[81] L. Lefort, A. Albert, V. Couderc, and A. Barthélémy, "Highly stable 68-fs pulse generation from a stretched-pulse $Yb^{(3+)}$-doped fiber laser with frequency shifted feedback," *IEEE Photonics Technology Letters*, vol. 14, pp. 1674–1676, 2002.

[82] J. M. Sousa and O. Okhotnikov, "Short pulse generation and control in Er-doped frequency-shifted-feedback fibre lasers," *Optics Communications*, vol. 183, pp. 227–241, 2000.

[83] M. P. Nikodem, E. Kluźniak, and K. Abramski, "Wavelength tunability and pulse duration control in frequency shifted feedback Er-doped fiber lasers," *Optics Express*, vol. 17, pp. 3299–3304, 2009.

[84] M. Y. Jeon, H. K. Lee, J. T. Ahn, D. S. Lim, and S. B. Kang, "Wideband wavelength tunable mode-locked fibre laser over 1557-1607 nm," *IET Electronics Letters*, vol. 36, pp. 300–302, 2000.

[85] S. U. Alam and A. B. Grudinin, "Tunable picosecond frequency-shifted feedback fiber laser at 1550 nm," *IEEE Photonics Technology Letters*, vol. 16, pp. 2012–2014, 2004.

[86] N. Akhmediev and A. Ankiewicz, "Dissipative solitons in the complex Ginzburg-Landau and Swift-Hohenberg equations," *Lecture Notes in Physics*, vol. 661, pp. 1–17, 2005.

[87] ——, "Dissipative solitons: From optics to biology and medicine," *Lecture Notes in Physics*, vol. 751, pp. 1–28, 2008.

[88] ——, "Soliton around us: Integrable, Hamiltonian and Dissipative systems," *Lecture Notes in Physics*, vol. 613, pp. 105–126, 2002.

[89] J. M. Soto-Crespo and P. Grelu, "Temporal multi-soliton complexes generated by passively mode-locked lasers," *Lecture Notes in Physics*, vol. 661, pp. 207–239, 2005.

[90] P. Grelu, M. Grapinet, J. M. Soto-Crespo, and N. Akhmediev, "Nonlinear dynamics of temporal optical soliton molecules in lasers," *PIERS Online*, vol. 3, pp. 357–359, 2007.

[91] N. Akhmediev, J. M. Soto-Crespo, M. Grapinet, and P. Grelu, "Dissipative soliton interactions inside a fiber laser cavity," *Optical Fiber Technology*, vol. 11, pp. 209–228, 2005.

[92] P. Grelu and N. Akhmediev, "Group interactions of dissipative solitons in a laser cavity: the case of $2+1$," *Optics Express*, vol. 12, pp. 3184–3189, 2004.

[93] L. M. Zhao, D. Y. Tang, H. Zhang, and X. Wu, "Bunch of restless vector solitons in a fiber laser with SESAM," *Optics Express*, vol. 17, pp. 8103–8108, 2009.

[94] D. Y. Tang, B. Zhao, D. Y. Shen, and C. Lu, "Bound-soliton fiber laser," *Physical review A*, vol. 66, p. 033806, 2002.

[95] P. Grelu and J. M. Soto-Crespo, "Temporal soliton "molecules" in mode-locked lasers: collisions, pulsations, and vibrations," *Lecture Notes in Physics*, vol. 751, pp. 137–173, 2008.

[96] S. Chouli and P. Grelu, "Rains of solitons in a fiber laser," *Optics Express*, vol. 17, pp. 11 776–11 781, 2009.

[97] ——, "Soliton rains in a fiber laser: An experimental study," *Physical review A*, vol. 81, p. 063829, 2010.

[98] S. M. Kelly, "Characteristic sidebands instability of periodically amplified average soliton," *IET Electronics Letters*, vol. 28, pp. 806–807, 1992.

[99] A. Chong, W. H. Renninger, and F. W. Wise, "Properties of normal-dispersion femtosecond fiber lasers," *Journal of Optical Society America B*, vol. 25, pp. 140–148, 2008.

[100] P. Grelu and N. Akhmediev, "Dissipative solitons for mode-locked lasers," *Nature Photonics*, vol. 6, pp. 84–92, 2012.

[101] J. Sotor, G. Sobon, and K. M. Abramski, "Scalar soliton generation in all-polarization-maintaining, graphene mode-locked fiber laser," *Optics Letters*, vol. 37, pp. 2166–2168, 2012.

[102] M. Yasin, S. W. Harun, and H. Arof, *Recent progress in optical fiber research*. Croatia: INTECH, 2012.

[103] C. R. Menyuk, "Stability of solitons in birefringent optical fibers. I: Equal propagation amplitudes," *Optics Letters*, vol. 12, pp. 614–616, 1987.

[104] ——, "Stability of solitons in birefringent optical fibers. II. Arbitrary amplitudes," *Journal of Optical Society America B*, vol. 5, pp. 392–402, 1988.

[105] ——, "Nonlinear pulse propagation in birefringent optical fibers," *IEEE Journal of Quantum Electronics*, vol. 23, pp. 174–176, 1987.

[106] D. N. Christodoulides and R. I. Joseph, "Vector solitons in birefringent nonlinear dispersive media," *Optics Letters*, vol. 13, pp. 53–55, 1988.

[107] B. Collings, S. Cundiff, N. N. Akhmediev, J. M. Soto-Crespo, K. Bergman, and W. Knox, "Polarization-locked temporal vector solitons in a fiber laser: experiment," *Journal of Optical Society America B*, vol. 17, pp. 354–365, 2000.

[108] S. Cundiff, B. C. Collings, and W. H. Knox, "Polarization locking in an isotropic, modelocked soliton Er/Yb fiber laser," *Optics Express*, vol. 1, pp. 12–21, 1997.

[109] J. M. Soto-Crespo, N. Akhmediev, B. C. Collings, S. Cundiff, K. Bergman, and W. K. Knox, "Polarization-locked temporal vector solitons in a fiber laser: theory," *Journal of Optical Society America B*, vol. 17, pp. 366–372, 2000.

[110] G. P. Agrawal, *Applications of nonlinear fiber optics*. UK: ACADEMIC PRESS, 2001.

[111] S. T. Cundiff, B. C. Collings, N. N. Akhmediev, J. M. Soto-Crespo, K. Bergman, and W. H. Knox, "Observation of polarization-locked vector solitons in an optical fiber," *Physical Review Letters*, vol. 82, pp. 3988–3991, 1999.

[112] H. Zhang, D. Y. Tang, L. Zhao, and H. Y. Tam, "Induced solitons formed by cross-polarization coupling in a birefringent cavity fiber laser," *Optics Letters*, vol. 33, pp. 2317–2319, 2008.

[113] M. N. Islam, C. D. Poole, and J. P. Gordon, "Soliton trapping in birefringent optical fibers," *Optics Letters*, vol. 14, pp. 1011–1013, 1989.

[114] A. E. Korolev, V. N. Nazarov, D. A. Nolan, and C. M. Truesdale, "Experimental observation of orthogonally polarized time-delayed optical soliton trapping in birefringent fibers," *Optics Letters*, vol. 30, pp. 132–134, 2005.

[115] L. M. Zhao, D. Y. Tang, H. Zhang, X. Wu, and N. Xiang, "Soliton trapping in fiber lasers," *Optics Express*, vol. 16, pp. 9528–9533, 2008.

[116] W. H. Renninger, A. Chong, and F. W. Wise, "Area theorem and energy quantization for dissipative optical solitons," *Journal of Optical Society America B*, vol. 27, pp. 1978–1982, 2010.

[117] A. Chong, W. H. Renninger, and F. W. Wise, "All-normal-dispersion femtosecond fiber laser with pulse energy above 20 nJ," *Optics Letters*, vol. 32, pp. 2408–2410, 2007.

[118] A. Cabasse, B. Ortaç, G. Martel, A. Hideur, and J. Limpert, "Dissipative solitons in a passively mode-locked Er-doped fiber laser with strong normal dispersion," *Optics Express*, vol. 16, pp. 19 322–19 329, 2008.

[119] N. Akhmediev, J. M. Soto-Crespo, and P. Grelu, "Roadmap to ultra-short record high-energy pulses out of laser oscillators," *Physics LettersA*, vol. 372, pp. 3124–3128, 2008.

[120] W. Chang, A. Ankiewicz, J. M. Soto-Crespo, and N. Akhmediev, "Dissipative soliton resonances in laser models with parameter management," *Journal of Optical Society America B*, vol. 25, pp. 1972–1977, 2008.

[121] K. Kieu, W. H. Renninger, A. Chong, and R. W. Wise, "Sub-100 fs pulses at watt-level powers from a dissipative-soliton fiber laser," *Optics Letters*, vol. 34, pp. 593–595, 2009.

[122] C. Lecaplain, M. Baumgartl, T. Schreiber, and A. Hideur, "On the mode-locking mechanism of a dissipative-soliton fiber oscillator," *Optics Express*, vol. 19, pp. 26 742–26 751, 2011.

[123] B. G. Bale, J. N. Kutz, A. Chong, W. H. Renninger, and F. W. Wise, "Spectral filtering for mode locking in the normal dispersive regime," *Optics Letters*, vol. 33, pp. 941–943, 2008.

[124] C. Ouyang, L. Chai, H. Zhao, M. Hu, Y. Song, Y. Li, and C. Wang, "Pulse-shaping dynamics controlled by four structural parameters in an all-normal-dispersion mode-locked fiber laser," *Journal of Optical Society America B*, vol. 26, pp. 1875–1881, 2009.

[125] W. Chang, A. Ankiewicz, J. M. Soto-Crespo, and N. Akhmediev, "Dissipative soliton resonances," *Physical review A*, vol. 78, p. 023830, 2008.

[126] P. Grelu, W. Chang, A. Ankiewicz, J. M. Soto-Crespo, and N. Akhmediev, "Dissipative soliton resonance as a guideline for high-energy pulse laser oscillators," *Journal of Optical Society America B*, vol. 27, pp. 2336–2341, 2010.

[127] Z.-C. Luo, Q.-Y. Ning, H. L. Mo, H. Chui, J. Liu, L.-J. W. A.-P. Luo, and W.-C-Xu, "Vector dissipative soliton resonance in a fiber laser," *Optics Express*, vol. 21, pp. 10 199–10 204, 2013.

[128] D. Mortag, D. Wandt, U. Morgner, D. Kracht, and J. Neumann, "Sub-80-fs pulses from an all-fiber-integrated dissipative-soliton laser at 1 μm," *Optics Express*, vol. 19, pp. 546–551, 2011.

[129] X. Liu, "Dissipative soliton evolution in ultra-large normal-cavity-dispersion fiber lasers," *Optics Express*, vol. 17, pp. 9549–9557, 2009.

[130] K. Özgören and F. Ö. Ilday, "All-fiber all-normal dispersion laser with a fiber-based Lyot filter," *Optics Letters*, vol. 35, pp. 1296–1298, 2010.

[131] J.-B. Lecourt, C. Duterte, F. Narbonneau, D. Kinet, Y. Hernandez, and D. Giannone, "All-normal dispersion, all-fibered PM laser mode-locked by SESAM," *Optics Express*, vol. 20, pp. 11 918–11 923, 2012.

[132] B. Ortaç, M. Plötner, J. Limpert, and A. Tünnermann, "Self-starting passively mode-locked chirped-pulse fiber laser," *Optics Express*, vol. 15, pp. 16 794–16 799, 2007.

[133] R. Gumenyuk, J.Puustinen, A. V. Shubin, I. A. Bufetov, E. M. Dianov, and O. G. Okhotnikov, "1.32 μm mode-locked bismuth-doped fiber laser operating in anomalous and normal dispersion regimes," *Optics Letters*, vol. 38, pp. 4005–4007, 2013.

[134] R. Wang, Y. Dai, L. Yan, J. Wu, K. Xu, Y. Li, and J. Lin, "Dissipative soliton in actively mode-locked fiber laser," *Optics Express*, vol. 20, pp. 6406–6411, 2012.

[135] N. A. Koliada, B. N. Nyushkov, A. V. Ivanenko, S. M. Kobtsev, P. Harper, S. K. Turitsyn, V. I. Denisov, and V. S. Pivtsov, "Generation of dissipative solitons in an actively mode-locked ultralong fibre laser," *Quantum Electronics*, vol. 43, pp. 95–98, 2013.

[136] B. Ortaç, M. Baumgartl, J. Limpert, and A. Tünnermann, "Approaching microjoule-level pulse energy with mode-locked femtosecond fiber lasers," *Optics Letters*, vol. 34, pp. 1585–1587, 2009.

[137] S. Lefrancois, K. Kieu, Y. Deng, J. D. Kafka, and F. W. Wise, "Scaling of dissipative soliton fiber lasers to megawatt peak powers by use of large-area photonic crystal fiber," *Optics Letters*, vol. 35, pp. 1569–1571, 2010.

[138] B. G. Bale, S. Boscolo, and S. K. Turitsyn, "Dissipative dispersion-managed solitons in mode-locked lasers," *Optics Letters*, vol. 34, pp. 3286–3288, 2009.

[139] S. Kivistö, T. Hakulinen, M. Guina, and O. G. Okhotnikov, "Tunable raman soliton source using mode-locked Tm-Ho fiber laser," *IEEE Photonics Technology Letters*, vol. 19, pp. 934–936, 2007.

[140] J. N. Kutz, B. C. Collings, K. Bergman, and W. H. Knox, "Stabilized pulse spacing in soliton lasers due to gain depletion and recovery," *IEEE Journal of Quantum Electronics*, vol. 34, pp. 1749–1757, 1998.

[141] A. N. Pilipetskii, E. A. Golovchenko, and C. R. Menyuk, "Acoustic effect in passively mode-locked fiber ring lasers," *Optics Letters*, vol. 20, pp. 907–909, 1995.

[142] A. B. Grudinin, D. J. Richardson, and D. N. Payne, "Passively harmonic modelocking of a fiber soliton ring laser," *IET Electronics Letters*, vol. 29, pp. 1860–1861, 1993.

[143] K. Smith and L. F. Mollenauer, "Experimental observation of soliton interaction over long fiber paths: discovery of a long-range interaction," *Optics Letters*, vol. 14, pp. 1284–1286, 1989.

[144] J. M. Soto-Crespo, N. Akhmediev, P. Grelu, and F. Belhache, "Quantized separations of phase-locked soliton pairs in fiber lasers," *Optics Letters*, vol. 28, pp. 1757–1759, 2003.

[145] A. Efimov, A. V. Yulin, D. V. Skryabin, J. C. Knight, N. Joly, F. G. Omenetto, A. J. Taylor, and P. Russell, "Interaction of an optical soliton with a dispersive wave," *Physical Review Letters*, vol. 95, p. 213902, 2005.

[146] S. Wabnitz, "Control of soliton train transmission, storage, and clock recovery by cw injection," *Journal of Optical Society America B*, vol. 13, pp. 2739–2749, 1996.

[147] X. Wu, D. Y. Tang, X. N. Luan, and Q. Zhang, "Bound states of solitons in a fiber laser mode locked with carbon nanotube saturable absorber," *Optics Communications*, vol. 284, pp. 3615–3618, 2011.

[148] L. M. Zhao, D. Y. Tang, and B. Zhao, "Period-doubling and quadrupling of bound solitons in a passively mode-locked fiber laser," *Optics Communications*, vol. 252, pp. 167–172, 2005.

[149] J. M. Soto-Crespo, P. Grelu, N. Akhmediev, and N. Devine, "Soliton complexes in dissipative systems: Vibrating, shaking, and mixed soliton pairs," *Physical review E*, vol. 75, p. 016613, 2007.

[150] B. Ortaç, A. Hideur, T. Chartier, M. Brunel, P. Grelu, H. Leblond, and F. Sanchez, "Generation of bound states of three ultrashort pulses with a passively mode-locked high-power Yb-doped double-clad fiber laser," *IEEE Photonics Technology Letters*, vol. 16, pp. 1274–1276, 2004.

[151] D. Y. Tang, B. Zhao, D. Y. Shen, C. Lu, W. S. Man, and H. Y. Tam, "Compound pulse solitons in a fiber ring laser," *Physical review A*, vol. 68, p. 013816, 2003.

[152] L. M. Zhao, D. Y. Tang, and D. Liu, "Ultrahigh-repetition-rate bound-soliton fiber laser," *Applied Physics B*, vol. 99, pp. 441–447, 2010.

[153] Y. Gong, P. Shum, T. Hiang, Cheng, Q. Wen, and D. Tang, "Bound soliton pulses in passively mode-locked fiber laser," *Optics Communications*, vol. 200, pp. 389–399, 2001.

[154] A. Hideur, B. Ortaç, T. Chartier, M. Brunel, H. Leblond, and F. Sanchez, "Ultra-short bound states generation with a passively mode-locked high-power Yb-doped double-clad fiber laser," *Optics Communications*, vol. 225, pp. 71–78, 2003.

[155] P. Grelu, F. Belhache, F. Gutty, and J. M. Soto-Crespo, "Relative phase locking of pulses in a passively mode-locked fiber laser," *Journal of Optical Society America B*, vol. 20, pp. 863–870, 2003.

[156] L. Gui, X. Xiao, and C. Yang, "Observation of various bound solitons in a carbon-nanotube-based erbium fiber laser," *Journal of Optical Society America B*, vol. 30, pp. 158–164, 2013.

[157] X. Liu, "Dynamic evolution of temporal dissipative-soliton molecules in large normal path-averaged dispersion fiber lasers," *Physical review A*, vol. 82, p. 063834, 2010.

[158] L. Yun and D. Han, "Bound state of dissipative solitons in a nanotube-mode-locked fiber laser," *Optics Communications*, vol. 313, pp. 70–73, 2014.

[159] P. Grelu, J. Beál, and J. M. Soto-Crespo, "Soliton pairs in a fiber laser: from anomalous to normal average dispersion regime," *Optics Express*, vol. 11, pp. 2238–2243, 2003.

[160] M. Olivier and M. Piché, "Origin of the bound states of pulses in the stretched-pulse fiber laser," *Optics Express*, vol. 17, pp. 405–418, 2009.

[161] S. Chouli and P. Grelu, "Solitons rains in a fiber laser: An experimetal study," *Physical review A*, vol. 81, p. 063829, 2010.

[162] P. Grelu, S. Chouli, J. M. Soto-Crespo, W. Chang, A. Ankiewicz, and N. Akhmediev, "Dissipative solitons for mode-locked fiber lasers," in *Photonics Global Conference*, 2010.

[163] C. Bao, X. Xiao, and C. Yang, "Soliton rains in a normal dispersion fiber laser with dual-filter," *Optics Letters*, vol. 38, pp. 1875–1877, 2013.

[164] R. Gumenyuk, D. A. Korobko, I. O. Zolotovskii, and O. G. Okhotnikov, "Role of cavity dispersion on soliton grouping in fiber lasers," *Optics Express*, vol. 22, pp. 1896–1905, 2014.

[165] I. Razdobreev and L. Bigot, "On the multiplicity of Bismuth active centers in germano-alumosilicate preform," *Optical Materials*, vol. 33, pp. 973–977, 2011.

[166] I. Razdobreev, H. E. Hamzaoui, V. Y. ivanov, E. F. Kustov, B. Capoen, and M. Bouazaoui, "Optical spectroscopy of bismuth dosped pure silica fiber preform," *Optics Letters*, vol. 35, pp. 1341–1343, 2010.

[167] R.Gumenyuk, M. Melkumov, V. F. Khopin, E. M. Dianov, and O. Okhotnikov, "Pulse grouping in a 1460 nm mode-locked bismuth-doped fiber laser," prepared for submission.

Appendix 1

Publication 1

R. Gumenyuk, K. Golant and O. G. Okhotnikov, "Energy transition characterization of 1.18- and 1.3-μm bands of bismuth fiber by spectroscopy of the transient oscillations", Apllied Physics Letters, Vol. 98, No. 19, pp. 191108, (2011).

Energy transition characterization of 1.18 and 1.3 μm bands of bismuth fiber by spectroscopy of the transient oscillations

Regina Gumenyuk,[1,a)] Konstantin Golant,[2] Oleg. G. Okhotnikov,[1] Regina Gumenyuk,[3] Konstantin Golant,[4,b)] and Oleg G. Okhotnikov[5,c)]
[1]*Optoelectronics Research Centre, Tampere University of Technology, P.O. Box 692, FIN-33101 Tampere, Finland*
[2]*Kotel'nikov Institute of Radioengineering and Electronics, Russian Academy of Science, Mokhovaya 11, bld.7, 125009 Moscow, Russian Federation*
[3]*Optoelectronics Research Centre, Tampere University of Technology, P.O. Box 692, FIN-333101 Tampere, Finland*
[4]*Kotel'nikov Institute of Radioengineering and Electronics, Russian Academy of Science, Mokhovaya 11, bld.7, 125009 Moscow, Russian Federation*
[5]*Optoelectronics Research Centre, Tampere University of Technology, P.O. Box 692, FIN-333101 Tampere, Finland*

(Received 11 March 2011; accepted 21 April 2011; published online 11 May 2011)

The experimental evidence of laser transition type in bismuth-doped silica fibers operating at different spectral bands is presented. Spectrally resolved transient (relaxation) oscillations studied for a Bi-doped fiber laser at room and liquid-nitrogen temperatures allow to identify the three- and four-level energy bands. 1.18 μm short-wavelength band is found to be a three-level system at room temperature with highly populated terminal energy level of laser transition. The depopulation of ground level by cooling the fiber down to liquid-nitrogen temperature changes the transition to four-level type. Four-level energy transition distinguished at 1.32 μm exhibits the net gain at room temperature. © *2011 American Institute of Physics*. [doi:10.1063/1.3590266]

Bismuth-doped glasses have been recently shown to represent a novel promising active material for broadband near-infrared amplification. The emission spectrum of Bi glass in a broadband 1.0–1.5 μm spectral range was shown to depend on the excitation wavelength. Recently developed Bi-doped fibers have the ability to provide gain within the 1100–1500 nm wavelength range[1,2] and thus expand the advantages of fiber lasers and fiber amplifiers to new applications. Watt-level continuous wave and mode-locked Bi-doped fiber lasers have been reported.[3–7] Though, the luminescent properties and amplification of bismuth-doped silica glass have been reported, the nature of the active center responsible for the observed luminescence is still unclear and is the subject of intensive study. The infrared luminescence has been attributed to electronic transition of Bi^{5+},[8] Bi^{+},[9] clusters of Bi atoms,[10] and $\{[AlO_{4/2}]^{-},Bi^{+}\}$ complexes.[1]

Bi-doped fiber pumped at various wavelengths reveals the simultaneous presence of different active centers. The luminescence spectra shown in Fig. 1 disclose the number of emission bands emerging for 808 and 980 nm pumping. Since each center requires individual excitation source, pumping Bi fiber at a single wavelength could not saturate the loss induced by unpumped centers which explains the high background losses observed in these fibers. This phenomenon provides a detrimental impact at 1.18 μm band where Bi-fiber amplifiers operate as a three-level system with terminal laser level highly populated at room temperature. Consequently, the practical gain can be achieved at this band only by deep cooling the fiber or by using multicolor pumping. Alternatively, the selective control of active centers during fiber fabrication would be a practical technology of Bi-doped fiber intended to a specific spectral band.

In this letter, we report the study of relaxation oscillations in the bismuth alumosilicate and phosphosilicate-core fiber lasers. It was shown that spectrally resolved transient oscillations offer a useful analysis of emission buildup, dynamics of population inversion and the nature of laser transition.[11–13] This technique is applied here to bismuth-doped fiber lasers operating at various spectral bands. We performed spectroscopic measurements of the relaxation oscillations in a tunable Bi-doped fiber laser at liquid-nitrogen and room temperatures and identified three-level and four-

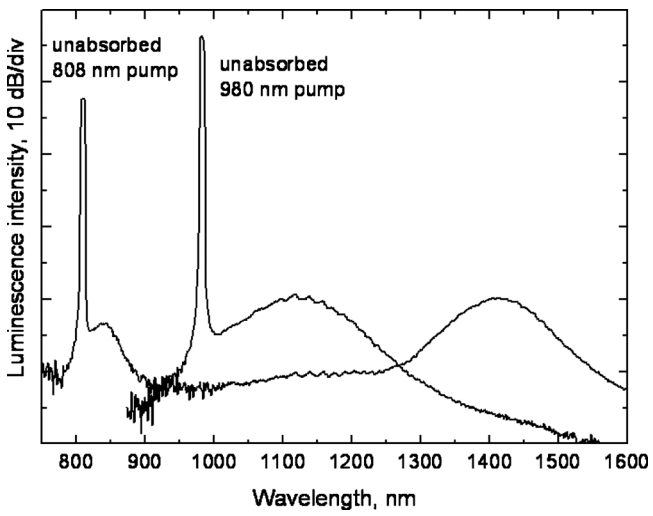

FIG. 1. Luminescent spectra from Bi-doped alumosilicate fiber pumped at 808 and 980 nm. The fiber details are given in Ref. 14.

[a)]Author to whom correspondence should be addressed. Electronic mail: regina.gumenyuk@tut.fi.
[b)]Electronic mail: golant@cplire.ru. Tel.: +7 (495) 629 33 20. FAX: +7 (495) 629 35 74.
[c)]Electronic mail: oleg.okhotnikov@tut.fi. Tel.: +358 40 849 0010. FAX: +358 3 3115 3400.

level transitions. The results particularly explain the strong temperature dependence of gain in Bi-fiber operating at 1.18 μm band.

The origin of the wavelength dependence of ω_{relax} for three-level systems can be understood from the small-signal analytic solution of the rate equations, taking into account the thermal level population as follows:

$$\omega_{relax}^2 = \frac{1}{\tau_c \tau_s}(1 + \tau_c \sigma c \eta f^l N)(r-1), \quad (1)$$

where N is total number of active ions, c, σ are the speed of light and laser transition cross section, $\eta = l/[L + l(n-l)]$, where L, l are the total cavity length and the length of the gain medium, n is the refractive index, f^l is the fractional thermal occupation of the lower laser level, and τ_c, τ_s are the cavity and laser transition lifetimes. r is a pumping rate normalized to threshold.

From this relation it is clear that the wavelength dependent term in the bracket disappears for all lasers operating with negligible population on the terminal level, as it occurs in four-level transitions. In addition, the cross sections for emission and absorption at each transition may be also determined directly using the experimentally measured wavelength dependencies of the relaxation oscillation frequency and threshold pumping rate. It should be then noted that the relaxation oscillation frequency depends directly on the absorption at the signal wavelength ($\sim \sigma f^l$) as a result of the finite thermal population of the ground level. Thus the wavelength dependence of transient oscillation provides a method to determine the energy level character of optical transition in laser material.

The transient oscillations were studied in linear cavity comprising piece of Bi-doped fiber, pump coupler, a segment of air space with chopper and diffraction grating in Littrow configuration, and loop mirror acting as an output coupler. An antireflection coated lens was used to collimate the beam from the active fiber to the reflection grating. The laser was pumped by 1.06 μm Yb-doped fiber laser for operation around 1170 nm and by 1.24 μm laser diode to achieve oscillation at 1.32 μm spectral band. The chopper placed in a collimated beam operating at rate of 650 Hz was used to observe the transient evolution of the laser emission toward its steady-state condition.

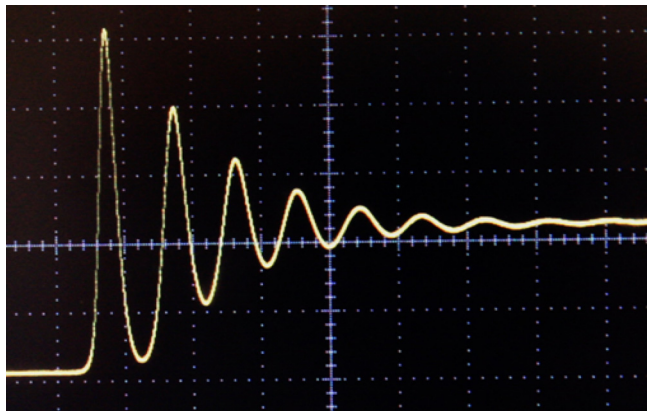

FIG. 2. (Color online) Typical transient oscillations from Bi-doped phosphosilicate-core fiber laser for pumping rate of $r-1=0.46$. Time scale: 40 μs/div.

First, 20 m long Bi-doped silicate glass fiber designed for operation at 1160–1180 nm band has been examined. Fiber with absorption of ~1.2 dB/m at 1062 nm was core-pumped by a 1 W Yb-doped single-mode fiber laser through a 1062/1165 pump coupler. The threshold pump power was in a range from 55 to 70 mW depending on lasing wavelength. The output was taken via fiber loop mirror with reflectivity of 97%. The length of the doped fiber was optimized in order to achieve efficient pump absorption.

Typical relaxation oscillations are shown in Fig. 2. The frequency of oscillations ω_{relax} was determined from the repetition period of strongly damped small-amplitude nearly sinusoidal oscillations which correspond to small-signal analytic solution of rate equations. The relaxation oscillation frequency was measured at liquid-nitrogen (77 °K) and room temperature (297 °K). Figures 3(a) and 3(b) show the dependence of $(\omega_{relax}/2\pi)^2$ versus normalized pumping rate for different lasing wavelengths. The slope of the dependences exhibits noticeable variation with wavelength at room temperature which indicates the change in the population of the sublevel of ground manifold. This behavior is a clear signature of three-level origin of laser transition. In a contrast, at liquid-nitrogen temperature the population of ground manifold is negligible ($\sigma f^l = 0$) resulted in insignificant absorption of individual transitions from ground sublevels and,

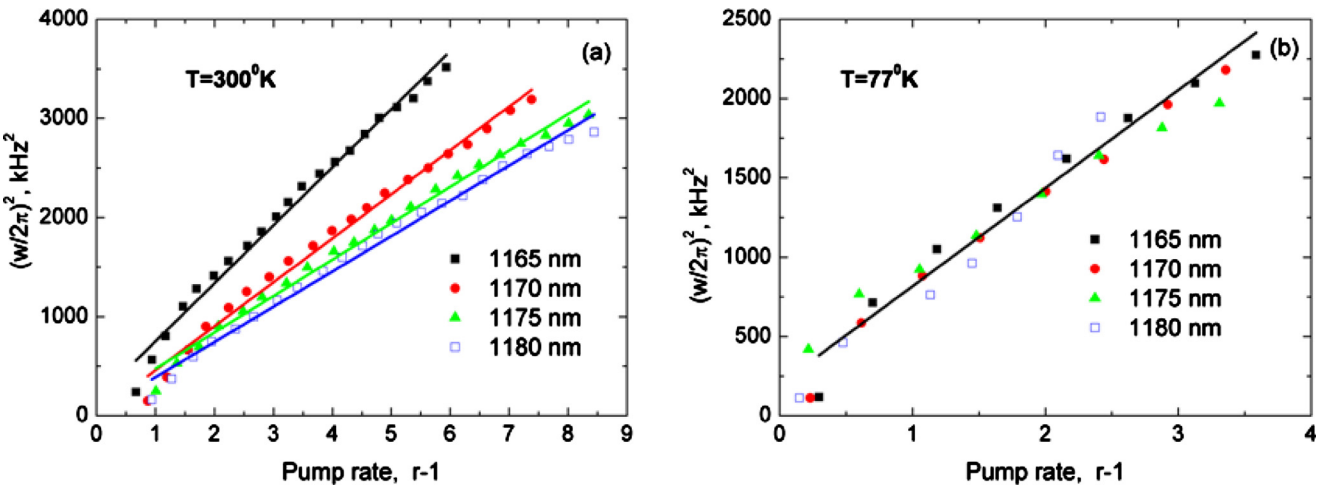

FIG. 3. (Color online) $(\omega_{relax}/2\pi)^2$ vs pumping rate $(r-1)$ for 1160–1180 nm spectral band. Bi-doped fiber is pumped by 1.07 μm Yb-fiber laser.

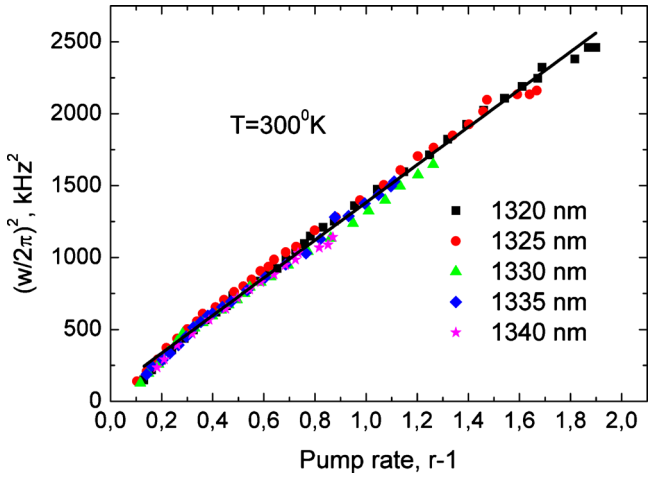

FIG. 4. (Color online) $(\omega_{relax}/2\pi)^2$ vs $(r-1)$ dependence for 1.32–1.34 μm wavelength range measured at room temperature. Pumping source is 1.24 μm laser diode.

consequently, in four-level operation of active medium. The large scatter of the data in Fig. 3(b) is because practically difficult to ensure a uniform temperature distribution along the entire length of the fiber when the fiber is immersed in liquid nitrogen.

Next, 30 m long Bi-doped fiber optimized for operation at 1.32–1.34 μm (Ref. 14) was tested in a similar laser cavity. 200 mW of pump power from 1236 nm laser diode was coupled to Bi-doped fiber via 1230/1320 nm dichroic pump combiner. The threshold pump power was varied from 60 to 80 mW depending on operation wavelength. The wavelength independent behavior of $(\omega_{relax}/2\pi)^2$ versus $(r-1)$ dependence seen from Fig. 4 even at room temperature indicates a four-level character of laser transition at this spectral band.

In conclusion, three- and four-level transitions in bismuth fiber have been established by the spectral analysis of transient oscillations at room and liquid nitrogen temperatures. It was found that 1.18 μm short-wavelength band pumped at 1.07 μm performs as a three-level system at room temperature with highly populated terminal energy level of laser transition resulted in a strong wavelength dependence of relaxation oscillations. Depopulation of ground level at temperature of liquid nitrogen turns the system to four-level scheme which allows sensible gain to be achieved at this spectral band. Long-wavelength band at 1.32 μm belongs to a four-level energy transition scheme and, consequently, exhibits the net gain at room temperature when excited at wavelength of 1.24 μm. It should also be noted that various luminescent centers are created in Bi-fiber during fabrication. Since these centers require different pump wavelengths for activation, single-wavelength resonant pumping of specific spectral band cannot prevent the losses induced by the unpumped centers, which validates the high background absorption observed typically in Bi-doped fibers. Simultaneous multiple-wavelength pumping could suppress this type of losses.

[1]V. V. Dvoyrin, V. M. Mashinsky, E. M. Dianov, A. A. Umnikov, M. V. Yashkov, and A. N. Guryanov, Proceedings of ECOC, 2005, Vol. 4, p. 949, Glasgow, UK, 25–29 September.
[2]I. Bufetov, S. Firstov, V. Khopin, O. Medvedkov, A. Guryanov, and E. Dianov, Opt. Lett. **33**, 2227 (2008).
[3]E. M. Dianov, A. V. Shubin, M. A. Melkumov, O. I. Medvedkov, and I. A. Bufetov, J. Opt. Soc. Am. B **24**, 1749 (2007).
[4]A. B. Rulkov, A. A. Ferin, S. V. Popov, J. R. Taylor, I. Razdobreev, L. Bigot, and G. Bouwmans, Opt. Express **15**, 5473 (2007).
[5]E. M. Dianov, A. A. Krylov, V. V. Dvoyrin, V. M. Mashinsky, P. G. Kryukov, O. G. Okhotnikov, and M. Guina, J. Opt. Soc. Am. B **24**, 1807 (2007).
[6]S. Kivistö, J. Puustinen, M. Guina, O. G. Okhotnikov, and E. M. Dianov, Electron. Lett. **44**, 1456 (2008).
[7]I. A. Bufetov, K. M. Golant, S. V. Firstov, A. V. Kholodkov, A. V. Shubin, and E. M. Dianov, Appl. Opt. **47**, 4940 (2008).
[8]H.-P. Xia and X.-J. Wang, Appl. Phys. Lett. **89**, 051917 (2006).
[9]M. Peng, J. Qiu, D. Chen, X. Meng, and C. Zhu, Opt. Express **13**, 6892 (2005).
[10]M. Peng, J. Qiu, D. Chen, X. Meng, and C. Zhu, Opt. Lett. **30**, 2433 (2005).
[11]L. Orsila and O. G. Okhotnikov, Opt. Express **13**, 3218 (2005).
[12]O. G. Okhotnikov and J. R. Salcedo, Appl. Phys. Lett. **64**, 2619 (1994).
[13]O. G. Okhotnikov and J. R. Salcedo, Opt. Lett. **19**, 1445 (1994).
[14]K. M. Golant, A. P. Bazakutsa, O. V. Butov, Y. K. Chamorovskij, A. V. Lanin, and S. A. Nikitov, Proceedings of ECOC, 2010, Torino, Italy, 19–23 September.

Appendix 2

Publication 2

R. Gumenyuk, I. Vartiainen, H. Tuovinen and O. G. Okhotnikov, "Dissipative dispersion-managed soliton 2 μm thulium/holmium fiber laser", Optics Letters, Vol. 36, No. 5, pp. 609–611, (2011).

Dissipative dispersion-managed soliton 2 μm thulium/holmium fiber laser

Regina Gumenyuk,[1,*] Ismo Vartiainen,[2] Hemmo Tuovinen,[2] and Oleg G. Okhotnikov[1]

[1]*Optoelectronics Research Centre, Tampere University of Technology, Korkeakoulunkatu 3, Tampere, FIN-33101, Finland*

[2]*Department of Physics and Mathematics of the University of Eastern Finland, Yliopistokatu 7 Joensuu, FIN-80101, Finland*

**Corresponding author: regina.gumenyuk@tut.fi*

Received November 9, 2010; revised January 18, 2011; accepted January 25, 2011;
posted January 31, 2011 (Doc. ID 137902); published February 17, 2011

We report a first dissipative dispersive-managed soliton fiber laser operating at 2 μm. The cavity comprised of all-anomalous-dispersion fiber employs chirped fiber Bragg grating, which ensures net-normal cavity dispersion and semiconductor saturable absorber for mode-locking. © 2011 Optical Society of America

OCIS codes: 060.2320, 060.2410, 140.4050, 140.7090.

Over the past decade, ultrafast fiber laser technology has progressed remarkably and now it starts to challenge other laser technologies, particularly those based on bulk solid state lasers. Advantages of ultrafast fiber lasers include excellent beam and pulse quality, high efficiency, and turn-key operation. Pulse generation covering a large wavelength range from 895 to 1560 nm have been reported using neodymium, ytterbium, bismuth and erbium mode-locked fiber systems [1–3]. Mode-locked Raman fiber lasers, demonstrated recently, open another interesting opportunity for wavelength tailoring [4,5]. Extending the operation wavelength toward the midinfrared range is triggered by a large number of applications. Thulium- and thulium-holmium doped fibers are demonstrated to be a major candidate for high-power sources operating around 2 μm. Thulium fiber has a broad amplification bandwidth between 1.65 μm and 2.1 μm and is, therefore, suitable for short pulse generation and wide spectral tuning [6–9].

A specific feature of optical fiber operating at 2 μm is a large anomalous dispersion which causes the operation in a soliton pulse regime. Normal-dispersion lasers supporting dissipative solitons (DS) exhibit, however, superior performance over lasers exploiting dispersion-managed (DM) solitons. DS lasers have demonstrated the highest femtosecond pulse energy produced to date by lasers made of standard fiber [10].

Contrary to conservative solitons where only the balance between dispersion and nonlinearity is required, in laser supporting dissipative solitons the dispersion is only one among many other parameters that determines the laser dynamics [11]. Particularly, proper balance between gain and loss is needed to achieve operation with high-energy DS solitons [12,13]. The space of the system parameters where high-energy dissipative solitons exist is described by Akhmediev *et al.* [14].

The laser cavity supporting the DS regime should be built of an all-normal-dispersion cavity [10] or at least cavity segments with normal dispersion should provide the dominant contribution to the cavity dispersion [15]. This requirement becomes increasingly difficult to fulfill for longer wavelengths due to limited availability of fibers with normal dispersion. If at shorter wavelengths all-normal-dispersion laser supporting dissipative solitons could be constructed from conventional fibers, above 1.2 μm fiber or bulk compensators producing normal dispersion should be employed thus inducing the dispersion map.

A promising solution was proposed recently which extends the dispersion-managed soliton theory to dissipative DM solitons (DDM) [16]. It was shown that DDM solitons could be generated at higher strengths of the dispersion map as compared with DM strategy, leading to stable pulses with an increased energy. This finding is particularly important for construction of long-wavelength dissipative soliton systems.

In this paper, we demonstrate a mode-locked 2 μm thulium-holmium doped fiber laser that exploits dissipative dispersion-managed soliton pulse shaping. The DDM laser operates in a stable single-pulse regime and demonstrates an increase in the pulse energy as compared with a DM net anomalous-dispersion cavity.

The mode-locked fiber laser with linear cavity is shown schematically in Fig. 1. The gain was provided by a 1.2 m-long Tm-Ho fiber with absorption of 14 dB/m at 1564 nm and anomalous dispersion of 0.13 ps^2/m at 1985 nm. The cavity was terminated by chirp fiber Bragg grating (CFBG) and a semiconductor saturable absorber mirror (SESAM) described in detail elsewhere [17]. SESAM producing self-amplitude modulation ensured a self-starting character of the mode-locking. The CFBG had a chirp of 130 nm/cm and acted as an output coupler and dispersion compensator which provided the net-normal cavity dispersion. The CFBG was imprinted in the single-mode fiber using phase mask, fabricated by e-beam technology. The 4 mm-long grating had the bandwidth of 82 nm with a central wavelength of 1986 nm, reflectivity of ~30%, and generated the normal dispersion of 1.07 ps^2. Thus, the dispersion map of the cavity consisted of a fiber segment with anomalous dispersion and normal-dispersion CFBG,

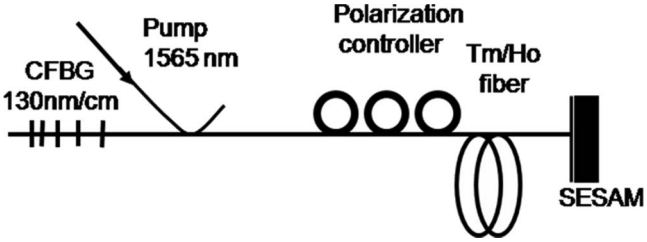

Fig. 1. Schematic of mode-locked Tm-Ho fiber laser.

0146-9592/11/050609-03$15.00/0

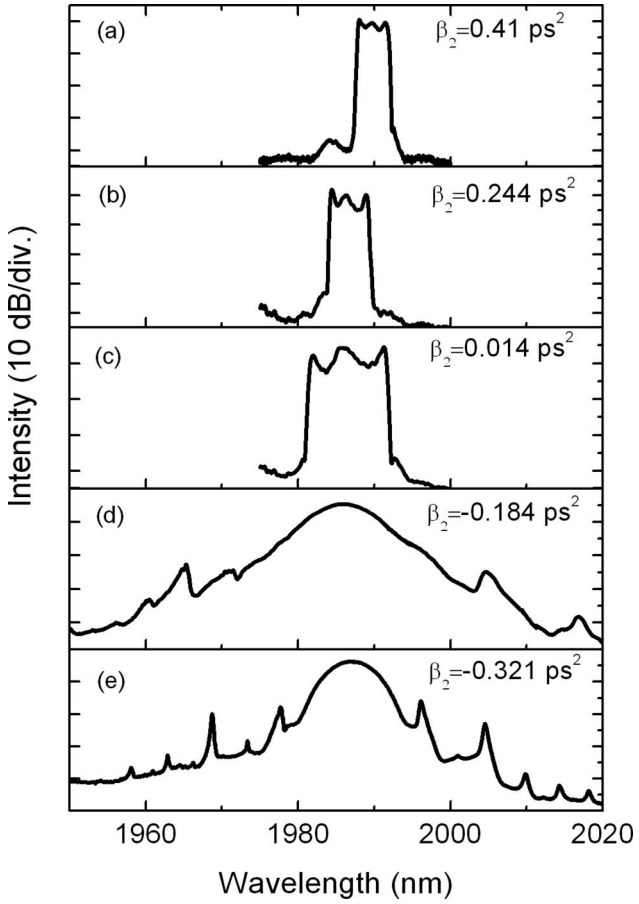

Fig. 2. The evolution of the pulse spectrum with cavity dispersion.

which meant that it could support DM solitons. By changing the length of passive fiber, the net cavity dispersion could be either normal or anomalous in a range from $0.47\,\mathrm{ps}^2$ to $-0.32\,\mathrm{ps}^2$. The total length of the laser cavity was varied from 3 to 8.5 m changing the repetition rate in a range of 12.2 to 33.3 MHz. All data were collected after CFBG output. The gain fiber was pumped by a 1565 nm Er-fiber laser via a fiber pump combiner.

The evolution of the pulse spectrum with the cavity dispersion is shown in Fig. 2. As the normal group velocity dispersion (GVD) decreases from 0.47 to $0.02\,\mathrm{ps}^2$, the spectrum bandwidth increases from 3 to 10 nm, as seen from Figs. 2(a)–2(c). The spectrum steep spectral edges are a signature of dissipative solitons [11]. With anomalous GVD, the pulse spectral bandwidth increases from 6 nm to 7 nm when dispersion decreases from $-0.32\,\mathrm{ps}^2$ to $-0.18\,\mathrm{ps}^2$, Fig. 2(d) and 2(e). The spectra exhibit distinct Kelly sidebands inherent to DM solitons at anomalous GVD. It should be noted that self-stated mode-locking could be achieve regardless the sign and value of GVD owing to the high modulation depth of the saturable absorber.

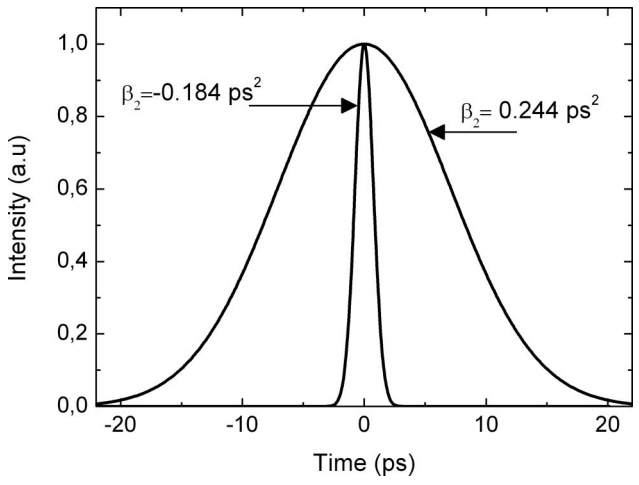

Fig. 3. The pulse autocorrelation traces for large net normal dispersion of $0.25\,\mathrm{ps}^2$ and anomalous GVD of $-0.18\,\mathrm{ps}^2$.

With the normal dispersion of $0.25\,\mathrm{ps}^2$, the cavity length was 4.5 m corresponding to the repetition rate of 22.7 MHz and the bandwidth of 5 nm with the central wavelength of 1987 nm, as seen from Fig. 2(b). Figure 3 shows that autocorrelation of 11.7 ps strongly up-chirped pulses corresponding to a time-bandwidth product of 15.69. As expected, the single-pulse regime was maintained over the whole range of pump power since the normal-dispersion regime of the cavity prevents wave breaking [10,18]. The average output power was limited to 50 mW at a pump power of 470 mW due to excessively large outcoupling provided by CFBG.

For net anomalous GVD of $-0.18\,\mathrm{ps}^2$, Fig. 2(d), the spectrum bandwidth, pulse width, and average power are 7.3 nm, 1.54 ps, and 20 mW, respectively. Multiple-pulse operation sets in with a minor increase in pump power expected with the DM soliton laser.

In conclusion, we have demonstrated a dissipative dispersion-managed soliton thulium-holmium fiber laser mode-locked by an antimonide-based saturable absorber mirror. The normal-dispersion regime of the cavity consisting solely of anomalous-dispersion fiber was achieved by chirped fiber Bragg grating. A future work will be focused on pulse compression and power scaling.

This work was supported by the Graduate School in Electronics, Telecommunications and Automation (GETA). O. G. Okhotnikov thanks S. Turitsyn from Aston University for valuable discussions.

References

1. O. G. Okhotnikov, L. Gomes, N. Xiang, T. Jouhti, and A. B. Grudinin, Opt. Lett. **28**, 1522 (2003).
2. S. Kivistö, J. Puustinen, M. Guina, O. G. Okhotnikov, and E. M. Dianov, Electron. Lett. **44**, 1456 (2008).
3. O. G. Okhotnikov, T. Jouhti, J. Konttinen, S. Karirinne, and M. Pessa, Opt. Lett. **28**, 364 (2003).
4. A. Chamorovskiy, J. Rautiainen, J. Lyytikäinen, S. Ranta, M. Tavast, A. Sirbu, E. Kapon, and O. G. Okhotnikov, Opt. Lett. **35**, 3529 (2010).
5. A. Chamorovskiy, J. Rantamäki, A. Sirbu, A. Mereuta, E. Kapon, and O. G. Okhotnikov, Opt. Express **18**, 23872 (2010).
6. S. D. Jackson and S. Mossman, Appl. Opt. **42**, 2702 (2003).
7. R. L. Shubochkin, V. A. Kozlov, A. L. G. Carter, and T. F. Morse, IEEE Photonics Technol. Lett. **10**, 944 (1998).
8. L. E. Nelson, E. P. Ippen, and H. A. Haus, Appl. Phys. Lett. **67**, 19 (1995).
9. R. C. Sharp, D. E. Spock, N. Pan, and J. Elliot, Opt. Lett. **21**, 881 (1996).
10. K. Kieu, W. H. Renninger, A. Chong, and F. W. Wise, Opt. Lett. **34**, 593 (2009).

11. N. Akhmediev, J. M. Soto-Crespo, and Ph. Grelu, Phys. Lett. A **372**, 3124 (2008).
12. J. M. Soto-Crespo, N. Akhmediev, and G. Town, Opt. Commun. **199**, 283 (2001).
13. N. Akhmediev and A. Ankiewicz, in *Optical Solitons: Theoretical and Experimental Challenges*, K. Porsezian and V. C. Kurakose eds. (Springer, 2003).
14. W. Chang, A. Ankiewicz, J. M. Soto-Crespo, and N. Akhmediev, J. Opt. Soc. Am. B **25**, 1972 (2008).
15. A. Cabasse, B. Ortac, G. Martel, A. Hideur, and J. Limpert, Opt. Express **16**, 19322 (2008).
16. B. G. Bale, S. Boscolo, and S. Turitsin, Opt. Lett. **34**, 3286 (2009).
17. S. Kivistö, T. Hakulinen, M. Guina, and O. G. Okhotnikov, IEEE Photonics Technol. Lett. **19**, 934 (2007).
18. R. Herda and O. G. Okhotnikov, IEEE J. Quantum Electron. **40**, 893 (2004).

Appendix 3

Publication 3

R. Gumenyuk and O. G. Okhotnikov, "Temporal control of vector soliton bunching by slow/fast saturable absorption", J. Opt. Soc. Am. B, Vol. 29, No. 1, pp. 1–7, (2012)

Temporal control of vector soliton bunching by slow/fast saturable absorption

Regina Gumenyuk* and Oleg G. Okhotnikov

Optoelectronics Research Centre, Tampere University of Technology, Korkeakoulunkatu 3, Tampere FIN-33101, Finland
**Corresponding author: regina.gumenyuk@tut.fi*

Received August 3, 2011; revised October 18, 2011; accepted October 21, 2011;
posted October 21, 2011 (Doc. ID 152272); published December 7, 2011

Saturable absorbers exhibiting complex dynamics are shown to provide efficient means for control of soliton interactions. This study, focused specifically on dynamics of vector soliton interactions, demonstrates that a soliton bunch can be efficiently compressed by attractive force generated in a saturable absorber. Effect of absorption recovery time on soliton bunching is explored by using fast and slow semiconductor and carbon nanotube absorbers.

OCIS codes: 320.7110, 060.3510, 140.4050, 190.5530.

1. INTRODUCTION

It is well documented that lasers mode locked in the anomalous dispersion regime tend to produce multiple soliton pulses with pulse number increasing with pump power [1–4]. When the multiple-pulse regime sets in, the temporal pulse position in a cavity is not firmly determined. Nevertheless, soliton self-ordering resulted in an equally spaced harmonically mode-locked pulse train was frequently observed [1]. Several physical effects are established to be responsible for this behavior. Repulsing forces in soliton lasers have been considered and analyzed in a number of studies, e.g., in [3]. It was shown that the interpulse dynamics in a harmonic passively mode-locked soliton laser is mainly determined by gain depletion in conjunction with its recovery, which provides an effective repulsion force between adjacent solitons by imparting a group velocity drift proportional to the interpulse spacings. It was also suggested that the electrostriction and acoustic effect could play the significant role in pulse interaction as the next largest perturbation to the gain recovery. In addition to equal spacing, the acoustic effect modulating the refractive index could lead to pulse bunching [5].

Since the actual non-polarization-maintaining fibers exhibit some birefringence resulting in polarization mode dispersion, the unequal propagation velocities of polarization modes need to be included in a complete consideration of pulse propagation. The vector nature of nonlinear pulse propagation in the birefringent environment has been established both theoretically and experimentally [6–8]. Importantly, it was shown that a pulse comprising both polarization components can propagate as a vector soliton with equalized group velocities. Both the polarization-locking, so-called polarization-locked vector soliton (PLVS), regime when polarization does not evolve and the regime exhibiting the gradual polarization evolution have been observed [7].

Vector soliton interaction inside laser cavity is another essential aspect. Recently nonlinear dynamics in a form of vector soliton bunching has been observed [5]. Specifically, the vector solitons exhibit contractive and repulsive motions within the bunch. Thus, contrary to static behavior of scalar solitons in a bunch, the vector solitons move repeatedly with respect to each other.

Semiconductor saturable absorbers are proven to be key components for short pulse generation [9–13]. Based on mature semiconductor technology, MBE or MOCVD, semiconductor saturable absorber mirrors (SESAMs) offer flexible tailoring of their optical characteristics. An alternative technique is based on carbon nanotubes (CNTs), which provide fast broadband absorption achievable with large diameter distribution, compromised, however, by insertion loss [14].

It should be noted that semiconductor absorber could exhibit both fast and slow temporal components in the recovery dynamics. These components, originated from the intraband and band-to-band transitions, influence the start-up of mode locking and the pulse shaping process. Generally, the intensity-dependent temporal response of semiconductor saturable absorbers originates from resonant and nonresonant absorption in bulk or quantum-confined semiconductors, quantum wells, or dots. Resonant absorption effects involving carrier excitation and relaxation provide a slow saturable absorption mechanism. Near-resonant band edge effects and intraband carrier–carrier scattering and thermalization processes induce a subpicosecond fast component to the absorption recovery [15]. This subpicosecond recovery time of saturable absorber forms a low-loss temporal window constructive to the shortest pulse shaping. The fast recovery mechanism can be further enhanced by using low-temperature growth, ion-irradiation, surface-state assistance, metamorphic growth [15–18]. Both resonant and nonresonant effects are favorable to the initiation of the passive mode-locking and the steady-state short pulse regimes [11]. The typical analysis of mode-locked lasers is usually focused on reliable start-up of the short pulse regime, robustness against the low-frequency Q-switching instability, and the breakup into multiple pulses.

Here we examine the effect of saturable absorption on the dynamic of a vector soliton laser. It is demonstrated that pulse bunching in a vector soliton fiber laser mode locked with saturable absorber depends primarily on the recovery time of absorption. Though the gain depletion and acoustic effect could also contribute to interpulse dynamics, as mentioned

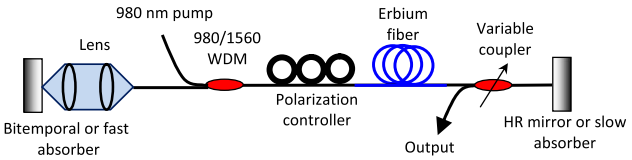

Fig. 1. (Color online) Experimental setup of mode-locked erbium-doped fiber laser. WDM, wavelength-division multiplexer; HR mirror, high reflective mirror.

above, the effects governed by saturable absorbers are shown to provide the dominant impact on the solitonlike pulse bunching. To identify the role of saturable absorber, the laser cavity was kept unchanged throughout the measurements except for a set of different absorbers used consecutively for mode locking and temporal pulse control.

2. LASER DETAILS

Based on the above consideration, we consider the saturable absorber as a nonlinear element having a temporal response on two time scales, fast and slow. It is assumed that the slow component exhibits the recovery time comparable to interpulse spacing, and therefore it would provide the mechanism for pulse attraction. Intuitively, it is expected that closely spaced pulses forming the bunch acquire reduced losses in a saturable absorber as compared to a pulse train having the temporal spacing (or average pulse period) larger than recovery time of the absorption.

The experimental procedure of this study employs various saturable absorbers or their combination, which allows us to engineer the bitemporal response. The linear cavity of the fiber laser is shown in Fig. 1. The gain is provided by a 2 m long erbium-doped fiber pumped by a 980 nm diode laser through a dichroic coupler. The laser cavity is terminated by the lens-coupled absorber and broadband mirror or second absorber butt coupled to the fiber. The 10.3 m long cavity corresponds to a fundamental repetition rate of 10 MHz and generates a net cavity dispersion of 0.27 ps/nm. The signals examined at the output ports of the polarization-maintaining variable coupler were used to distinguish scalar and vector soliton operation.

Since the main subject of this study is soliton interactions and bunching inside a laser cavity enforced with saturable absorption, various saturable absorbers or their combination have been employed. Particularly, the study examines the effect of specific temporal dynamics of absorption saturation on the soliton interactions in a passively mode-locked laser. The absorbers with a single-exponential fast or slow recovery mechanism and two-exponential absorption recovery comprising both fast and slow components resulting in the bitemporal dynamics have been implemented as a cavity mirrors in a fiber laser. SESAM or CNT-based fast absorbers described in detail in [9,14] have picosecond-to-subpicosecond recovery time and are optimized for easy startup of mode-locked operation. Slow absorbers exploit slow recovery in a GaInAsP quantum well achieved by accurate setting of growth condition [19]. These absorbers exhibit typically the recovery times above 100 ps and cannot initiate and sustain mode locking. The absorbers exhibiting biexponential absorption recovery were prepared by using metamorphic growth providing simultaneously strong fast and slow components [16,17].

3. EXPERIMENTAL RESULTS

As a starting point we first examine the performance of the laser using an SESAM with dominant fast recovery dynamics assembled as one cavity reflector [9], while another end of the fiber cavity is butt coupled to highly reflective mirror, as shown in Fig. 1. The laser exploiting fast absorber with sufficient ultrafast time response produces stable nearly transform-limited 1 ps sech^2 pulses. Because of relatively high anomalous dispersion, the resonant sidebands are seen in the optical spectrum resulted from periodic perturbations in a laser cavity (Fig. 2). Since the laser is mode locked in the soliton dispersion regime, it tends to produce multiple pulses per round trip because pulse energy is locked to the fundamental soliton energy [1–4]. The total number of pulses in the cavity gradually increases with the output power. The distinct feature of this regime is random and unstable temporal spacing between the pulses.

Similar behavior was observed with the CNT-based absorber, which also exhibits picosecond recovery [14]. The slow SESAM used instead of the fast one could not initiate the mode-locked operation and provides low-frequency Q-switched instability only. Poor starting capability of slow absorbers was found to originate somewhat from the high level of amplified spontaneous emission in fiber lasers [20].

Next, a fast absorber was replaced with the SESAM exhibiting a distinct bitemporal response [Fig. 3(a)]. Recently, we have demonstrated that MBE growth can be employed to fabricate the metamorphic SESAMs with scalable recovery time of the nonlinear response on GaAs substrates. Using

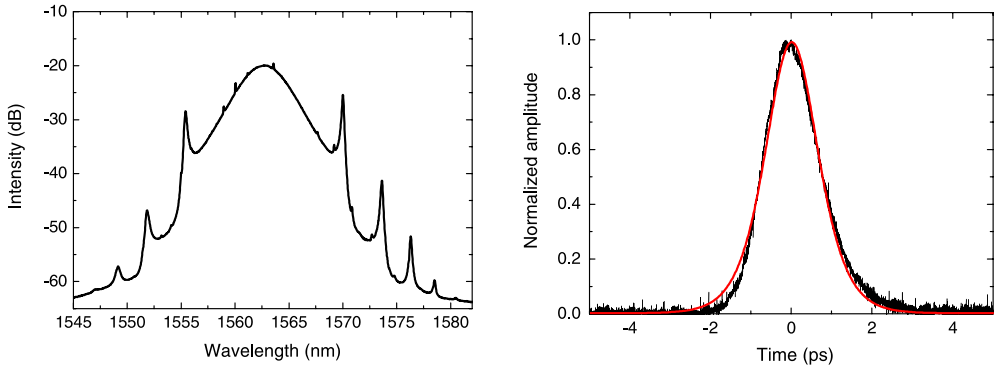

(a) (b)

Fig. 2. (Color online) (a) Spectrum and (b) corresponding autocorrelation of erbium fiber laser with a solitary absorber based on fast SESAM. The red line presents sech^2 fitting of the autocorrelation trace.

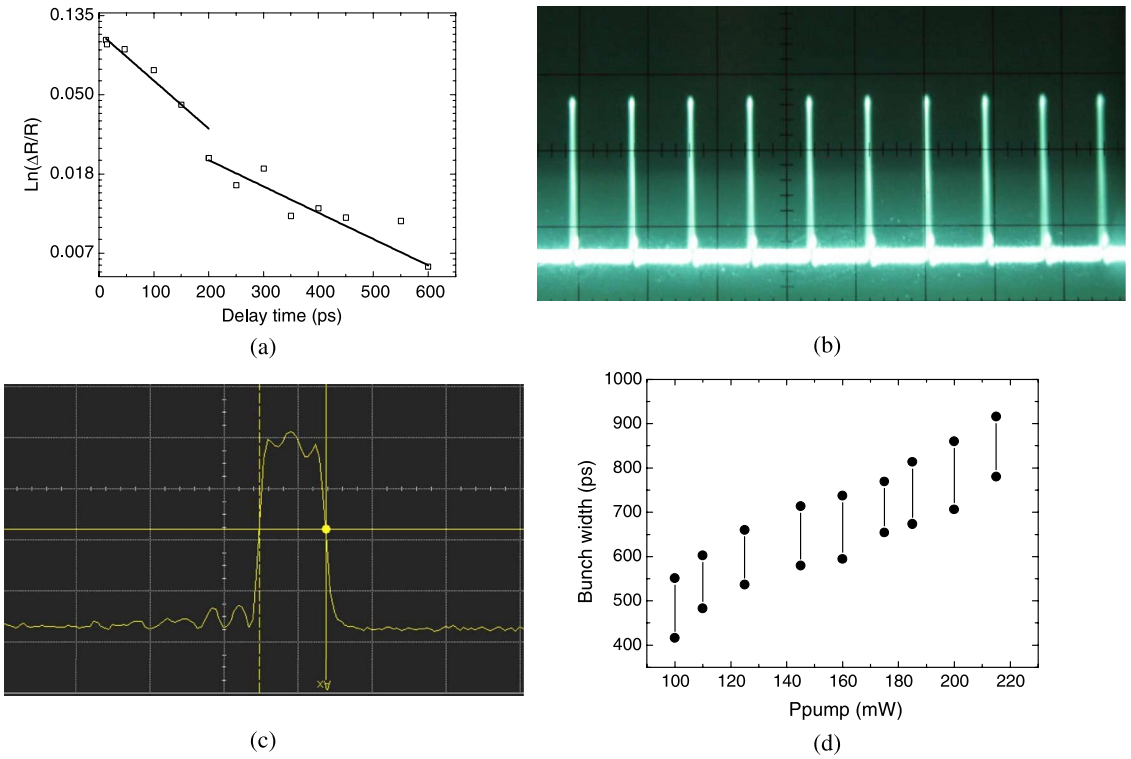

Fig. 3. (Color online) (a) Reflectivity response of SESAM with biexponential recovery time dynamics shown at logarithmic scale. The time constants of fast and slow components are 170 and 300 ps, respectively. (b) Pulse train measured by 250 MHz oscilloscope (100 ns/div.); (c) the oscilloscope picture of a soliton bunch observed with 9 GHz detection system (1 ns/div.); (d) the bunch duration versus pump power. Dots limit the upper and lower values of bunch width variation with time.

an intermediate "reformation" layer placed between the GaAs-based reflector and the InP-based absorbing section allows for flexible adjustment of absorption recovery. Self-starting mode-locked operation ensured by the SESAM with bitemporal response is achieved for pump power exceeding a certain level. The typical mode-locked pulse train measured by a 250 MHz bandwidth oscilloscope is presented in Fig. 3(b). Monitoring the scope trace reveals a surprising observation: the pulse amplitude progressively increases with pump power without signature of pulse energy "quantization" and multiple-pulse breakup expected for the soliton laser operating with anomalous dispersion. For a detailed inspection of a single bunch, we used a 9 GHz detection system, which allowed us to measure the temporal variations of the bunch width. The measurements disclosed that a "single" pulse observed in Fig. 3(b) is in fact a bunch of closely spaced pulses [Fig. 3(c)]. The bunch amplitude does not depend on output power confirming the soliton nature of pulses comprised in the bunch. The temporal length of the bunch increases with the output power, as shown in Fig. 3(d). It was also confirmed that the pulses oscillate within the bunch, which appears as a "breathing" of bunch width [5]. The competition between the repulsing and attractive forces results in oscillatory motion of the pulses within the bunch. This repetitive motion is indirectly confirmed by the presence of pedestal seen in the autocorrelation trace, shown in Fig. 4(b). The direct observation of bunches with large pulse separation suggests that the pulse oscillation is quasiperiodic.

Apparent distinctions with the regular soliton behavior are a narrower spectrum band, suppressed soliton sidebands with

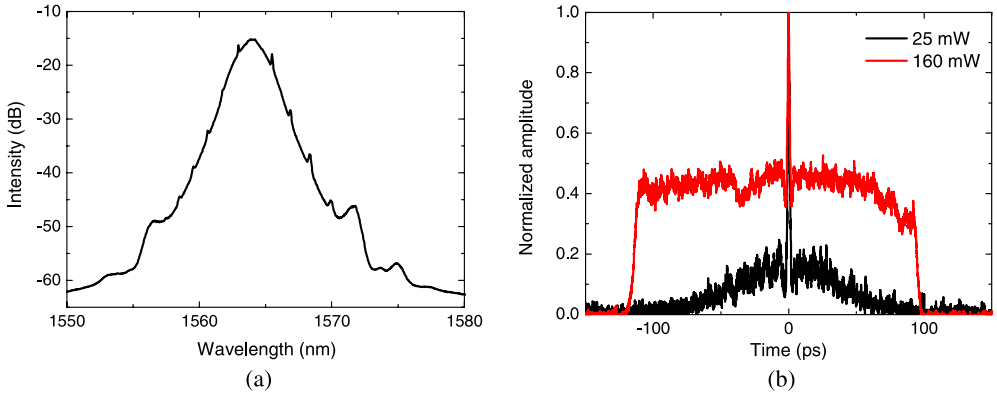

Fig. 4. (Color online) (a) Output laser spectrum and (b) autocorrelation traces at different pump power of erbium fiber laser mode locked by SESAM with bitemporal response.

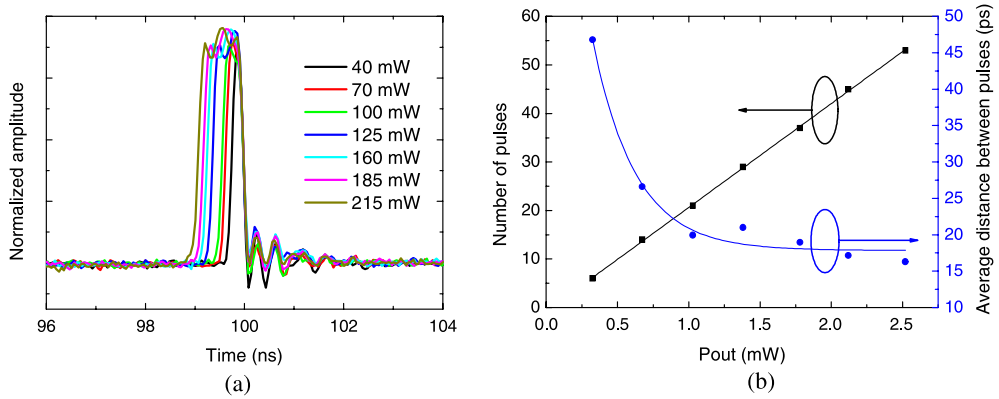

Fig. 5. (Color online) (a) Dependence of the bunch width on the pump power and number of pulses within the bunch and (b) the average distance between pulses versus output power.

wide width, and a huge pedestal in the autocorrelation. These attributes were concluded to originate from dynamic properties of bunched solitons. Indeed, large timing jitter of the pulses results in large deviations in a carrier frequency, which deteriorates the coherency of soliton perturbation inside the cavity providing a larger width of soliton sidebands. This was confirmed by observation of the correlation between the temporal width of the sidebands and spacing between the pulses for the multiple-pulse regime [21]. The bunch of randomly oscillating solitons manifests as an autocorrelation trace with a large pedestal seen from Fig. 4(b). In addition to soliton sidebands, the spectrum also contains the small-amplitude regular features independent on polarization setting known as polarization sidebands [Fig. 4(a)] [22].

Noticeable birefringence of the cavity suggests vector character of soliton in this cavity. By placing the polarization beam splitter at the laser output, we observed the stable output pulses for both polarization components [22]. Such stationary solitons composed of two orthogonally polarized phase-locked components present so-called PLVSs [7]. Prominently, this property maintains for the whole bunch of jittering vector solitons, which circulates in a cavity as a unified entity [5]. Though the presented laser supported only vector solitons, we believe that a scalar solitonlike pulse should also exhibit bunching with the presence of slowly recovering absorption in a cavity.

Comparison of single-temporal and bitemporal dynamics of absorption allows us to draw the conclusion that a slow recovery component plays a key role for bunch formation. Qualitatively, it is evident that the cluster of closely spaced soliton pulses with a duration smaller than the recovery time of the absorber suffers reduced loss compared to the train of individual pulses with a large repetition period.

The bunch collapse due to soliton merging has never been observed for any output power. This observation suggests that there is repulsive force that balances the attractive force generated by the absorber and prevents contractive collapse of the bunch. Namely, it was shown that the soliton and the nonsoliton component interaction force becomes repulsive for all solitons within a bunch [1]. The joint action of these forces provides the mechanism for pulse oscillations within the bunch, which effectively result in the autocorrelation pedestal.

Figure 5(a) shows the gradual increase of the bunch width with pump power. This dependence corresponds to the nearly linear increase in the number of soliton pulses in a bunch, shown in Fig. 5(b). The bunch amplitude independent on the pump power, as seen from Fig. 5(a), confirms the soliton origin of the pulses. These data together with measured energy of a single vector soliton allow us to estimate the number of pulses in a bunch and the average pulse separation assuming the equidistant pulse spacing, as shown in Fig. 5(b). The number of pulses increases linearly with pump power, while the pulse separation decreases with the output power and approaches asymptotically the value of ~17 ps. This interpulse interval corresponds to the ultimate contraction achievable with a given absorber. We believe that this value depends on the recovery time of slow component and saturation fluence of the absorber.

The evolution of the pulse polarization state can be examined by monitoring the radio-frequency (RF) spectrum of the pulses passed through polarization beam splitter [22]. The sidebands around the harmonics of the repetition rate frequency are the signature of the evolution of the pulse polarization since the polarization variations transform into amplitude modulation at the output of the polarizer [22]. It was shown that the sideband frequency offset from cavity harmonics, denoted as polarization evolution frequency (PEF), is a rate at which polarization evolves [7]. When polarization is locked, e.g., when the PLVS regime sets in, the RF spectrum does not exhibit sidebands, i.e., PEF = 0. A tenth harmonic of the pulse RF spectrum is shown in Fig. 6. As can be seen, the adjacent frequency components in the RF spectrum are suppressed by more than 50 dB, indicating that soliton polarization does not evolve, which confirms the formation of the PLVS within the laser cavity [7,22].

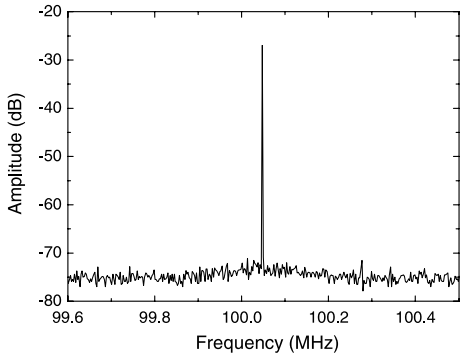

Fig. 6. Tenth cavity frequency harmonic of RF spectrum.

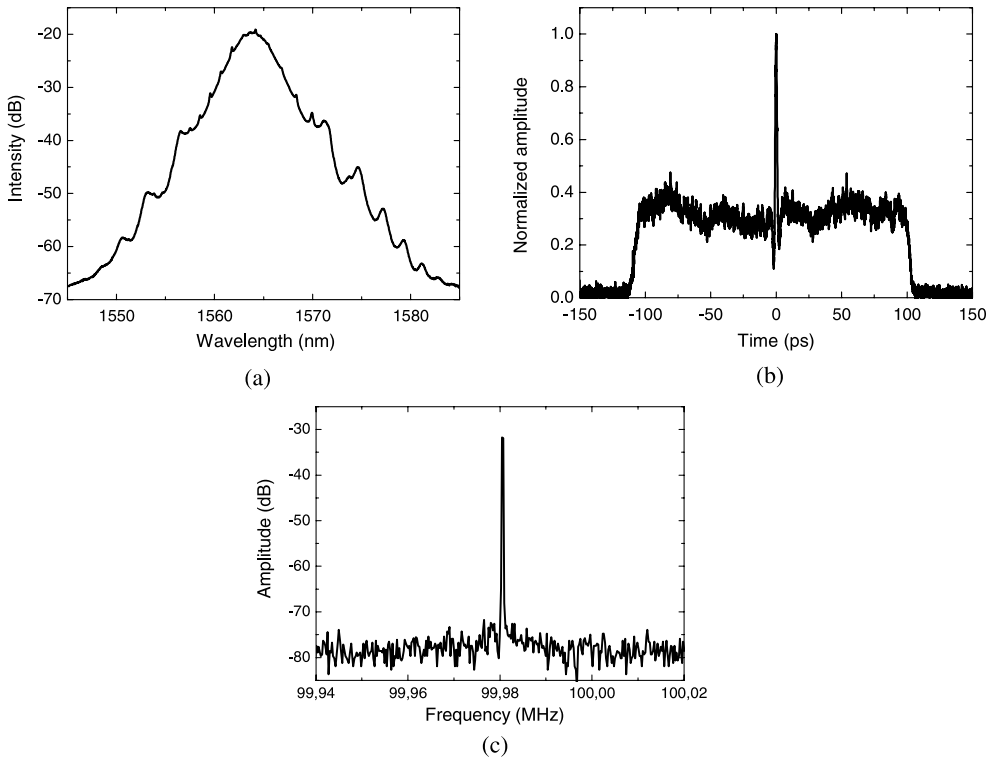

Fig. 7. (a) Laser spectrum and (b) autocorrelation trace with separate slow and fast SESAMs in the cavity; (c) RF spectrum of the tenth harmonic of pulse repetition rate frequency.

To further confirm the dominant role of slow absorption as an attractive force for vector soliton bunch formation, we have replaced the SESAM with combined bitemporal slow-and-fast response and the broadband mirror by two individual SESAMs, each producing single-exponential absorption recovery, one fast and another slow. Otherwise the laser cavity remained unchanged. With only a fast SESAM in a cavity, vector soliton bunching was not observed here for the full range of pump power. The mode-locking characteristics are shown in Fig. 2. A slow SESAM could not initiate passive mode locking by any means. The laser using individual fast and slow SESAMs in the cavity, shown in Fig. 7, reveals the behavior similar with soliton dynamics observed with a single SESAM exhibiting bitemporal response (Figs. 3–5).

The variation of the bunch width and estimated number of the pulses in the bunch are presented in Fig. 8. We believe that these measurements provide reliable evidence of the principal role of slow saturable absorption in the vector soliton bunching.

Finally, the CNT absorber was tested in the cavity instead of a fast SESAM in combination with a slow SESAM used before. The pulse spectrum and autocorrelation plotted in Fig. 9 indicate similar strong vector soliton bunching. Therefore, we can generally conclude that the principal factor responsible for the vector soliton the bunching is a presence of a slowly recovering component in the saturable absorption. The state when the pulses perfectly overlap each other, i.e., bunch collapse, was never observed, indicating that this regime is not stable against perturbations.

It should be noted that the soliton bunches observed with fast absorption only, e.g., nonlinear polarization rotation, exhibit different behavior. Particularly, pulse separation in the bunch is much larger, typically a few nanoseconds [23]. This is mainly because the strength of attractive force between

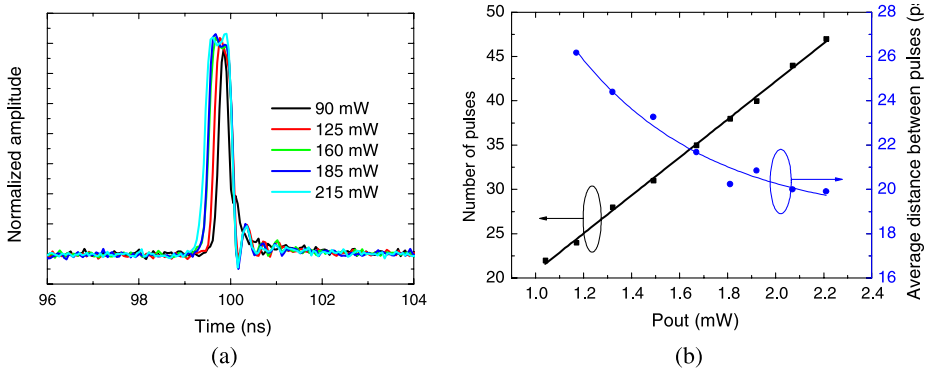

Fig. 8. (Color online) Laser with slow and fast SESAMs in the cavity. (a) Bunch width of the vector soliton depending on the pump power and variation of the pulse number and (b) the distance between pulses with the output power.

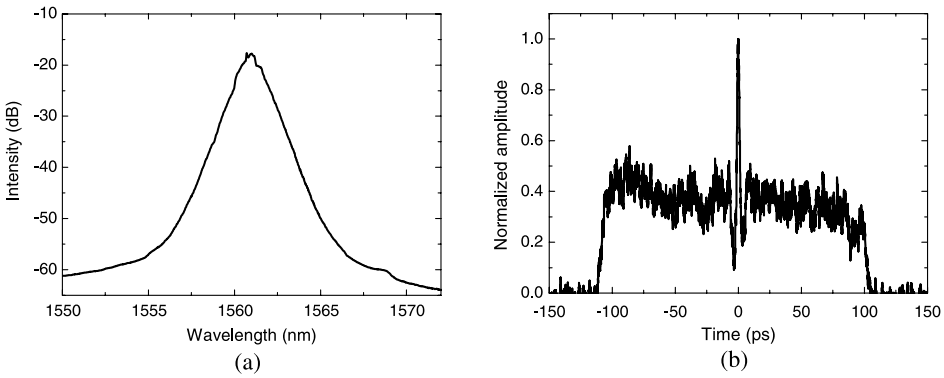

Fig. 9. (a) Spectrum and (b) autocorrelation trace of fiber laser with CNT absorber and slow SESAM in the cavity.

solitons is weak, so the repulsive force is dominant. In contrast, bunches formed with the presence of slow absorption are stationary, stable against environmental disturbances, and have temporal pulse distribution of a few tens of picoseconds. Using an SESAM with various recovery times allows us to manipulate the bunch length, particularly, to compress it. Mode-locking techniques based on artificial absorption, e.g., nonlinear polarization evolution, do not offer flexible control of the soliton interaction. Though the presented laser supported only vector solitons, we believe that a scalar solitonlike pulse should also exhibit bunching with the presence of slowly recovering absorption in a cavity.

4. CONCLUSION

The balance of the fast and slow time constants and relative contribution to the nonlinear response are shown to be a valuable instrument in laser dynamics control. It was clearly observed that, by adding the slow recovery component to the absorption, it is possible to change radically the vector soliton interaction. The slow response of absorption creates an attractive force between solitons and brings pulses closer together.

The bunch always manifests at the oscilloscope as a single pulse per cavity round trip with the number of pulses within the bunch dependent on the pump power. It indicates that the vector solitons are tightly bound in a bunch, which propagates in a cavity as a particle. The temporal width of the bunch increases with output power, indicating the increase in number of pulses in a bunch. Also, it indicates that interpulse spacing cannot be exceedingly small. It was suggested that soliton–soliton repulsive interaction pushes the solitons away. Subjected to the joint action of attractive and repulsive forces, the solitons tend to oscillate within the bunch, which is detectable as a pulse pedestal in the autocorrelation. These soliton oscillations are clearly detected as an oscillation of the bunch width observed at the autocorrelator.

The specific form of pulse interaction in a bunch also affects the optical spectrum of the pulses. Particularly, soliton oscillations in a bunch result in a significant frequency jittering. This feature results in a broadening of soliton sidebands and decreases of their amplitude, which is expected with carrier frequency fluctuations of vector solitons permanently shifting within the bunch.

If the given application has a characteristic time comparable or longer than bunch length, the group of pulses will be treated as a single pulse with total bunch energy. By varying the recovery time of slow component, it would be possible to change the temporal length of the pulse bunch. Using a saturable absorber with adjustable characteristics, e.g., an SESAM comprising the p–n junction, could provide the flexible control of pulse interaction.

REFERENCES

1. B. Grudinin and S. Gray, "Passive harmonic mode locking in soliton fiber lasers," J. Opt. Soc. Am. B **14**, 144–154 (1997).
2. J. N. Kutz, B. C. Collings, K. Bergman, S. Tsuda, S. T. Cundiff, W. H. Knox, P. Holmes, and M. Weinstein, "Mode-locking pulse dynamics in a fiber laser with a saturable Bragg reflector," J. Opt. Soc. Am. B **14**, 2681–2690 (1997).
3. J. N. Kutz, B. C. Collings, K. Bergman, and W. H. Knox, "Stabilized pulse spacing in soliton lasers due to gain depletion and recovery," IEEE J. Quantum Electron. **34**, 1749–1757 (1998).
4. M. J. Lederer, B. Luther-Davis, H. H. Tan, C. Jagadish, N. Akhmediev, and J. M. Soto-Crespo, "Multipulse operation of a Ti:sapphire laser mode locked by an ion-implanted semiconductor saturable absorber mirror," J. Opt. Soc. Am. B **16**, 895–904 (1999).
5. L. M. Zhao, D. Y. Tang, H. Zhang, and X. Wu, "Bunch of restless vector solitons in a fiber laser with SESAM," Opt. Express **17**, 8103–8108 (2009).
6. S. T. Cundiff, B. C. Collings, N. N. Akhmediev, J. M. Soto-Crespo, K. Bergman, and W. H. Knox, "Observation of polarization-locked vector solitons in an optical fiber," Phys. Rev. Lett. **82**, 3988–3991 (1999).
7. C. Collings, S. T. Cundiff, N. N. Akhmediev, J. M. Soto-Crespo, K. Bergman, and W. H. Knox, "Polarization-locked temporal vector solitons in a fiber laser: experiment," J. Opt. Soc. Am. B **17**, 354–365 (2000).
8. J. M. Soto-Crespo, N. N. Akhmediev, B. C. Collings, S. T. Cundiff, K. Bergman, and W. H. Knox, "Polarization-locked temporal solitons in a fiber laser: theory," J. Opt. Soc. Am. B **17**, 366–372 (2000).
9. O. Okhotnikov and M. Pessa, "Dilute nitride saturable absorber mirrors for optical pulse generation," J. Phys. Condens. Matter **16**, S3107 (2004).
10. H. A. Haus and Y. Silberberg, "Theory of mode locking of a laser diode with multiple-quantum-well structure," J. Opt. Soc. Am. B **2**, 1237–1243 (1985).
11. O. G. Okhotnikov and R. Herda, "Effect of complex recovery of saturable absorption on the performance of mode-locked lasers," Quantum Electron. **41**, 610–613 (2011).
12. M. Guina, N. Xiang, A. Vainionpää, O. G. Okhotnikov, T. Sajavaara, and J. Keinonen, "Self-starting stretched-pulse fiber laser mode locked and stabilized with slow and fast semiconductor saturable absorbers," Opt. Lett. **26**, 1809–1811 (2001).
13. M. Guina, N. Xiang, and O. G. Okhotnikov, "Streched-pulse fiber lasers based on semiconductor saturable absorbers," Appl. Phys. B **74**, S193–S200 (2002).
14. S. Kivistö, T. Hakulinen, A. Kaskela, D. P. Brown, A. G. Nasibulin, E. I. Kauppinen, A. Härkönen, and O. G.

Okhotnikov, "Carbon nanotube films for ultrafast broadband technology," Opt. Express **17**, 2358–2363 (2009).
15. O. Okhotnikov, A. Grudinin, and M. Pessa, "Ultra-fast fibre laser systems based on SESAM technology: new horizons and applications," New J. Phys. **6**, 177 (2004).
16. A. Vainionpää, S. Suomalainen, O. Tengvall, T. Hakulinen, R. Herda, S. Karirinne, M. D. Guina, and O. G. Okhotnikov, "Metamorphic growth of long-wavelength saturable absorber on GaAs substrates," in *Proceedings of the 18th Annual Meeting of the IEEE Lasers and Electro-Optics Society* (LEOS, 2005), paper ThN3.
17. S. Suomalainen, A. Vainionpää, O. Tengvall, T. Hakulinen, S. Karirinne, M. Guina, O. G. Okhotnikov, T. G. Euser, and W. L. Vos, "Long-wavelength fast semiconductor saturable absorber mirrors using metamorphic growth on GaAs substrates," Appl. Phys. Lett. **87**, 121106 (2005).
18. S. Suomalainen, M. Guina, T. Hakulinen, R. Koskinen, J. Paajaste, M. Karjalainen, S. Marcinkevicius, and O. G. Okhotnikov, "Semiconductor saturable absorbers with recovery time controlled by lattice mismatch and band-gap engineering," Mater. Sci. Eng. B **147**, 156–160 (2008).
19. N. Xiang, O. G. Okhotnikov, A. Vainionpää, M. Guina, and M. Pessa, "Broadband semiconductor saturable absorber mirror at $1.55\,\mu$m using Burstein–Moss shifted $Ga_{0.47}In_{0.53}As/InP$ distributed Bragg reflector," Electron. Lett. **37**, 374–375 (2001).
20. R. Herda and O. G. Okhotnikov, "Effect of amplified spontaneous emission and absorber mirror recovery time on the dynamics of the mode-locked fiber lasers," Appl. Phys. Lett. **86**, 011113 (2005).
21. R. Weill, A. Bekker, V. Smulakovsky, and B. Fischer, "Spectral sidebands and multiple formation in passively mode-locked lasers," Phys. Rev. A **83**, 043831 (2011).
22. S. T. Cundiff, B. C. Collings, and W. H. Knox, "Polarization locking in an isotropic, mode-locked soliton Er/Yb fiber laser," Opt. Express **1**, 12–21 (1997).
23. D. Y. Tang, B. Zhao, D. Y. Shen, C. Lu, W. S. Man, and H. Y. Tam, "Bound-soliton fiber laser," Phys. Rev. A **66**, 033806 (2002).

Appendix 4

Publication 4

R. Gumenyuk, M. S. Gaponenko, K. V. Yumashev, A. A. Onuschenko and O. G. Okhotnikov, "Vector Soliton Bunching in Thulium-Holmium Fiber Laser Mode-Locked with PbS Quantum-Dot-Doped Glass Absorber", IEEE Journal of Quantum Electronics, Vol. 48, No. 7, pp. 903–907, (2012).

Vector Soliton Bunching in Thulium-Holmium Fiber Laser Mode-Locked with PbS Quantum-Dot-Doped Glass Absorber

Regina Gumenyuk, Maxim S. Gaponenko, Konstantin V. Yumashev, Alexei A. Onushchenko, and Oleg G. Okhotnikov

Abstract— Saturable absorber based on PbS quantum-dot doped glasses exhibiting bi-temporal recovery dynamics provides effective means for control of vector soliton bunching in 2 μm spectral range. The slow response of absorption creates an attractive force between pulses and a bunch of tightly bounded vector solitons propagates in a cavity as an entity. Subjected to the joint action of attractive and repulsive forces, the solitons tend to oscillate within the bunch.

***Index Terms*—fiber laser, laser mode-locking, nonlinear optics, optical solitons.**

I. Introduction

SOLITON dynamics has been subject of intensive research [1-3]. Self-ordering, harmonic mode-locking, period-doubling and soliton bunching are examples of phenomena that deserved substantial theoretical and experimental efforts [4-6]. Menyuk et al. showed that two orthogonally polarized components of pulse propagating in a birefringent nonlinear environment can be coupled and propagate with equal group velocity [7]. This phenomenon underlies the formation of vector solitons in the laser cavity [8-10]. With multiple-pulse regime typical for cavities with anomalous dispersion, the vector soliton interaction could lead to a bunch development propagating as an entity at fundamental repetition rate. It was found that contrary to scalar soliton bunch behavior, the vector solitons exhibit periodic-like contractive and repulsive motion within the bunch. As it was disclosed recently [11], the slow response of absorption induces an attractive force between vector solitons resulting in a tight bunch formation with pulse temporal separation at a picoseconds scale. Therefore, it was established that details of absorption recovery could be an instrumental for vector soliton control.

Semiconductor absorbers exhibit typically both fast and slow temporal components in the recovery dynamics originated from the intraband and band-to-band transitions and resulted in bi-exponential recovery process. The balance of the fast and slow time constants and relative contribution to the nonlinear response was shown to be valuable for reliable start-up of mode-locking and pulse shaping process [12]. It was recently shown that glasses doped with PbS quantum dots (QDs) demonstrate similar bi-exponential dynamics of absorption [13]. The saturable absorption of PbS QD-doped glasses can be tailored over broad spectral range from 1 to 2.5 μm by changing the size of the dots. The nanometer size of PbS quantum dots provides strong quantum confinement effect resulted in a blue shift of the energy band gap and a strong nonlinearity close to the first excitation resonance. The large exciton Bohr radius of 18 nm and narrow bandgap of 0.41 eV produce strong confinement effect even with relatively large crystals and allow to tune the absorption resonance over 2 μm range [14]. PbS based absorbers have been used to date only with solid-state lasers [13-17].

In this article we report the first fiber laser mode-locked by PbS QD glasses. The Tm-Ho-doped fiber laser, operating in the vector soliton regime is found to exhibit tendency to strong pulse bunching. This phenomenon induced by the complex dynamics of PbS QDs absorption recovery modifies both optical spectrum and autocorrelation due to repetitive oscillations of solitons inside the bunch.

II. Setup

The setup of Tm-Ho fiber laser is shown in Fig. 1. The gain was provided by 3 m-long Tm-Ho fiber with 14 dB/m absorption at 1564 nm and anomalous dispersion 0.065 (ps/nm)/m at 1985 nm. The active fiber was pumped by 1565 nm laser through fiber pump combiner. 40%-reflectivity loop mirror was used as an output coupler while another cavity mirror was the saturable absorber. The total cavity length is 4.5 m with corresponding repetition rate of 22.75 MHz and 0.43 ps/nm net cavity dispersion.

Manuscript received January 23, 2012, revised March 16, 2012. This work was supported in part by the Graduate school in electronics, telecommunications and automation (GETA).

R. Gumenyuk and O. G. Okhotnikov are with Optoelectronics Research Centre, Tampere University of Technology, FIN-33101 Tampere, Finland (e-mail: regina.gumenyuk@tut.fi, oleg.okhotnikov@tut.fi).

M. G. Gaponenko and K. V. Yumashev are with Center for Optical Materials and Technologies, Belarusian National Technical University, 220013 Minsk, Belarus (e-mail: gap@bntu.by, kyumashev@bntu.by).

Alexei A. Onushchenko is with Research and Technological Institute of Optical Material Science, 193171 St. Petersburg, Russia (e-mail: alarkon@goi.ru).

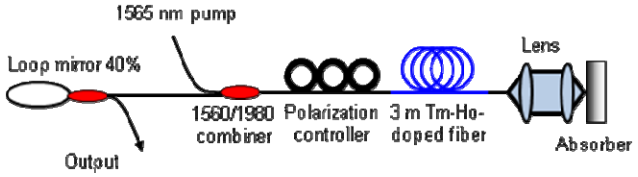

Fig. 1. The scheme of mode-locked Tm-Ho fiber laser.

Firstly, we examined the performance of the laser using SESAM with dominant fast recovery dynamics. The laser exploiting fast absorber with sufficient ultrafast time response produces stable 980 fs sech^2-pulses. Because of relatively high anomalous dispersion, the resonant sidebands are seen in optical spectrum resulted from periodic perturbations in a laser cavity (Fig. 2a). Since the laser is mode-locked in the soliton dispersion regime, it tends to produce multiple pulses per round trip because pulse energy is locked to the fundamental soliton energy (Fig. 2b). The total number of pulses in the cavity gradually increases with the output power. The distinct feature of this regime is random and unstable temporal spacing between the pulses.

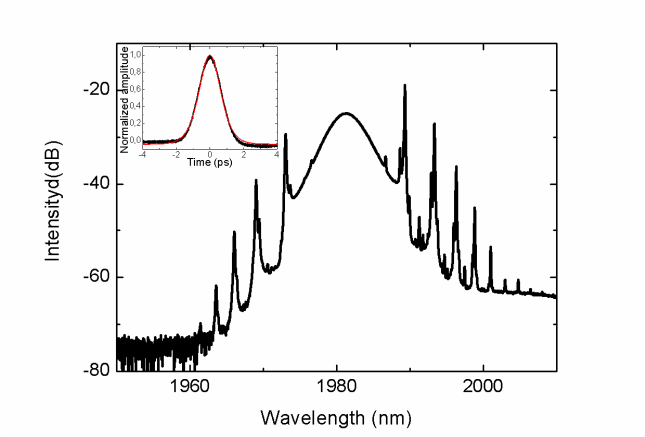

(a)

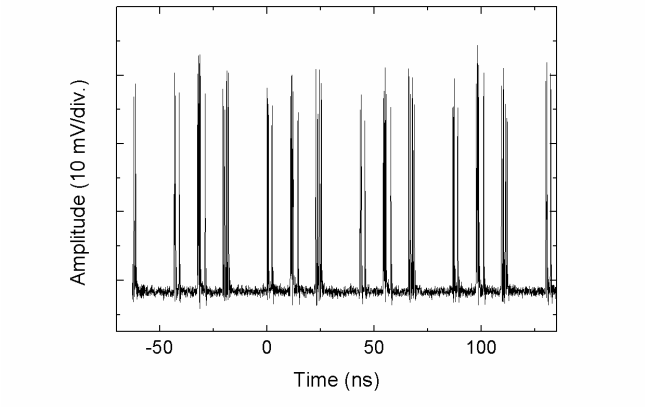

(b)

Fig. 2. Mode-locked Tm-Ho-doped fiber laser with a fast SESAM. a - spectrum and corresponding autocorrelation trace of 980 fs pulses (inset). The red line presents sech^2-fitting. b – oscilloscope view of the pulse sequence.

Soliton bunching has been never observed for whole range of available pump power, when SESAM was implemented as a mode-locking element.

III. PBS QD ABSORBER

A sample of SiO_2-Al_2O_3-NaF-Na_2O-ZnO silicate glass doped with PbS QDs quantum dots was prepared using the technique reported elsewhere [17]. The thermal treatment was adjusted to produce the PbS QDs with the absorption band edge in the spectral range of ~2 μm. The mean diameter of quantum dots in the sample was estimated to be 9 nm. Absorption spectrum of the sample is shown in the Fig. 3. The distinct absorption bands correspond to the allowed exciton states in the PbS QDs in the regime of strong quantum confinement, namely 1S-1S (1.9 μm) and 1P-1P (1.45 μm) states.

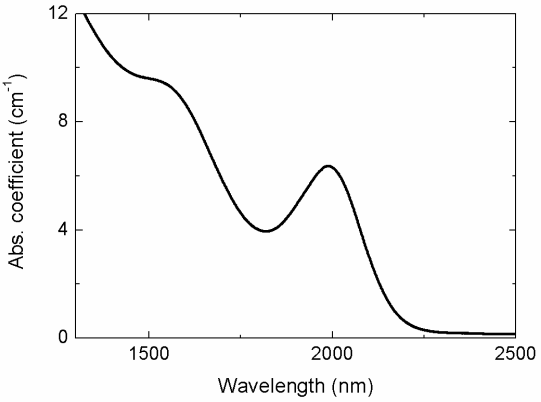

Fig. 3. Absorption spectrum of PbS QD-doped glass sample.

Intensity dependent optical transmission of PbS QD-doped glass was measured using Q-switched holmium laser with 50 ns pulse duration at 2090 nm wavelength. The saturable absorption observed in PbS-doped glass at high intensities is caused by the excitation induced state-filling effect. The intensity dependent transmission, shown in Fig. 4, was approximated using model of fast four-level nonlinear transmission with absorption from excited states. The saturation intensity derived from the simulation was 2 MW/cm2 and the ratio of excited-state absorption cross-section to the ground-state absorption cross-section was 0.1.

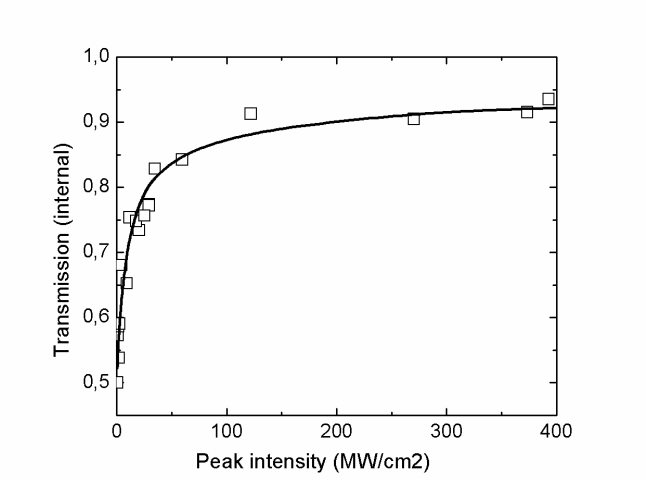

Fig. 4. Nonlinear transmission of PbS QD-doped glass sample at 2090 nm.

The nonlinear response of the sample is shown in Fig. 5. The measurement was provided by pump-probe techniques at the probe wavelength of 1.5 μm. The relaxation time constants were observed to be τ_f =6.5 and τ_s =220 ps assuming bi-temporal recovery:

$$-\Delta\mathrm{OD} = A_\mathrm{f} \exp(-t/\tau_f) + A_s \exp(-t/\tau_s), \qquad (1)$$

where ΔOD is differential absorption, A_f, A_s, τ_f and τ_s are amplitudes and relaxation times constant of fast and slow components. Since the bleaching dynamics of PbS QD-doped glasses, studied in details in [18, 19], are fairly independent on nanocryctal size, we believe that the slow and fast recovery constants at 2 μm have similar values.

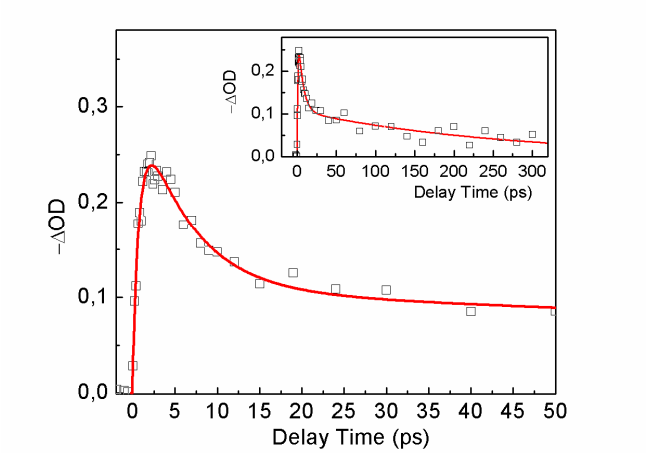

Fig. 5. The fast and slow (inset) bleaching relaxation of PbS sample. The squares are experiment data, the solid line is fitting within the two-exponential model.

IV. EXPERIMENTAL RESULTS

After complete characterization, PbS QDs-doped glass sample was used instead of SESAM in the same cavity described above. PbS absorber provides robust start-up of mode-locking with pulse characteristics shown in Fig. 6a. Monitoring the oscilloscope trace reveals remarkable observation: pulse amplitude progressively increases with pump power without signature of pulse energy "quantization" and multiple pulse break-up expected for soliton laser operating with anomalous dispersion. As it was shown earlier, this is the attribute of the vector solitons bunch formation with average pulse separation of few picoseconds, therefore, the individual pulses within the bunch cannot be distinguished by slow detection system [11]. The slow temporal component in absorber recovery was shown to generate an attractive force which organizes the solitons in a stable compact bunch propagating in a cavity at fundamental repetition rate as an integrated entity. Joint action of contraction force induced by saturable absorber and repulsive force due to soliton-soliton interaction forces the solitons oscillation within the bunch.

Figs. 6b and 6c show output spectrum and corresponding autocorrelation trace. Apparent disparities with the regular soliton behavior are reduced spectrum bandwidth, suppressed large-width soliton sidebands and remarkable pedestal in the autocorrelation. These attributes were concluded to originate from dynamic properties of bunched solitons. Indeed, large timing jitter of the pulses results in large deviations in a carrier frequency which deteriorates the coherency of soliton perturbation inside the cavity providing a larger width of soliton sidebands. This was confirmed by observation of the correlation between the temporal width of the sidebands and spacing between the pulses for multiple-pulse regime [20]. The bunch of randomly oscillating solitons manifests as an autocorrelation trace with a large pedestal seen from Fig. 6c.

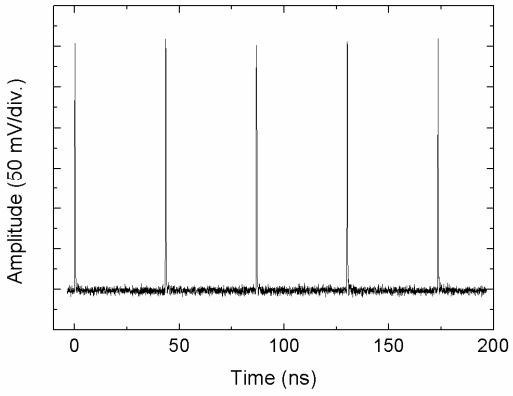

(a)

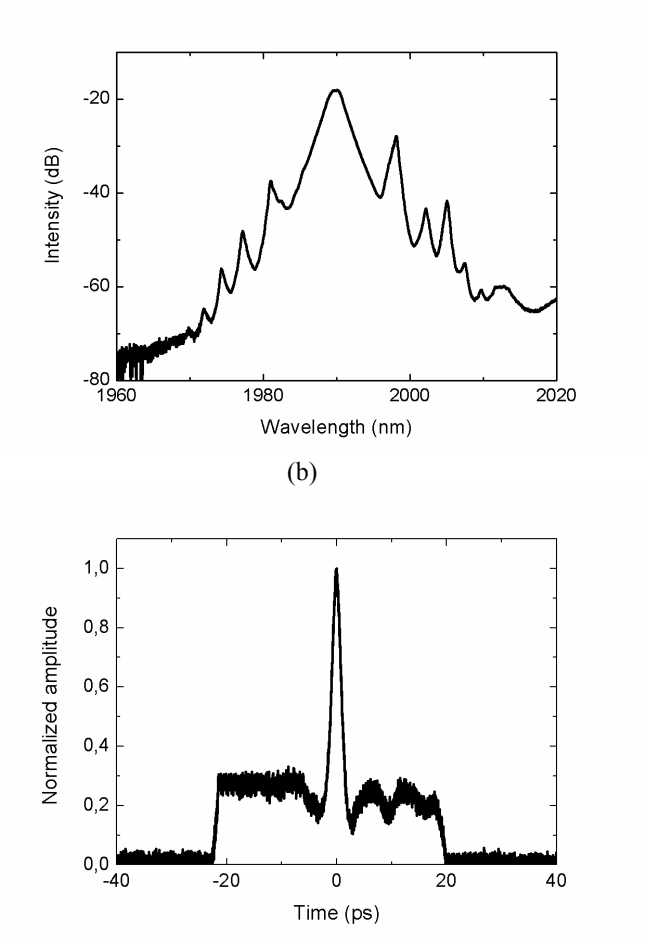

Fig. 6. Tm-Ho-doped fiber laser mode-locked by PbS QDs-doped glass absorber. a – oscilloscope picture of the pulse train; b – optical spectrum; c – autocorrelation trace.

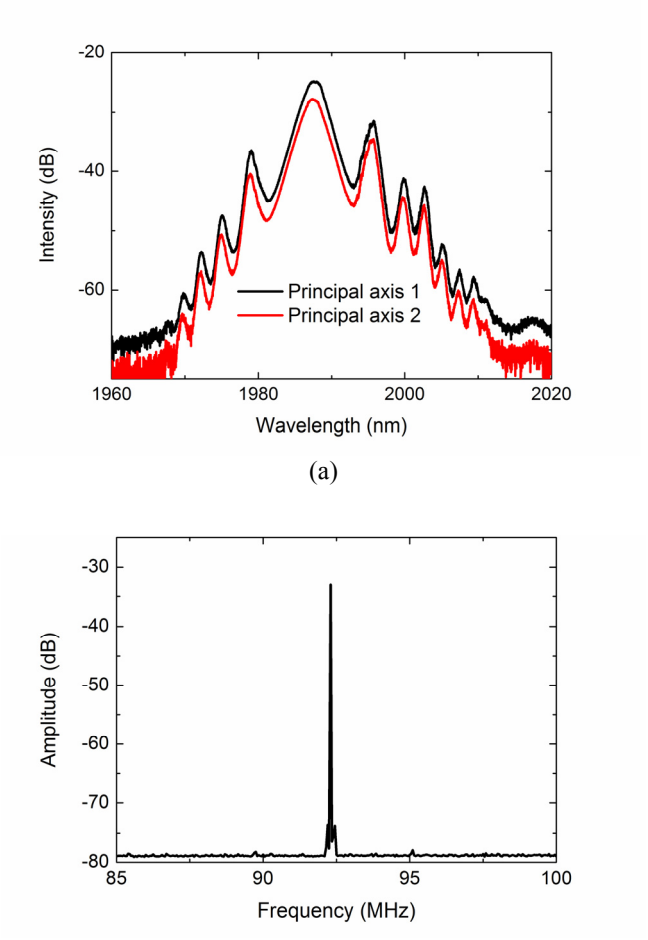

Fig. 7. a - Optical spectra for orthogonal polarizations measured at the output of polarizer; b – RF spectrum of the 4th harmonic of pulse repetition rate frequency.

The vector nature of soliton polarization state was verified from the measurement of pulses spectrum passed through the polarization beam splitter. Fig. 7a shows that pulse spectrum does not depend on the polarization indicating the vector nature of solitons. The evolution of pulse polarization state was further examined by monitoring the radio-frequency (RF) spectrum of the pulses [8]. The sidebands around the harmonics of the repetition rate frequency are the signature of the temporal evolution of pulse polarization since the polarization variations transform into amplitude modulation at the output of polarizer. It was shown that the sideband frequency offset from cavity harmonics denoted as polarization evolution frequency (PEF), is a rate at which polarization evolves [9]. When polarization is locked, e.g. polarization-locked vector solitons (PLVS) regime sets in, the RF spectrum does not exhibit sidebands, i.e. PEF=0. A 4th harmonic of pulse RF spectrum is shown in Fig. 7b. As it can be seen, the adjacent frequency components in RF spectrum are strongly suppressed indicating that soliton polarization does not evolve which confirms the formation of PLVS within the laser cavity [9, 20].

The state when the pulses perfectly overlap each other was never observed indicating that this regime is not stable against perturbations.

V. CONCLUSIONS

In conclusions, we investigated the formation of vector soliton bunches in the Tm-Ho-doped fiber laser mode-locked by PbS QD-doped glasses. Slow recovery component of the PbS absorber exhibiting bi-temporal dynamics generates an attractive force between the pulses while fast recovery mechanism provides start-up of mode-locking and contributes to pulse shaping. The soliton-soliton interaction induces the repulsive force between pulses balancing the contractive force and leads to stable bunch formation. The joint action of two forces results in solitons oscillation within the bunch which is detectable as a pulse pedestal in the autocorrelation. Specific form of vector soliton interaction in a bunch affects also the optical spectrum of the pulses. Particularly, soliton oscillation in a bunch results in a significant frequency jittering. This feature results in broadening of soliton sidebands and decrease of their amplitude which is expected with carrier frequency fluctuations of vector solitons oscillating within the bunch.

REFERENCES

[1] W. H. Loh, A.B. Grudinin, V.V. Afanasjev, and D.N. Payne, "Soliton interaction in the presence of a weak nonsoliton component," Opt. Lett., vol. 19, pp. 698 – 700, 1994.

[2] D.Y. Tang, B. Zhao, and L.M. Zhao, "Soliton interaction in a fiber ring laser," Phys. Rev. E, vol. 72, 016616, 2005.

[3] L.M. Zhao, D.Y. Tang, and D. Liu, "Ultrahigh-repetition-rate bound-soliton fiber laser," Appl. Phys. B, vol. 99, pp. 441-447, 2010.

[4] A.B. Grudinin, D.J. Richardson, and D.N. Payne, Electron. Lett., vol. 29, 1860, 1993.

[5] L.M. Zhao, D.Y. Tang, F. Lin and B. Zhao, "Observation of period-doubling bifurcations in a femtosecond fiber soliton laser with dispersion management cavity," Opt. Exp., vol. 12, pp. 4573-4578, 2004.

[6] D.J. Richardson, R.I. Laming, D.N. Payne, V.J. Matsas, and M.W. Philips, Electron. Lett., vol. 27, 1451, 1991.

[7] C.R. Menyuk, "Stability of solitons in birefringent optical fibers. I: Equal propagation amplitudes" Opt. Lett., vol. 12, pp. 614-616, 1987.

[8] S.T. Cundiff, B.C. Collings, and W.H. Knox, "Polarization locking in an isotropic, modelocked soliton Er/Yb fiber laser," Opt. Exp., vol. 1, pp. 12 – 20, 1997.

[9] B.C. Collings, S.T. Cundiff, N.N. Akhmediev, J.M. Soto-Crespo, K. Bergman, and W.H. Knox, "Polarization-locked temporal vector solitons in a fiber laser: experiment," J. Opt. Soc. Am. B, vol. 17, pp. 354–365, 2000.

[10] L.M. Zhao, D.Y. Tang, H. Zhang, and X. Wu, "Polarization rotation locking of vector solitons in a fiber ring laser," Opt. Exp. vol. 16, pp. 10053–10058, 2008.

[11] R. Herda and O.G. Okhotnikov, "Effect of complex recovery of saturable absorber on the performance of mode-locked lasers", IOP Quantum Electronics, vol. 41, pp. 610-613, 2011.

[12] R. Gumenyuk and O.G. Okhotnikov, "Temporal control of vector soliton bunching by slow/fast saturable absorption," J. Opt. Soc. Am. B, vol. 29, 1-7, 2012.

[13] K. Wudke, S. Pötting, J. Auxier, A. Schülzgen, N. Peyghambarian, and N.F. Borelli, "PbS quantum-dot-doped glasses for ultrashort-pulse generation," Appl. Phys. Lett., vol. 76, pp. 10-12, 2000.

[14] A.A. Lagatsky, C.G. Leburn, C.T.A. Brown, W. Sibbett, S.A. Zalotovskaya, E.U. Rafailov, "Ultrashort-pulse lasers passively mode locked by quantum-dot-based saturable absorbers," Progress in Quantum Electron., vol. 34, pp. 1-45, 2010.

[15] K. Wudke, S. Pötting, J. Auxier, A. Schülzgen, N. Peyghambarian, and N.F. Borelli, "PbS quantum-dot-doped glasses for ultrashort-pulse generation," Appl. Phys. Lett. vol. 76, pp. 10-12, 2000.

[16] A.A. Lagatsky, A.M. Malyarevich, V.G. Savitsky, M.S. Gaponenko, K.V. Yumashev, A.A. Zhilin, C.T.A. Brown, and W. Sibbett, "PbS quantum-dot-doped glass for efficient passive mode-locking in a CW Yb:KYW laser," IEEE Photon. Technol. Lett., vol. 18, pp. 259-261, 2006.

[17] A.M. Malyarevich, V.G. Savitski, M.S. Gaponenko, K.V. Yumashev, A.A. Lagatsky, W. Sibbett, A.A. Lipovskii, H. Raaben, and A.A. Zhilin, "PbS-doped glass saturable absorbers for mode-locked and Q-switched near IR lasers," in Conference *Advanced Solid-State Photonics* (Optical Society of America, 2005), paper 102.

[18] A.A. Onushchenko, A.A. Zhilin, G.T. Petrovskii, E.L. Raaben, M.S. Gaponenko, A.M. Malyarevich, K.V. Yumashev, and V.V. Golubkov, "Nanostructured glass-crystal materials with lead sulfide for passive Q switching of IR lasers," J. Opt. Technol., vol. 73, pp. 576-583, 2006.

[19] M. S. Gaponenko, O. V. Buganov, A. A. Onushchenko, S. G. hickey, A. M. Malyarevich, S. A. Tikhomirov, and K. V. Yumashev, "Exiton relaxation in PbS quantum dots," Phys. Status Solidii RRL vol. 4, pp. 341-343, 2010.

[20] R. Weill, A. Bekker, V. Smulakovsky, and B. Fischer, "Spectral sidebands and multiple formation in passively mode-locked lasers," Phys. Rev. A, vol. 83, 043831, 2011.

Regina Gumenyuk (M'08) received the M.Sc. degree in microelectronics from Saint-Petersburg State Electrotechnical University, Russia, in 2008. She is currently working towards the Ph.D. degree at the Optoelectronics Research Centre, Tampere University of Technology, Tampere, Finland.

Her doctoral research concerns applications of ultrafast fiber lasers.

Maxim Gaponenko graduated from Belarusian State University in 2003 and received the Ph.D. degree in optics from Belarusian National Technical University in 2011.

He is presently a Head of Department of Optics of Glass and Crystalline Materials, Center for Optical Materials and Technologies of Belarusian National Technical University. His research interests include spectroscopy of rear-earth doped laser materials and semiconductor nanostructures, as well as investigation and development of infrared lasers.

Konstantin Yumashev received the M.S. degree in physics from Belarusian State University, Minsk in 1979 and Doctor of Science degree in laser physics from Institute of Physics of Belarusian Academy of Science, Minsk in 2003, and the Professor degree in physics from Belarusian National Technical University in 2005.

He is presently a Head of the Center for Optical Material and Technologies of Belarusian National Technical University, where he conducts research on the optical properties of new laser materials and development of Q-switched and mode-locked lasers. His professional research has involved the ultrafast spectroscopy of crystals doped with transition metal ions and rear-earth elements as well as semiconductor nanocrystals.

Alexei Onushchenko graduated from Leningrad State University in 1975 where received the B.S. degree in physics of semiconductors. The Ph.D. degree in optics of low dimensional systems he received from S.I. Vavilov State Optical Institute, Leningrad, in 1989.

He is a Senior Researcher in Glass-Ceramics Lab, Research and Technology Institute of Optical Materials Science, St. Petersburg. His current research interests include study of formation and structure of semiconductor doped glasses, their spectroscopic and non-linear optical properties.

Oleg G. Okhotnikov received the Ph.D. degree from the P. N. Lebedev Physical Institute, Moscow, Russia, and the D.Sc. degree from the General Physics Institute, Russian Academy of Sciences, Moscow, Russia, in 1981 and 1992, respectively, both in laser physics.

Since 1999, he has been a Full Professor at the Optoelectronics Research Centre, Tampere University of Technology, Tampere, Finland. He has published over 100 journal papers.

Appendix 5

Publication 5

R. Gumenyuk and O. G.Okhotnikov, ”Impact of gain medium dispersion on stability of soliton bound states in fiber laser”, IEEE Photonics Technology Letters, Vol. 25, No. 2, pp. 133–135 (2013).

Impact of gain medium dispersion on stability of soliton bound states in fiber laser

Regina Gumenyuk and Oleg G. Okhotnikov

***Abstract*— Effect of the gain medium dispersion on stability of soliton groups in fiber laser has been studied. An attractive force produced by bi-temporal saturable absorber was used to enhance the soliton interaction and resulted in a firm bound state formation. It was found that active media supporting soliton formation cause their irregular bunching in the fiber cavity, while the gain media with normal non-soliton dispersion demonstrate stationary bound state soliton generation. The results provide guidelines for synthesis of optimal dispersion map for soliton fiber lasers.**

***Index Terms*— fiber laser, laser mode-locking, nonlinear optics, optical solitons.**

I. Introduction

Over the last decade, the soliton interaction in fiber lasers have attracted considerable attention, particularly the soliton bunching, bound states dynamics, vector and dissipative soliton generation. Though the soliton laser operates in the net negative (anomalous) cavity dispersion regime, the details of dispersion map produce tremendous impact on the character of the soliton interactions.

Due to generic property of soliton known as energy quantization, the multiple soliton regime sets in at sufficient level of pumping. Various scenarios of multiple soliton operation have been observed. The role of specific form of the dispersion map on the soliton bunching has not been clearly addressed. Though the bound states of solitons in fiber lasers have been observed either with normal and anomalous cavity net dispersion, the gain section of the laser always exhibited normal dispersion [1]-[4]. This paper presents the results that clearly demonstrate the imperative role of dispersion of the gain medium. The effect of gain medium dispersion has been experimentally examined in the two versions of similar fiber laser, one with anomalous and another with normal dispersion. The net cavity dispersion was kept unchanged after switching the sign of gain medium dispersion.

We use the semiconductor saturable absorber mirror (SESAM) having a temporal response on two time scales, fast and slow, as describe earlier [5]. The slow component, exhibiting the recovery time comparable to interpulse spacing, provides the mechanism for pulse attraction and results in reduced losses for closely-spaced pulses forming the bunch. The absorbers exhibiting bi–exponential absorption recovery were prepared by using metamorphic growth providing simultaneously strong fast and slow components [6], [7].

Manuscript received July 3, 2012, revised October 23, 2012, accepted November 19, 2012. This work was supported in part by the Graduate school in electronics, telecommunications and automation (GETA).

R. Gumenyuk and O. G. Okhotnikov are with Optoelectronics Research Centre, Tampere University of Technology, FIN-33101 Tampere, Finland (e-mail: regina.gumenyuk@tut.fi, oleg.okhotnikov@tut.fi).

II. Experimental

The effect of gain medium dispersion on the soliton interaction was studied in fiber laser shown in Fig. 1 using two erbium fibers with opposite sign of group–velocity dispersion (GVD). One 13 m long segment has anomalous dispersion of +1.1 (ps/nm)/ km at 1600 nm and another 0.5 m long erbium fiber has normal dispersion of –46 (ps/nm)/ km at 1560 nm. Both Er–doped fibers were pumped by 980 nm diode laser through dichroic fiber coupler. All passive fibers used in the cavity are standard single mode fibers with anomalous dispersion of +18 (ps/nm)/ km. The cavity was terminated by butt-coupled high reflective mirror from one side and lens-coupled SESAM from another side. To identify the role of gain dispersion, after switch of the active medium the cavity dispersion was kept the same by varying the length of passive fiber. The net cavity dispersion was +0.16 ps/nm for each case.

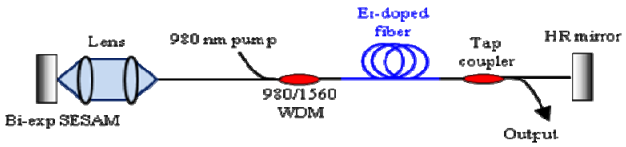

Fig. 1. Experimental setup of mode-locked erbium doped fiber laser.

Since the laser is mode-locked in the soliton dispersion regime, it tends to produce multiple pulses per round trip because pulse energy is locked to the fundamental soliton energy [8]-[10]. The total number of pulses in the cavity gradually increases with the output power. The distinct feature of this regime is random and unstable temporal spacing between the pulses.

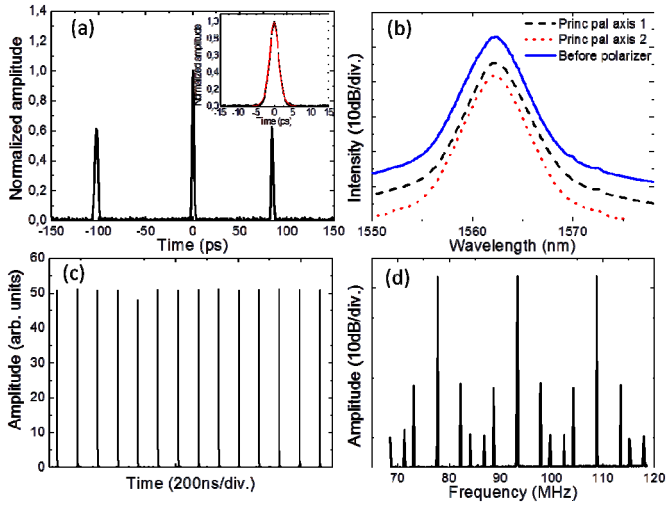

Fig. 2. Output laser characteristics with normal dispersion of Er-doped fiber. a – autocorrelation trace (in the inset central pulse and its fitting); b – corresponding spectra, measured before and after polarizer; c – oscilloscope picture of the pulse train; d – RF spectrum.

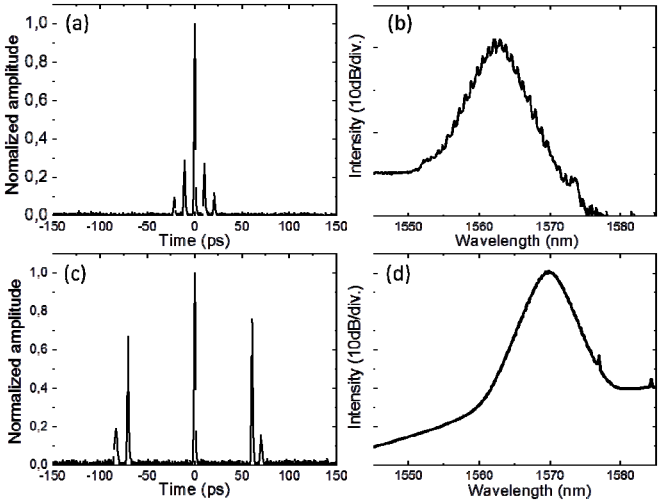

Fig. 3. Bound soliton group autocorrelations and corresponding spectra for normal dispersion of the gain medium and SESAM with the recovery time of saturable absorption of ~1 ps (a, b) and ~100 ps (c, d).

First we described the laser with the gain medium having normal GVD. Fig. 2(a, b) show the autocorrelation and optical spectrum representing typical characteristics of bound solitons.

Large separation of bound states we ascribed to the action of SESAM having ~100 ps recovery of slow component. Steady-state bound soliton groups circulate in the cavity at the fundamental repetition rate of 15.7 MHz (Fig. 2c). Only bound soliton pairs were observed within the group, likely due to relatively large separation of pulses. The notable feature of the laser exploiting bi-temporal SESAM as a mode-locking element is that the soliton interaction is strongly affected by an attractive force induced by saturable absorption [5]. Particularly, it was found that the separation of bound soliton decreases with the decrease in the recovery time of the saturable absorber, as seen from Fig. 3, however, the group formation was never observed with SESAM exhibiting only fast sub-picosecond component in absorption recovery. The examination of soliton polarization indicates their vector nature (Fig. 2b). RF spectrum, shown in Fig. 2d, comprises the fundamental frequency of the cavity and its harmonics separated by 4.5 MHz and 5.625 MHz.

Next, the gain section with normal dispersion was replaced by 13 m of erbium fiber with anomalous dispersion. The value of net cavity dispersion was kept the same by changing the length of passive fiber. The fundamental repetition rate in this case was 6.2 MHz. The distinct feature of the operation is soliton bunching with irregular nonstationary soliton behavior within the bunch, as shown in Fig. 4. It was recently shown that the soliton and the nonsoliton components interaction force provides the mechanism for pulse oscillations within the bunch. The repulsive soliton force is balanced by the attractive force generated by slowly recovering component of saturable absorber. Apparent distinctions of bunched soliton are narrower spectrum band, suppressed soliton sidebands with large pedestal in the autocorrelation. These attributes were concluded to originate from irregular dynamic properties of bunched solitons as discussed in [5], [12]. The larger bandwidth of Kelly sidebands indicates that the resonant phase-matching condition is strongly violated by significant random phase component of the solitons. Random motion of the pulses provoked by joint action of SESAM induced soliton attraction and soliton repulsive force could be avoided neither by polarization adjusting nor by changing other laser parameters. At the autocorrelation trace shown in Fig. 4a, these chaotic oscillations of multiple pulses manifest as a large pedestal due to averaging effect induced by slow scanning of autocorrelator. The bunched pulses still preserved the vector nature, as can be concluded from Fig. 4b. The operation regime with stationary bound solitons has never been observed with anomalous GVD gain medium neither by changing the pump power level nor by aligning the cavity. It can, therefore be concluded that gain media with anomalous dispersion provokes temporal instability within the soliton group. This phenomenon can be attributed to an explosive increase in amplitude and corresponding pulsewidth change observed for soliton formed in gain media which eventually leads to soliton collapse [13], [14]. The results of this study are in agreement with the observation made in number of publications showing that stable bound soliton states with fixed separation have never been obtained in lasers with soliton supporting gain media [5], [12], [15].

Though, the models of fiber laser, operated in the bound states regime, were developed earlier [1], [13], [14], [16], the analysis has been done in terms of net cavity dispersion without close inspection of the effect of dispersion map shape. Particularly, the imperative role of gain medium dispersion in soliton regime for small-scale temporal instability within soliton group was not shown. The detailed simulations of fiber lasers with various dispersion maps are now in progress.

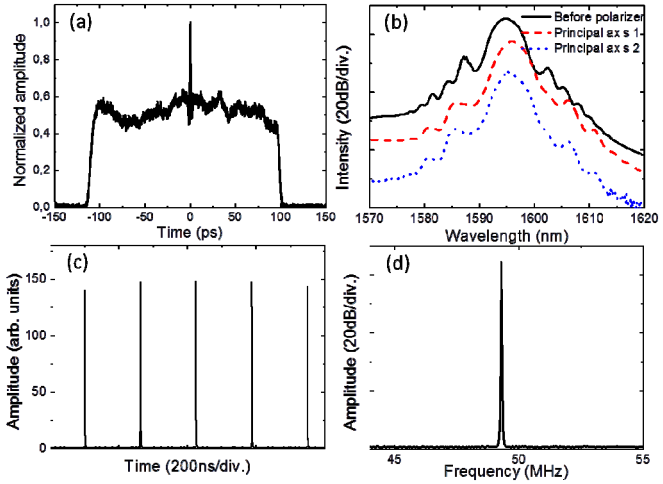

Fig. 4. Er-doped fiber laser with anomalous dispersion of active medium. a – autocorrelation trace; b - corresponding spectra, measured before and after polarizer; c – oscilloscope image of pulse train; d - RF spectrum of 8th cavity harmonic.

III. Conclusion

In conclusion, we demonstrate the crucial impact of gain medium dispersion on the formation of soliton bound states. The soliton interaction enhanced by an attractive force produced by the slow recovering component of saturable absorber allows for the detail investigation of soliton group structure and stability. The mechanism of soliton group formation with the presence of the slow recovering saturable absorber is apparent: tightly spaced solitons suffer reduced loss, which promotes soliton group formation. Slower recovery time provides larger time frame for the group. Moreover, the fast recovery component is responsible for short pulse regime start-up, while the slow component brings solitons together, enhances their interaction and results in soliton group formation.

Though the role of the dispersion map strength on the soliton energy was studied theoretically by Bale et al. [17], in this study we consider another aspect of dispersion mapping, particularly, the impact of gain medium dispersion when the average dispersion and the map strength are kept unchanged. We have found that the dispersion map strength and average dispersion have little effect for a given sign of active medium dispersion. However, the switching of the gain dispersion from normal to anomalous changes radically the soliton dynamics. Although the cavity with normal dispersion gain medium supports stable bound solitons, the anomalous gain dispersion leads to soliton bunch formation with irregular pulse motion.

Acknowledgment

This work was supported by the Federal Agency on Science and Education in the course of the federal targeted programs "Research and Development in Priority Fields of the Scientific and Technical Complex of Russia (2007–2012)" and "Scientific and Pedagogical Personnel of Innovative Russia (2009–2013)."

The authors thank I.O. Zolotovskii from Ul'yanovsk State University, Russia, for helpful discussions.

IV. References

[1] D. Y. Tang, B. Zhao, D. Y. Shen, and C. Lu, W. S. Man and H. Y. Tam, "Bound-soliton fiber laser," Phys. Rev A 66, no. 3, pp. 033806-1-033806-6 , 2002.

[2] D. Y. Tang, W. S. Man and H. Y. Tam, P. D. Drummond, "Observation of bound states of solitons in a passively mode-locked fiber laser," Phys. Rev. A 64, no. 3, pp. 033814-1-033814-3, 2001.

[3] Y. D. Gong, P. Shum, D. Y. Tang, C. Lu, T. H. Cheng, Z. W. Qi, Y. L. Guan, W. J. Lai, W. S. Man, and H. Y. Tam, "Bound solitons with 103-fs pulse width and 585.5-fs separation from Di-NOLM figure-8 fiber laser," Microwave and Optical Technology Letters 39, no. 2, pp. 163-164, 2003.

[4] B. Ortaç, A. Hideur, T. Chartier, M. Brunel, P. Grelu, H. Leblond, and F. Sanchez, "Generation of bound states of three ultrashort pulses with a passively mode-locked high-power Yb-doped double-clad fiber laser," IEEE Photon. Tech. Lett. 16, no. 5, pp. 1274-1276, 2004.

[5] R. Gumenyuk, O.G. Okhotnikov, "Temporal control of vector soliton bunching by slow/fast saturable absorption," J. Opt. Soc. Amer. B 29, no. 1, pp. 1-7, 2012.

[6] Vainionpää, S. Suomalainen, O. Tengvall, T. Hakulinen, R. Herda, S. Karirinne, M. D. Guina and O. G. Okhotnikov, **"**Metamorphic growth of long-wavelength saturable absorber on GaAs substrates", 18th Annual Meeting of the IEEE Lasers and Electro-Optics Society (LEOS), 2005, Sydney, Australia, paper ThN3.

[7] S. Suomalainen, M. Guina, T. Hakulinen, R. Koskinen, J. Paajaste, M. Karjalainen, S. Marcinkevicius and O. G. Okhotnikov, "Semiconductor saturable absorbers with recovery time controlled by lattice mismatch and band-gap engineering", Materials Science and Engineering B. 147, no. 2-3, pp. 156-160, 2008.

[8] B. Grudinin and S. Gray, "Passive harmonic mode locking in soliton fiber lasers," J. Opt. Soc. Amer. B 14, no.1, pp. 144–154, 1997.

[9] J. N. Kutz, B. C. Collings, K. Bergman, S. Tsuda, S. T. Cundiff, W. H. Knox, P. Holmes, and M. Weinstein, "Modelocking pulse dynamics in a fiber laser with a saturable Bragg reflector," J. Opt. Soc. Amer. B 14, no. 10, pp. 2681–2690, 1997.

[10] J. N. Kutz, B. C. Collings, K. Bergman, and W. H. Knox, "Stabilized pulse spacing in soliton lasers due to gain depletion and recovery", IEEE J. Quant, Electron 34, No. 9, pp. 1749-1757, 1998.

[11] C. Collings, S. T. Cundiff, N. N. Akhmediev, J.M. Soto-Crespo, K. Bergman, and W. H. Knox, "Polarization-locked temporal vector solitons in a fiber laser: experiment", J. Opt. Soc. Amer. B 17, no. 3, pp. 354-365, 2000.

[12] L. M. Zhao, D. Y. Tang, H. Zhang, and X. Wu, "Bunch of restless vector solitons in a fiber laser with SESAM," Opt. Exp. 17, no. 10, pp. 8103-8108, 2009.

[13] D. Y. Tang, L. M. Zhao and B. Zhao, "Soliton collapse and bunched noise-like pulse generation in a passively mode-locked fiber ring laser," Opt. Exp. 13, no. 7, pp. 2289-2294, 2005.

[14] A. I. Chernykh, and S. K. Turitsyn, "Soliton and collapse regimes of pulse generation in passively mode-locking laser systems," Opt. Lett. 20, no. 4, pp. 398-400, 1995.

[15] R. Gumenyuk, M.S. Gaponenko, K.V. Yumashev, A.A. Onushchenko, O.G. Okhotnikov, "Vector soliton bunching in thulium-holmium fiber laser mode-locked with PbS quantum-dot-doped glass absorber," IEEE J. Quant. Electron. 48, no. 7, pp.903-907, 2012.

[16] L. M. Zhao, D.Y. Tang, T.H. Cheng, C. Lu, H.Y. Tam, X. Q. Fu, S.C. Wen, "Passive harmonic mode locking of soliton bunches in a fiber ring laser," Opt. Quant. Electron 40, no. 13, pp. 1053-1064, 2008.

[17] B.G. Bale, S. Boscolo, S.K. Turitsyn, "Dissipative dispersion-managed solitons in mode-locked lasers," Opt. Lett 34, no. 21, pp. 3286-3288, 2009.

Appendix 6

Publication 6

R. Gumenyuk and O. G. Okhotnikov, ”Multiple Soliton Control in Fiber Lasers by Active Intensity Modulation”, IEEE Photonics Technology Letters, Vol. 25, No. 5, pp. 454–456 (2013).

Multiple Soliton Control in Fiber Lasers by Active Intensity Modulation

Regina Gumenyuk and Oleg G. Okhotnikov

***Abstract*—We demonstrate the method of stable bound solitons formation by applying the active loss modulation into the cavity. The modulation at high harmonic of cavity frequency could efficiently prevent irregular soliton bunching and result in the development of a stationary group of pulses with locked phases.**

***Index Terms*— fiber laser, mode-locking, optical solitons, bound solitons.**

I. Introduction

MULTIPLE pulse regime is a generic property of soliton fiber lasers originated from energy quantization in such systems [1-4]. Conclusions derived from the analysis using complex Ginzburg-Landau equation and then confirmed experimentally show that the separation and relative phases between the solitons determine the pulse states formed in the laser cavity [5]-[7]. Particularly, soliton interaction could lead to both bound solitons or bunches of chaotically oscillating solitons [8]. It was observed that random phase variations cause random soliton interaction [9]. Though the soliton bunch circulates as a unity in the laser cavity, the soliton separations in the bunch change randomly. Hence, the soliton bunch is nonstationary state, which is less stable than bound soliton state. Since the soliton interaction depends strongly on the relative phases of solitons, the presence of dispersive wave could cause irregular soliton motion. It was observed that soliton stability improves when background noise is suppressed [8]. The dispersive wave, however, always exists in a laser cavity indicating soliton perturbation at every round trip. The temporal stability can be improved by applying an active mode-locking using amplitude or phase modulation. The regular loss variation opens the low-loss window in time domain which reduces pulse excursion thus suppressing the phase noise and providing the stabilization of relative pulse position in the cavity. With a phase modulation, the noise accompanied the solitons experiences the gradual frequency shift and is eventually filtered out [10].

Manuscript received July 3, 2012, revised October 11, 2012. This work was supported in part by the Graduate school in electronics, telecommunications and automation (GETA).

R. Gumenyuk and O. G. Okhotnikov are with Optoelectronics Research Centre, Tampere University of Technology, FIN-33101 Tampere, Finland (e-mail: regina.gumenyuk@tut.fi, oleg.okhotnikov@tut.fi).

In this paper, we demonstrate the formation of stable bound solitons from irregular bunching state when active intensity modulation is induced into the cavity. Once the regular loss variations dominate over phase noise, the solitons appear in the cavity as a stationary group of pulses.

II. Experimental Work and Results

The linear cavity setup of fiber laser is shown in Fig. 1. The gain was provided by a 2 m-long erbium-doped fiber pumped by 980 nm diode laser through dichroic coupler. The pump and output power were 220 mW and 1.5 mW, respectively. The laser cavity is terminated by the lens-coupled bi-exponential absorber, described elsewhere [11], [12] and broadband mirror butt-coupled to the fiber. The output was taken from the 90% tap-coupler. The total cavity length was 10 m, corresponding to a pulse repetition rate of 10.3 MHz and 0.27 ps/nm net cavity dispersion. For intracavity control of pulse dynamics we used broad bandwidth $LiNbO_3$ intensity modulator. The modulator was driven by 30 GHz signal generator. The state of polarization was examined by placing the polarization analyzer at the laser output. The diagram shown in Fig.2a indicates that the pulses have orthogonal components with amplitude ratio of ≈14:1. These measurements confirm the vector character of soliton pulses.

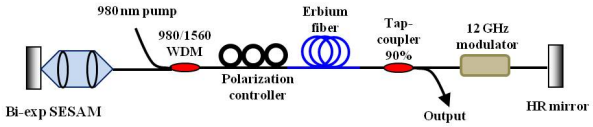

Fig. 1. Experimental setup of mode-locked Er-doped fiber laser.

As it was shown earlier [13], [14] the presence of absorber with bi-temporal recovery component in the cavity strongly affects the soliton dynamics in fiber laser. The slow recovery time induces the formation of attractive force, which in association with repulsive force formed due to soliton interactions, leads to continuous relative motion of the pulses within the bunch. This joint action of two counteractive forces causes the phase jittering of the pulses, which results in greatly reduced and broadened Kelly sidebands of the spectrum and pedestal in the autocorrelation trace. These features describe the nonstationary regime in vector soliton laser, so-called bunching. Without intensity modulation, the laser operated in bunching regime with the output laser parameters presented in Fig. 2 (b-d). Due to small soliton separations, the individual pulses within the bunch have not been resolved and the oscilloscope train is seen as a single pulse circulating at a fundamental frequency of the cavity.

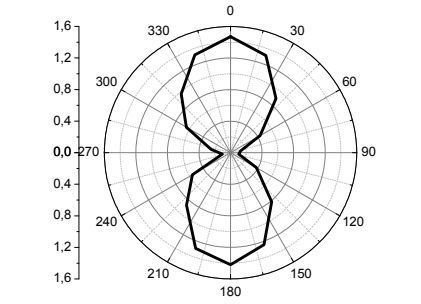

a

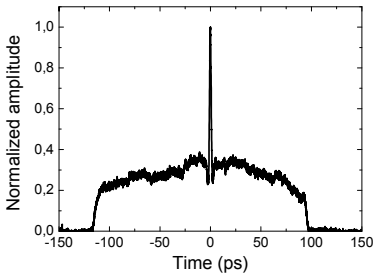

b

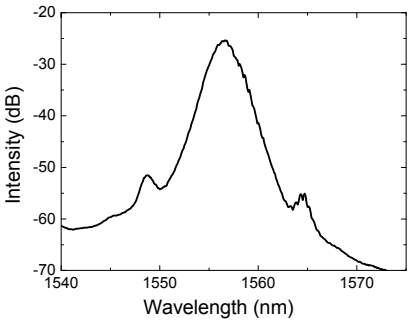

c

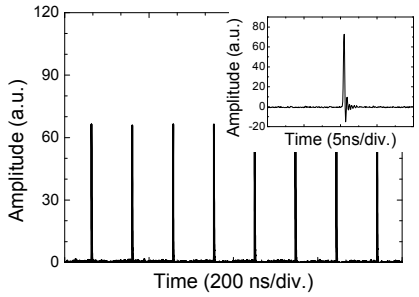

d

Fig. 2. Vector soliton laser output characteristics: a - polarization diagram of the laser output with intensity ratio of 14:1; b – autocorrelation trace; c – spectrum with 2.3 nm bandwidth; d – oscilloscope picture of the pulse train.

Random motion of the pulses provoked by joint action of SESAM induced soliton attraction and soliton repulsive force could not be avoided neither by polarization adjusting nor by changing other laser parameters. At the autocorrelation trace shown in Fig. 2b, these chaotic oscillations of multiple pulses manifest as a large pedestal due to averaging effect induced by slow scanning of autocorrelator.

Next to prevent irregular soliton motion within the group; the sinusoidal loss modulation of 8 dBm was applied at high harmonic of cavity frequency. The modulation frequency of ~12.3 GHz corresponding to 1195 cavity harmonic, provided selectivity sufficient to separate and stabilize the temporal position of soliton within the group. The modulation forces to operate the pulses in the stationary group in a bound soliton regime. The autocorrelation trace shows that irregular relative soliton movements have been suppressed and solitons propagate in the cavity with fixed time interval. The trace shown in Fig. 3a confirms the formation of stable pattern of soliton distribution. The pulse duration was 1 ps assuming $sech^2$-fitting. The modulation resulted in a larger spectral bandwidth of 3.2 nm and the sharp well-defined Kelly sidebands, which indicate the resonant phase-matching condition occurring with periodically perturbed pulses with low random phase component (Fig. 3b). The stabilization of pulse temporal position within the group is further evidenced by the periodic spectral fringes in the optical spectrum. The fragment of stabilized soliton spectrum plotted at linear scale is shown as inset to the Fig. 3b. The spectral period of 0.16 nm seen from the Figure corresponds to the periodic pulse sequence with the temporal separation of 50 ps. The contrast of the fringes is fairly low because instrument spectral resolution is close to the actual period of spectral modulation. Since the distance between pulses is small they cannot be clearly resolved on 2 GHz oscilloscope picture (Fig. 3c). The time-bandwidth product was equaled to 0.4 indicating slightly chirped pulse.

Though pulse synchronization and ordering induced by the amplitude modulation exhibit resonant character similar to actively mode-locked laser operating at high harmonics of cavity frequency, the locking pulse position within the bunch and formation of bound-state group of solitons shows specific features. As it was mentioned above, the saturable absorption exhibiting the slow component in the recovery provides strong force that brings the pulses in close proximity and, consequently, enhances the soliton interaction. It was demonstrated that such closely spaced solitons could form the stationary bounded group [15]. Then the strong attractive force between the pulses determines the steady-state pulse rather than the modulation frequency. Indeed, the actual pulse spacing within the group of 50 ps is somewhat shorter than 80 ps pulse period expected with 12.3 GHz frequency of modulation.

The groups of bound state behave as entities each similar to the solitary soliton in a passively mode-locked laser. The passive mechanism of mode-locking does not lock firmly the relative positions of pulses; consequently, they freely navigate along the cavity resulting in a large timing jitter. Applying loss modulation to the cavity provides pulse ordering mechanism. Qualitatively, the group sequence observed from the oscilloscope was found to exhibit much lower temporal excursion with increasing the modulation frequency. At 12.3 GHz the visual temporal jittering was completely disappeared. The relative positions of the pulses within the bound-state group were dominated by the soliton interaction enforced by the bi-temporal SESAM and were independent on the active loss modulation.

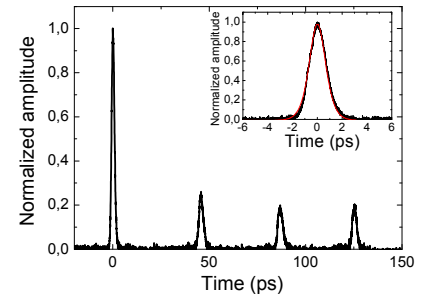

a

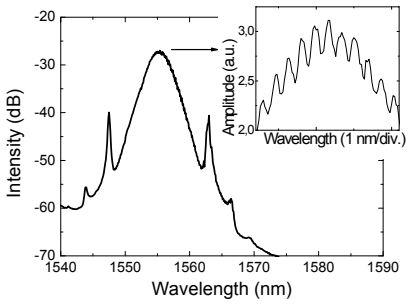

b

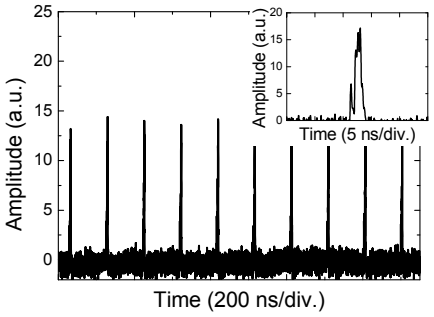

c

Fig. 3. Laser output characteristics with active modulation. a – autocorrelation trace. The inset shows the central pulse and its $sech^2$-fitting (red line); b – corresponding laser spectrum. The inset shows the spectrum fragment plotted in linear scale; c – oscilloscope picture of the pulse train.

III. Conclusion

We demonstrate the method of stable bound solitons formation by applying the loss modulation into the cavity. The loss modulation at high harmonic of cavity frequency provides efficient control of relative phases of solitons, prevent irregular soliton bunching and result in the formation of a stationary group of pulses with suppressed random relative phase variations.

The mode-locked fiber lasers offer attractive environment for generation new types of solitons and detailed study of soliton interaction. This knowledge would be particularly important for optical communication exploiting soliton propagation.

Acknowledgment

This work was supported by the Federal Agency on Science and Education in the course of the federal targeted programs "Research and Development in Priority Fields of the Scientific and Technical Complex of Russia (2007–2012)" and "Scientific and Pedagogical Personnel of Innovative Russia (2009–2013)."

The authors thank I.O. Zolotovskii from Ul'yanovsk State University, Russia, for helpful discussions.

References

[1] B. Grudinin and S. Gray, "Passive harmonic mode locking in soliton fiber lasers," J. Opt. Soc. Am. B 14, no. 1, 144–154 (1997).

[2] J. N. Kutz, B. C. Collings, K. Bergman, S. Tsuda, S. T. Cundiff, W. H. Knox, P. Holmes, and M. Weinstein, "Mode-locking pulse dynamics in a fiber laser with a saturable Bragg reflector," J. Opt. Soc. Am. B 14, no. 10, 2681–2690 (1997).

[3] J. N. Kutz, B. C. Collings, K. Bergman, and W. H. Knox, "Stabilized pulse spacing in soliton lasers due to gain depletion and recovery," IEEE J. Quantum Electron. 34, no. 9, 1749–1757 (1998).

[4] M. J. Lederer, B. Luther-Davis, H. H. Tan, C. Jagadish, N. Akhmediev, and J. M. Soto-Crespo, "Multipulse operation of a Ti:sapphire laser mode locked by an ion-implanted semiconductor saturable absorber mirror," J. Opt. Soc. Am. B 16, no. 6, 895–904 (1999).

[5] N. Akhmediev, J. M. Soto-crespo, M. Grapinet, Ph. Grelu, "Dissipative soliton interactions inside a fiber laser cavity," Optical Fiber Technology 11, no. 3, 209-228 (2005).

[6] J. M. Soto-Crespo, N. N. Akhmediev, B. C. Collings, S. T. Cundiff, K. Bergman, and W. H. Knox, "Polarization-locked temporal solitons in a fiber laser: theory," J. Opt. Soc. Am. B 17, no. 3, 366–372 (2000).

[7] Ph. Grelu and Soto-Crespo, "Multisoliton states and pulse fragmentation in passively ML fiber laser," J. Opt. B: Quantum Semiclass. Opt. 6, no. 5, S271-S278 (2004).

[8] D.Y. Tang, B. Zhao, L.M. Zhao, H.Y. Tam, "Soliton interaction in a fiber ring laser," Phys. Rev. E 72, no.1, 016616 (2005).

[9] D.Y. Tang, W.S. man, H.Y. Tam, P.D. Drummond, "Observation of bound states of solitons in a passively mode-locked fiber laser," Phys. Rev. A 64, no.3, 033814 (2001).

[10] W.W. Hsiang, C.-Y. Lin, and Y. Lai, "Stable new bound soliotn pairs in a 10 GHz hybrid frequency modulation mode-locked Er-fiber laser," Opt. Lett., 31, no. 11, 1627-1629 (2006).

[11] Vainionpää, S. Suomalainen, O. Tengvall, T. Hakulinen, R. Herda, S. Karirinne, M. D. Guina and O. G. Okhotnikov, **"**Metamorphic growth of long-wavelength saturable absorber on GaAs substrates", 18th Annual Meeting of the IEEE Lasers and Electro-Optics Society (LEOS), 2005, Sydney, Australia, paper ThN3.

[12] S. Suomalainen, M. Guina, T. Hakulinen, R. Koskinen, J. Paajaste, M. Karjalainen, S. Marcinkevicius and O. G. Okhotnikov, "Semiconductor saturable absorbers with recovery time controlled by lattice mismatch and band-gap engineering", Materials Science and Engineering B. 147, no. 2-3, 156-160 (2008).

[13] R. Gumenyuk and O.G. Okhotnikov, "Temporal control of vector soliton bunching by slow/fast saturable absorption," J. Opt. Soc. Am. B, vol. 29, no. 1, 1-7 (2012).

[14] L. M. Zhao, D. Y. Tang, H. Zhang, and X. Wu, "Bunch of restless vector solitons in a fiber laser with SESAM," Opt. Express vol. 17, no. 10, 8104-8108 (2009).

[15] R. Gumenyuk, and O.G. Okhotnikov, "Impact of gain medium dispersion on stability of soliton bound states in fiber laser," Accepted for publication in PTL 19.11.2012

Appendix 7

Publication 7

R. Gumenyuk and O. G. Okhotnikov, "Multiple solitons grouping in fiber lasers by dispersion management and nonlinearity control", J. Opt. Soc. Am. B, Vol. 30, No. 4, pp. 776–781 (2013).

Multiple solitons grouping in fiber lasers by dispersion management and nonlinearity control

Regina Gumenyuk* and Oleg G. Okhotnikov

Optoelectronics Research Centre, Tampere University of Technology, Korkeakoulunkatu 3, Tampere FIN-33101, Finland
**Corresponding author: regina.gumenyuk@tut.fi*

Received November 28, 2012; revised January 21, 2013; accepted January 31, 2013;
posted February 1, 2013 (Doc. ID 180801); published March 5, 2013

Dispersion-managed bound solitons and soliton bunches have been studied experimentally in a fiber laser mode-locked by saturable absorber with biexponential recovery dynamics, which enforces strongly the soliton interaction. The excessive nonlinearity and dispersion in a cavity was found to provoke the collapse of bound solitons states and induce the irregular soliton dynamics, which indicates the random relative phase variations between the solitons caused by the dispersive wave. © 2013 Optical Society of America

OCIS codes: 320.7110, 060.3510, 140.4050, 190.5530.

1. INTRODUCTION

With the net anomalous group velocity dispersion (GVD), the nonlinearity balances GVD resulting in a soliton-like pulse shaping, which implies that the fibers could support short pulse propagation with neither temporal nor spectral distortion as optical solitons. Net anomalous GVD compensates the accumulated pulse phase shift in a cavity consisting of segments with normal and anomalous GVD, representing a so-called dispersion map. With an increase in the pulse energy, however, the excessive nonlinear phase shift cannot be eventually compensated by the dispersion, giving rise to the phenomenon known as pulse breaking. Multiple pulsing is frequently observed in passively mode-locked fiber lasers as a result of energy quantization—the general attribute of soliton regime. Though the strong dispersion map was shown to increase the threshold for multiple pulse operation, the wave-breaking instability still prevents considerable energy scaling using this laser concept. Various short pulse regimes can then be supported, e.g., stretched-pulse [1–6], dissipative [7–13], vector [14–20], bound solitons [21–24] depending on the cavity design and the strength of the dispersion map.

It was recently shown that enhancement of soliton attractive force in the cavity can change dramatically their interaction [25,26]. Specifically, the saturable absorption can promote the stable soliton groups formation when the tightly bound cluster of pulses suffers reduced loss in absorber by saturating it together. This dynamic scenario could occur when the absorber recognizes the soliton group as a single entity. Intuitively, it is evident that when the group of pulses is confined within the time slot comparable with the recovery time of the absorber, it will saturate the absorber more strongly by joint action and, therefore, suffer lower loss. This mechanism was confirmed recently by using the semiconductor saturable absorber with slow and fast temporal dynamics [25]. The stable bunches of the vector solitons propagating in a cavity as an entity were observed [25–27].

Further study addressing the effect of dispersion map on the soliton bunching was focused on the imperative role of gain medium dispersion on the soliton dynamics within the group [28]. It was shown that either steady-state bound soliton ensemble with equally spaced pulses or nonstationary soliton group (bunch) are developed for normal and anomalous GVD of the gain medium, respectively, with the same net cavity dispersion in the anomalous regime.

The results presented in this study show the effect of the total cavity dispersion, the shape of dispersion map and nonlinearity on vector soliton interaction and group formation. Generally, the dispersion management in the fiber laser cavity can be accomplished either by using dispersion-compensation fiber or by using discrete component, e.g., grating pair, prism sequence, and chirped fiber Bragg grating, providing distributed and discrete strong dispersion map, respectively. In this study we used two options—dispersion-compensation fiber and grating pair to tune the cavity dispersion. The first adds significant nonlinearity into the cavity, while the latter one provides nonlinearity-free compensation. Using both compensation methods allowed to identify the separate impact of dispersion and nonlinearity on the soliton group formation.

2. EXPERIMENTAL

A. Soliton Laser with Dispersion Management by All-Fiber Compensator

The mode-locked erbium-doped fiber laser used in this experiment is shown schematically in Fig. 1. The gain was provided by a 0.5 m long erbium-doped fiber pumped by a 980 nm diode laser through the pump fiber combiner. The dispersion of the active fiber was −46 ps/nm × km at 1560 nm. The laser cavity was terminated by high reflective dielectric broadband mirror butt-coupled to the fiber and lens-coupled semiconductor saturable absorber mirror (SESAM) with bi-temporal slow/fast recovery dynamics described elsewhere [25]. The SESAM induces a strong attractive force between pulses, which supports the soliton group formation [25,26]. The passive fiber segments are made of standard single-mode fiber (SMF-28) with anomalous dispersion of 18 ps/nm × km at 1560 nm. The length of the passive compensating fiber was varied from

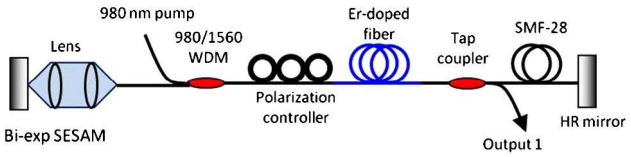

Fig. 1. (Color online) Erbium-doped soliton fiber laser with cavity dispersion adjusted by compensating fiber.

5.5 to 30 m tuning cavity dispersion from 0.15 to 1.1 ps/nm. The pulse parameters were measured using 10% output coupler with external pigtail length of 0.5 m. The polarization state was examined using a polarization analyzer inserted into the output beam.

The erbium fiber laser mode-locked by SESAM and operated in a vector soliton regime was found to produce

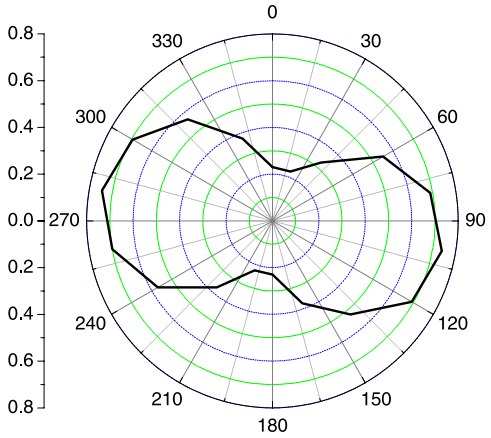

Fig. 2. (Color online) Polarization diagram of the laser output with intensity ratio of 3.7:1 confirms the vector character of solitons.

elliptically polarized pulses, as shown in Fig. 2. Figure 3 shows that by increasing the cavity dispersion, the type of the soliton group can be changed from stationary bound state to bunch. At low values of cavity dispersion, $D \leq 0.29$ ps/nm, the laser operated with the bound pair solitons for the whole range of available pump power, as seen from the autocorrelation plotted in Fig. 3(a).

The separation between solitons is firm, indicating that they propagate with the same GVD. With increasing the dispersion value, the solitons group together and circulate in the cavity as a unified bunch. The distinctive attribute of the bunch is a large pedestal in the pulse autocorrelation, which originates from the chaotic, nonstationary dynamics of solitons confined within the bunch [25]. The randomly oscillating pulses within the bunch effectively develop a large pedestal in the autocorrelation, as seen from Fig. 3(a) for $D > 0.26$ ps/nm [25]. Contrary to sharp Kelly spectral sidebands observed for steady bound state soliton pair, the sidebands are distorted, which results from the chaotic motion of soliton within the bunch [25]. The corresponding pulse trains are shown in Fig. 3(c). Due to small separation between the solitons, the group of pulses is seen on the scope as a "single pulse" with effective amplitude proportional to the number of pulses within the group. A "single pulse" train, which is actually a soliton bunch sequence circulating as a stable entity along the cavity. The large effective amplitude of these pulses (see the Y-scale) indicates the large number of solitary pulses trapped within the bunch.

The energy of the fundamental soliton and the number of pulses circulated in the laser cavity were estimated for various cavity lengths/dispersions. The results are summarized in Fig. 4. With increasing the net cavity dispersion, the energy of the fundamental soliton decreases, while the number of pulses in the cavity increases. With an increase in the cavity

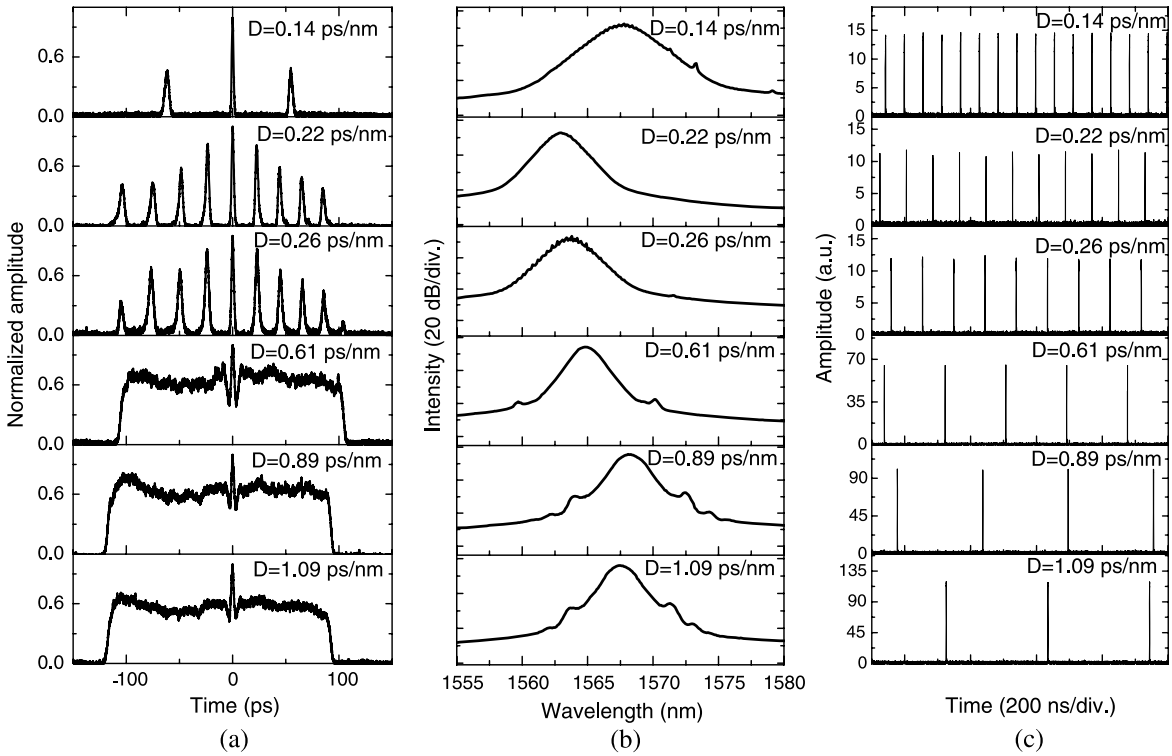

Fig. 3. Multiple pulse regime evolution with net cavity dispersion. (a) Pulse autocorrelations, corresponding, (b) pulse spectra and (c) oscilloscope pulse trains.

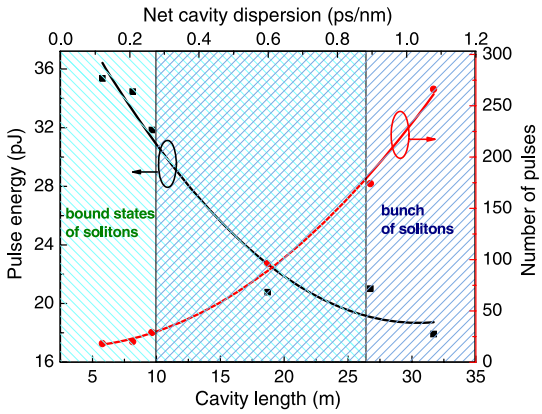

Fig. 4. (Color online) Energy and number of pulses versus cavity dispersion/length.

dispersion from 0.1 to 1.1 ps/nm, the number of pulses increases by order of magnitude. Figure 4 demonstrates that the stable bound soliton states have been observed for the cavity dispersion range below 0.26 ps/nm independent on the available pump power. For dispersion values from 0.26 to 0.89 ps/nm, the stationary bound soliton states observed at low pumping level collapse with an increase in pump power and transform into oscillating bunches. Above the cavity dispersion of 0.89 ps/nm, the soliton bunch formation has been observed for entire range of pump power.

Though the increase of anomalous dispersion apparently promotes the solitons bunch formation through enforced soliton–soliton interaction, it should be noted that the dispersion offset performed by changing the length of the fiber unavoidably changes the nonlinearity of the cavity, which would also affect the soliton interaction. To distinguish the role of dispersion and nonlinearity, a nonlinearity-free dispersion grating pair compensator was next implemented.

B. Soliton Laser with Grating Pair Compensator

A soliton fiber laser using a grating pair compensator is shown in Fig. 5. The pulse repetition rate varied slightly around ~36.6 MHz when the cavity dispersion was tuned by adjusting the grating pair separation, while the pulse energy was kept unchanged during the measurements. An essential feature of this setup is the nonlinearity independent dispersion management. Figure 6 shows the evolution of the laser output parameters with net cavity dispersion, which demonstrates that the character of the laser operation did not change with increasing the cavity dispersion from 0.37 to 0.75 ps/nm. Stationary bound solitons pairs have been observed for the entire ranges of available pump power and dispersion while the soliton separation in a group increases with the dispersion.

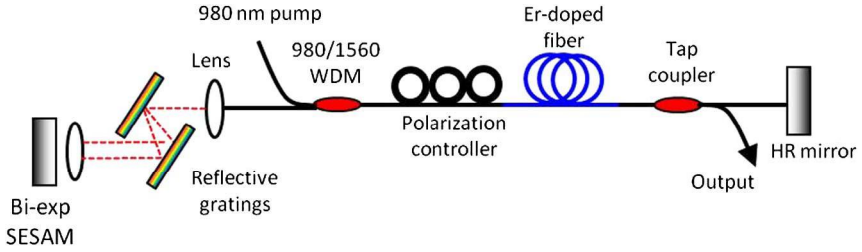

Fig. 5. (Color online) Soliton erbium fiber laser with 600 grooves/mm grating pair dispersion compensator.

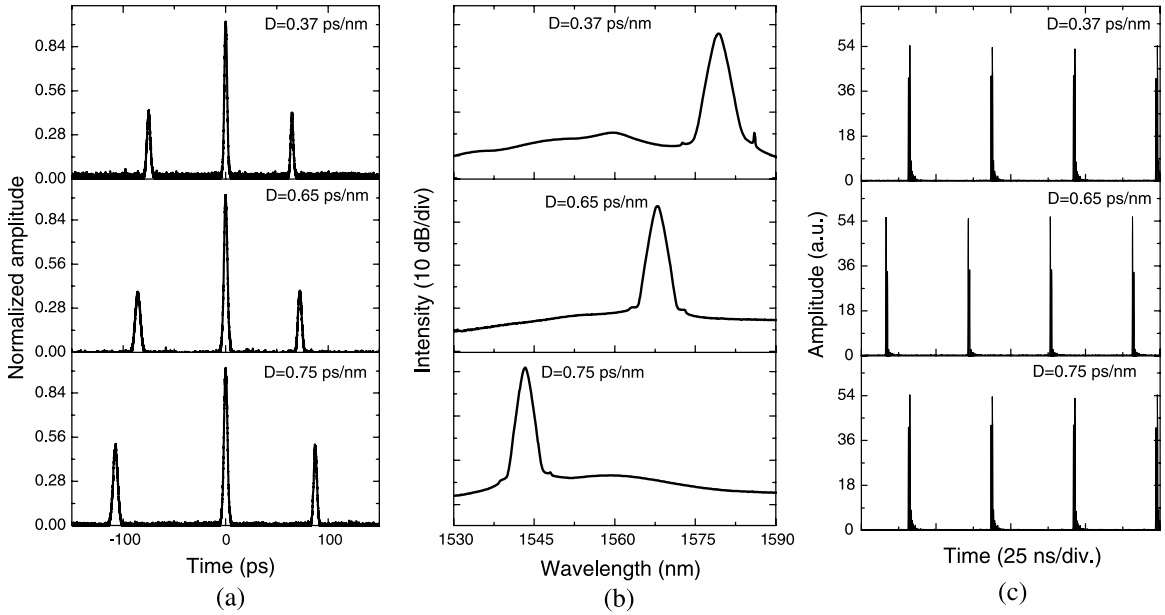

Fig. 6. (a) Pulse autocorrelations, (b) pulse spectra, and (c) oscilloscope waveforms of the pulse train for net anomalous cavity dispersion of $D = 0.37$, 0.65, and 0.75 ps/nm corresponding to 600/mm grating pair separation of 7, 12.3, and 13.5 cm.

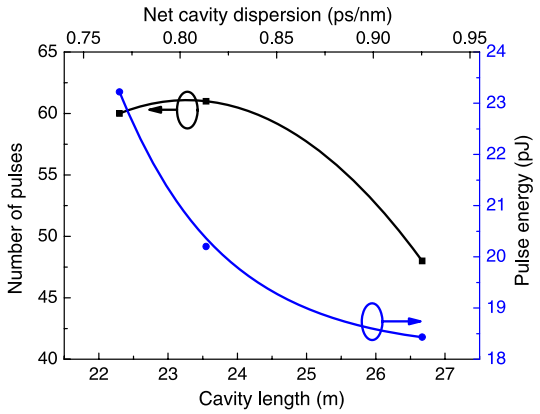

Fig. 7. (Color online) Soliton energy threshold of transition to bunch formation depending on length/dispersion of the compensating fiber.

The central wavelength shift, seen from Fig. 6(b), is caused by an increase of the intracavity loss with increasing of the gratings separation. To preserve the soliton parameters, the variation in the cavity loss was compensated by appropriate change in the pump power.

Comparison of the results presented in Figs. 3 and 6 indicates the noticeable effect of nonlinearity on the collapse of bound states. Particularly, the bound states have been observed only for dispersion below 0.26 ps/nm with a long-length fiber dispersion compensator exhibiting high nonlinearity (Fig. 3). In a contrary, the cavity with a short fiber section, the transition to the soliton bunching regime was not found for dispersion tuned by the grating pair up to 0.75 ps/nm.

C. Impact of Nonlinearity on the Soliton Interaction

The nonlinearity in a cavity leads to a nonlinear phase shift accumulation, which increases with the pulse energy and eventually cannot be controlled by the dispersion. This effect causes the pulse distortion and break-up resulting in a multiple pulse regime. The analysis shows that long-range soliton interaction mediated by the dispersive wave, may cause irregular soliton movements while the stability of relative separation between solitons increases with the spacing [29]. Then with an increase in the number of pulses and corresponding decrease in the average soliton spacing, the bound state of solitons collapses and bunch of pulses with random soliton oscillations sets in.

To further validate the impact of nonlinearity, we measured the critical number of pulses corresponding to the transition from bound state to soliton bunching. The typical scenario of soliton dynamics shows steady bound solitons formation at low pump power, while above the critical pumping level dependent on the cavity dispersion, the bunch of solitons develops. The soliton energy corresponding to the onset of transition from bound state to bunched solitons was varied by changing the length of fiber segment in the cavity. Figure 7 shows the soliton energy at the threshold of bunch formation. The pumping threshold for bunch formation gradually decreases with the cavity dispersion starting from the dispersion value of 0.27 ps/nm. At cavity dispersion of 0.89 ps/nm the soliton bunch regime has been observed for the entire range of pump power.

The evolution of the laser regime with a pump power for the total cavity dispersion of 0.82 ps/nm is further illustrated in Fig. 8. When the pulse number exceeds a critical value, the solitons grouped in a bunch circulate as an entity unit along the cavity. For high pump power, only soliton bunch formation has been observed.

3. DISCUSSION

The presented experimental findings indicate how the multiple pulse regime in soliton lasers in the presence of strong attraction force depends on the parameters of the laser cavity.

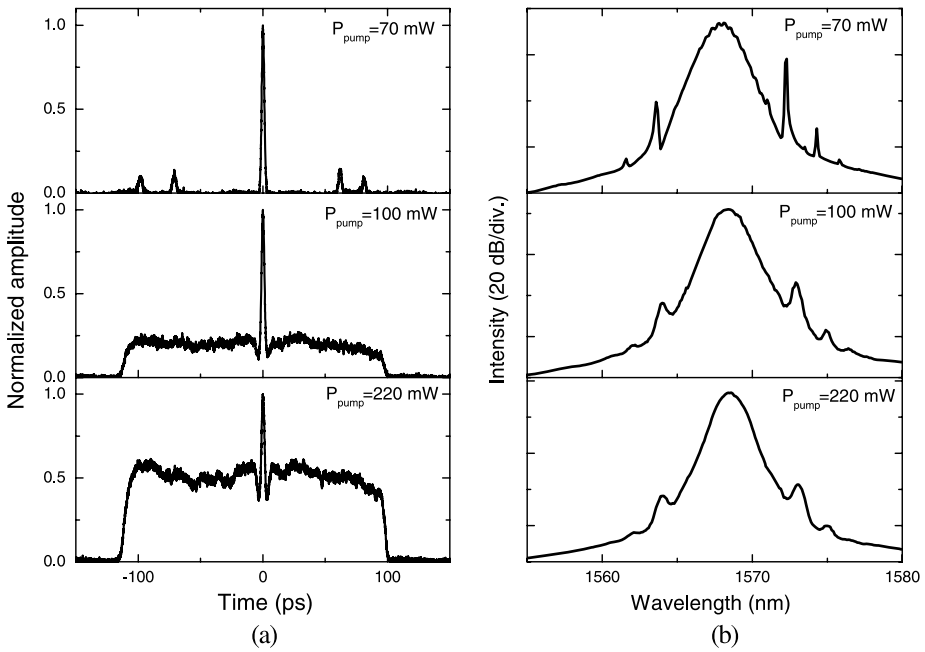

Fig. 8. Evolution of the laser regime with pump power, when passive fiber used as intracavity dispersion compensator. The net cavity dispersion was 0.82 ps/nm. (a) Autocorrelation traces and (b) pulse spectra.

Two distinct forms of a stable group of confined solitons have been identified. The autocorrelation functions measured with the temporal resolution of 1 fs and shown in Figs. 3(a), 6(a), and 8(a) allow to clearly resolve the substructure of the pulse group, particularly, to distinguish the stationary bound state from bunch of solitons with chaotic pulse oscillations. The autocorrelation traces of bound states shown in Fig. 3(a) (for $D = 0.14$ ps/nm; 0.22 ps/nm; 0.26 ps/nm), Figs. 6(a) and 8(a) (for 70 mW) reveal the actual interval of pulses in a group. The autocorrelation traces of bunches indicate that the rate of pulse oscillations within the bunch is much faster than the scanning speed of the autocorrelator. The cross-correlations of multiple pulses sweeping within the group form effectively the observed pedestal. The duration of the pedestal is larger than the scanning range of the autocorrelator (180 ps). Nevertheless, Kelly sidebands seen in the bunch spectra [Fig. 3(b) (for $D = 0.61$ ps/nm; 0.89 ps/nm; 1.09 ps/nm) and Fig. 8(a) (for 100 mW; 220 mW)] indicate that the pulses confined within the bunch are randomly oscillating actual solitons with duration of 1.2–2.5 ps assuming their nearly transform-limited characteristics. This feature provides the confident ground for nonstationary origin of the pedestal in the bunch autocorrelation.

Figures 4 and 7 show the estimated values of pulse energy and number of pulses inside the cavity. The output pulse characteristics measured at the output of 10% coupler were used to derive the estimation for the pulse energy and number of pulses propagated inside the cavity depending on the cavity dispersion. The figures illustrate the essential role of the dispersion for the multiple pulse regime. Indeed, the stable bound states of solitons have been observed for the cavity dispersion range below 0.26 ps/nm, while above 0.89 ps/nm, only soliton bunch formation has been observed for the entire range of pump power.

Another observation that can be derived from the experimental results shows that if the pulse energy or/and number of pulses circulating within the cavity become too large, the bound states of solitons become unstable eventually resulting in the transition to bunch formation with chaotic motion of solitons within the group. The evolution of the bound solitons toward bunch regime was thus ascribed to enforced soliton–soliton interaction.

The correct model of the multiple pulse soliton laser should include the temporal dynamics on the two scales. One relates to the absorber with bitemporal recovery. The slowly recovered component of the absorber causes the group formation with closely spaced pulses. When the temporal length of the group is below the decay time of the absorber, the joint action of the pulses forming the group provides more complete saturation of the absorption and thus the pulses suffer lower losses compared to the regime with absorber saturated by individual pulses. Thus, the absorber enhances strongly the pulse interaction by keeping them in a compact group with a short interpulse interval. The second dynamic scale concerns the soliton–soliton interaction within the group. The experimental results presented here reveal that there are two possible scenarios of the multiple pulse regime depending on the dispersion and nonlinearity of the laser cavity—stationary bound states of solitons or bunches with irregular chaotic motion of solitons. The model is now under development; however, the preliminary results suggest that the modulation instability is one of the main mechanisms responsible for multiple pulse dynamics.

4. CONCLUSIONS

In summary, we studied the formation of various regimes of the multiple solitons in a fiber laser. The excessive nonlinearity and dispersion in a cavity tend to destroy the stable bound solitons and lead to soliton bunch formation with chaotic motion of the pulses within the group. The collapse of bound states of solitons and transition to irregular soliton dynamics within the group, which signifies the random relative phase variations between the solitons, could be ascribed to combined effects dispersive wave and modulation instability.

REFERENCES

1. K. Tamura, E. P. Ippen, H. A. Haus, and L. E. Nelson, "77 fs pulse generation from a stretched-pulse mode-locked all-fiber ring laser," Opt. Lett. **18**, 1080–1082 (1993).
2. K. Tamura, E. P. Ippen, and H. A. Haus, "Pulse dynamics in stretched pulse fiber lasers," Appl. Phys. Lett. **67**, 158–160 (1995).
3. V. Cautaerts, D. J. Richardson, R. Paschotta, and D. C. Hanna, "Stretched pulse Yb3 + :silica fiber laser," Opt. Lett. **22**, 316–318 (1997).
4. H. A. Haus, K. Tamura, L. E. Nelson, and E. P. Ippen, "Stretched-pulse additive pulse mode-locking in fiber ring lasers: theory and experiment," IEEE J. Quantum Electron. **31**, 591–598 (1995).
5. F. Ö. Ilday and F. W. Wise, "Nonlinearity management: a route to high-energy soliton fiber lasers," J. Opt. Soc. Am. B **19**, 470–476 (2002).
6. F. Ö. Ilday, J. R. Buckley, H. Lim, F. W. Wise, and W. G. Clark, "Generation of 50 fs, 5 nJ pulses at 1.03 μm from a wave-breaking-free fiber laser," Opt. Lett. **28**, 1365–1367 (2003).
7. A. Chong, W. R. Renninger, and F. W. Wise, "Properties of normal-dispersion femtosecond fiber lasers," J. Opt. Soc. Am. B **25**, 140–148 (2008).
8. N. Akhmediev, J. M. Soto-Crespo, and Ph. Grelu, "Roadmap to ultra-short record high-energy pulses out of laser oscillators," Phys. Lett. A **372**, 3124–3128 (2008).
9. B. G. Bale, S. Boscolo, and S. K. Turitsyn, "Dissipative dispersion-managed solitons in mode-locked lasers," Opt. Lett. **34**, 3286–3288 (2009).
10. W. Chang, A. Ankiewicz, J. M. Soto-Crespo, and N. Akhmediev, "Dissipative soliton resonances in laser models with parameter management," J. Opt. Soc. Am. B **25**, 1972–1977 (2008).
11. C. Ouyang, L. Chai, H. Zhao, M. Hu, Y. Song, Y. Li, and C. Wang, "Pulse-shaping dynamics controlled by four structural parameters in an all-normal-dispersion mode-locked fiber laser," J. Opt. Soc. Am. B **26**, 1875–1881 (2009).
12. W. H. Renninger, A. Chong, and F. W. Wise, "Area theorem and energy quantization for dissipative optical solitons," J. Opt. Soc. Am. B **27**, 1978–1982 (2010).
13. R. Gumenyuk, I. Vartiainen, H. Tuovinen, and O. G. Okhotnikov, "Dissipative dispersion-managed soliton 2 μm thulium/holmium fiber laser," Opt. Lett. **36**, 609–611 (2011).
14. S. T. Cundiff, B. C. Collings, N. N. Akhmediev, J. M. Soto-Crespo, K. Bergman, and W. H. Knox, "Observation of polarization-locked vector solitons in an optical fiber," Phys. Rev. Lett. **82**, 3988–3991 (1999).
15. W. C. Chen, W. C. Xu, F. Song, M. C. Shen, D. A. Han, and L. B. Chen, "Vector solitons in femtosecond fibre lasers," Eur. Phys. J. D **48**, 255–260 (2008).
16. J. M. Soto-Crespo, N. N. Akhmediev, B. C. Collings, S. T. Cundiff, K. Bergman, and W. H. Knox, "Polarization-locked temporal vector solitons in a fiber laser: theory," J. Opt. Soc. Am. B **17**, 366–372 (2000).
17. B. C. Collings, S. T. Cundiff, N. N. Akhmediev, J. M. Soto-Crespo, K. Bergman, and W. H. Knox, "Polarization-locked temporal vector solitons in a fiber laser: experiment," J. Opt. Soc. Am. B **17**, 354–3765 (2000).

18. J. H. Wong, K. Wu, H. H. Liu, C. Ouyang, H. Wang, S. Aditya, P. Shum, S. Fu, E. J. R. Kelleher, A. Chernov, and E. D. Obraztsova, "Vector solitons in a laser passively mode-locked by single-wall carbon nanotubes," Opt. Commun. **284**, 2007–2011 (2011).
19. J. Yang, "Interactions of vector solitons," Phys. Rev. E **64**, 026607 (2001).
20. L. M. Zhao, D. Y. Tang, H. Zhang, and X. Wu, "Polarization rotation locking of vector solitons in a fiber ring laser," Opt. Express **16**, 10053–10058 (2008).
21. D. Y. Tang, W. S. Man, H. Y. Tam, and P. D. Drummond, "Observation of bound states of solitons in a passively mode-locked fiber laser," Phys. Rev. A **64**, 033814 (2001).
22. D. Y. Tang, B. Zhao, D. Y. Shen, and C. Lu, "Bound-soliton fiber laser," Phys. Rev. A **66**, 033806 (2002).
23. B. Ortaç, A. Hideur, T. Chartier, M. Brunel, P. Grelu, H. Leblond, and F. Sanchez, "Generation of bound states of three ultrashort pulses with a passively mode-locked high-power Yb-doped double-clad fiber laser," IEEE Photon Technol. Lett. **16**, 1274–1276 (2004).
24. Y. Cong, P. Shum, T. Hiang, C. Q. Wen, and D. Tang, "Bound soliton pulses in passively mode-locked fiber laser," Opt. Commun. **200**, 389–399 (2001).
25. R. Gumenyuk and O. G. Okhotnikov, "Temporal control of vector soliton bunching by slow/fast saturable absorption," J. Opt. Soc. Am. B **29**, 1–7 (2012).
26. L. M. Zhao, D. Y. Tang, H. Zhang, and X. Wu, "Bunch of restless vector solitons in a fiber laser with SESAM," Opt. Express **17**, 8103–8108 (2009).
27. R. Gumenyuk, M. S. Gaponenko, K. V. Yumashev, A. A. Onushchenko, and O. G. Okhotnikov, "Vector soliton bunching in thulium-holmium fiber laser mode-locked with PbS quantum-dot-doped glass absorber," IEEE J. Quantum Electron. **48**, 903–907 (2012).
28. R. Gumenyuk and O. G. Okhotnikov, "Impact of gain medium dispersion on stability of soliton bound states in fiber laser," IEEE Photon. Technol. Lett. **25**, 133–135 (2013).
29. D. Y. Tang, B. Zhao, L. M. Zhao, and H. Y. Tam, "Soliton interaction in a fiber ring laser," Phys. Rev. E **72**, 016616 (2005).

Tampereen teknillinen yliopisto
PL 527
33101 Tampere

Tampere University of Technology
P.O.B. 527
FI-33101 Tampere, Finland

ISBN 978-952-15-3312-9
ISSN 1459-2045